FACULTY OF EARTH
AND ENVIRONMENTAL SCIENCES
AND ENGINEERING

PhD Thesis

Nagham Amer Sami

Miskolc
2024

UNIVERSITY OF MISKOLC

Faculty of Earth and Environmental Sciences and Engineering

Institute of Mining and Energy

Forecasting of Intermittent Gas Lift Flow Parameters Using Computational Fluid Dynamics and Machine Learning Techniques

Research Topic Area:

Fluid Production and Transport Systems

Ph.D. Thesis

by

Nagham Amer Sami

Supervisor:

Dr. Zoltán Turzó

Mikoviny Sámuel Doctoral School of Earth Sciences

Head of the Doctoral School:

Prof. Dr. Péter Szűcs

Miskolc, Hungary, 2024

CONTENTS

ACKNOWDLEDGMENT

I want to express my deepest appreciation to my supervisor Dr. Zoltan Turzo, Professor and Head of the Petroleum Engineering Department, Miskolc University, for his valuable guidance, motivation, patience, and immense knowledge. His encouragement helped me all the time to complete this research program and to draft my thesis successfully.

I would also like to thank the rest of the petroleum engineering department staff, the Dean of earth science faculty, and my teachers in the Department for their support during the research program. I want to thank Stipendium Hungaricum Scholarship for its financial and academic support and for granting me this opportunity to complete my Ph.D. degree.

Life in Hungary would not be the same without my beloved family, my husband, Dr. Dhorgham, my daughter Rawan and my son Layth. Special thanks to my first teacher, my husband, Dr. Dhorgham, for his patience, support, and valuable comments to complete this research. I dedicated this work to all my family members; thanks for your care towards me during my study.

ABSTRACT

Intermittent gas lift is an artificial lift process used widely to enhance the productivity of oil wells. This process is based on the injection of gas as an external energy source at a regular time interval to lift the accumulated fluid from the bottom of the well to the surface. Despite the advanced works proposed by previous researchers, the interaction operating parameters of the intermittent gas lift remain poorly understood and need more investigation. A computational fluid dynamics model (CFD) is developed in this research to accurately predict the single and multiphase flow parameters of the intermittent gas lift process.

The simulation is conducted for a test section of an 18 m vertical tube with a 0.076 m diameter using air as injection gas and oil as a formation fluid. The results obtained from the CFD model validate the experiment results from the literature. The results obtained from this model show that as the gas injection pressure increases, the liquid slug velocity increase, and the region of the constant velocity decrease. The effect of the injected time and pressure on the fluid production rate has been studied. The developed model shows that more than 50% of the liquid product comes from after the flow period (the gas flow stopped).

Also, the effective parameters are organized into dimensionless ratios to reduce the complexity of the system and the required computational time. The production of the liquid slug for different injection pressures, tubing sizes, and starting submergence lengths were studied. The results obtained from the simulation model were validated with the results from the literature. The liquid production rate increases with the injection pressure, tubing size, and submergence length. The pressure profile can be easily obtained for various positions and conditions along the production string using the present developed model. The developed model achieved in this research shows that CFD is a proven model to describe the multiphase flow in such a complex system as intermittent gas lifting and can be used for further development in this field of research.

To design an efficient intermittent gas-lift installation, real information is needed to study all process components, from the outer boundary of the reservoir to the surface separators. The gas lift valve is the most critical component affecting the system's design. In an intermittent producing method, the pilot gas-lift valve is used to control the point of compressed gas entry into the production tubing and acts as a pressure regulator.

A novel approach using CFD simulation was performed in this study to develop a dynamic model for the gas passage performance of a 1-in. (25.4 mm), nitrogen-charged, pilot gas-lift valve. Dynamic performance curves were obtained using methane as an injection gas with flow rates reaching up to 4.5 MMscf/day (133 em^3/day). This study investigates the

effect of internal pressure, velocity, and temperature distribution within the pilot valve that cannot be predicted in the experiments and mathematical models during the flow-performance studies. A general equation of the nonconstant discharge coefficient has been developed for the 1-inch pilot valve to be used for further calculation in the industry without using the CFD model. The developed model significantly reduces the complexity of the data required to calculate the discharge coefficient.

Tubing pressure at gas injection depth in intermittent wells is one of the most critical parameters for production engineers to evaluate the system's performance. However, monitoring of the tubing pressure is not usually carried out in real-time.

Machine learning (ML) algorithms are utilized in this research to develop a model that can accurately predict tubing pressure in artificial intermittent gas lift wells. Intelligent algorithms built on the field data provide a solution that is easy to use and universally applicable to complex problems. Various non-linear regression ML methods are employed in this study, namely, Decision Tree- regression (DT), Random Forest- regression (RF), and K Nearest Neighbors- regression (KNN). All the tubing pressures obtained from ML models were compared with the actual values to ensure the effectiveness of the work. The developed models show that they can predict pressure with more than 99.9% accuracy. This is an exciting result, as such outcome accuracy has not been reported usually in the open literature.

1. INTRODUCTION

1.1. Background

In most oil reservoirs, oil exists under pressure from the natural energy that surrounds it (reservoir energy). When a well is drilled into the reservoir, the formation fluids start to flow due to the pressure difference between the reservoir and the producing facilities on the surface. With continuous natural oil production, the well will lose about 80% of the pressure required to lift the reservoir fluid to the surface, affecting the well deliverability (Winker and Smith, 1962). When the pressures in the reservoir and the wellbore equalize, it becomes very difficult to get the reservoir fluid to the surface without downhole artificial lift processes. In other wells, natural energy is not high enough to drive the oil to the surface in an economic volume, hence, one process of artificial lift must be utilized to sustain the reservoir's natural energy.

Gas lift is often an ideal selection of artificial lift, if gas is readily available on the surface, either from the produced gas, or from an outside gas source (Ortiz and Lagoven, 1990). The gas lift process is considered as a resemblance to the natural flow process of a well. In a naturally flowing well, the pressure is reduced as the fluid travels upward from the bottom of the well to the surface so that, the gas expands and moves faster upward. Continuous flow gas lift is also an expansion process of the natural flow phase, this process's adaptability changes in well conditions by providing additional gas to improve fluid production by increasing the gas-liquid ratio (GLR) and reducing the liquid column density (Fathi, 2017).

Gas lift is one of the artificial lift methods which can be selected for many reasons: availability of the gas since large quantities of gas are expected to be produced during the productive life of the well, the modest costs required for installation of downhole equipment, a flexibility of gas lift system maintenance by using side pocket mandrels compared with the other artificial lift systems, the initial design parameter of gas lift installations can be easier to adjust than other mechanical lift methods when some of the input parameters are unknown. Finally, with changing operating conditions, the gas lift has the potential to be more adaptable than other artificial lift methods. Elevated gas-to-liquid ratios (GLRs) usually improve the effectiveness of the gas lift method, whereas it has been found to cause problems in other lift processes, increase the failure frequency and limit the drawdown achieved by mechanical lift systems (Bilal et al., 2018).

There are two types of gas lift systems are used in industry, continuous and intermittent flow. The principle of gas lift is the same in both systems as high-pressure natural gas is injected from the surface to lift formation fluid upward, but the operation procedure is completely different.

The continuous flow technique is very similar to the natural flow, and it is the most common gas lift method used in the industry. As the name suggests, in this technique, gas is injected continuously into the flow stream at the designed injection depth. This injected gas creates bubbles that have a "scrubbing" action on the liquid and also, injection gas supplements the associated gas from the reservoir to reduce the density of the fluid column. Both actions act to reduce the flowing bottom hole pressure and improve the well productivity (Cedeno and Ortiz., 2007). When the reservoir pressure declines more in mature fields, the continuous gas-lift technique becomes no longer efficient and when the bottom hole pressure drops to the lowest value; at this point, the well may be converted to intermittent gas-lift (Alahmed and Bordalo, 2017).

The intermittent technique is based on the principle of injection gas at regular time intervals sequentially to the well loading by the reservoir. Although the need for high-pressure gas is periodic in intermittent flow and gives it the advantage over the continuous flow gas lift, intermittent flow is not capable of producing fluid at high volume rates compared to continuous flow gas lift. The process of intermittent gas lift starts by allowing the specified amount of formation fluid to build up in the tubing string at the bottom of the well. When the height of the liquid reaches a desired value at the gas-lift valve depth, high-pressure gas is injected at a specific high rate through the gas lift valve to push the accumulated liquid up to the surface. The casing pressure decreases, while gas is being injected into the tubing and build-up again when a new liquid column is accumulated in the tubing.

The energy of the flowing and expanding gas rises the liquid upward to the surface in the form of a slug or piston. During this stage, part of the liquid falls back into the gas in the form of droplets and/or liquid film on the pipe wall. The liquid fallback is due to the higher apparent velocity of the injection gas than the liquid slug velocity. When the liquid slug reaches the well head and starts to produce, more gas is injected into the tubing string through the gas lift valve as a result of the high-pressure difference between the tubing and the casing. The valve is then closed and the injection gas stop flowing when the casing pressure drops to the conditions of the valve closing pressure. A stabilization time occurs after the slug has

been produced, and the liquid fall back from the previous cycle flows down to the bottom of the well, and becomes a part of the next cycle (Brill et al., 1967).

Intermittent gas lift systems have different configurations including conventional intermittent systems, configurations that introduce plungers to reduce the fluid fallback, and chamber lift systems to increase the initial accumulated liquid volume. Despite their apparent configuration differences, the fundamental principles for each of these intermittent gas lift operations remain the same. In the subject area, to maximize fluid production over the well-expected production life, the well is first allowed to flow up naturally. As the well pressure depletes, it is placed to continuous flow gas lift. With further depletion, the well is finally converted to intermittent gas lift. In certain cases, plungers may be utilized to further enhance lift efficiency by limiting slippage and reducing fluid fallback. Later in the well life, the well can be converted to a chamber and produced with this method until abandonment (Sami N.A., Turzo Z., 2021).

A pilot valve is an ideal valve for intermittent lift, which provides greater port diameters required for high injection gas flow rates and, at the same time, allows the selection of the right valve spread. The pilot valve contains two parts: a pilot and the main section. The upper part (pilot section) usually a bellows charged unbalanced valve with or without a spring, controls the opening and closing pressures of the valve. The lower part (power or main section) allows a very high instantaneous injection gas flow to the production tubing. To design an efficient intermittent gas lift system, reliable information on the performance of all the installation components is needed. The gas lift valve is one of the critical components since it is acting as a pressure regulator and controls the injection gas flow rate for lifting the cumulated oil to the surface through tubing (Sarvestani et al., 2019). The performance curve of gas lift valves describes the effects of injection and production pressures on the gas flow rate. Pilot valves exhibit only orifice flow because the injection gas flows through the power section either fully opens or closes as soon as the upper part opens or closes and cannot take intermittent positions (Hernandez, 2013).

The gas passage characteristics and the performance curve of the gas lift valve are essential for any intermittent gas lift system including the pilot valve as a gas injection component. For many years, the Thornhill-Craver equation has been used to calculate the flow rate through the gas lift valve. This model was originally developed in 1964 to predict the gas flow rate through a choke. There is a lack of research regarding the pilot valve and a poor understanding of the physical description of compressible flow behavior within it.

Calculating tubing pressure at the operating intermittent gas lift valve are the most important parameters in determining the mass flow rate of injection gas as well as calculating the oil production rate per cycle. Tubing pressure is the connection parameter that combines casing annuls behavior with the tubing string behavior. These pressures, in such complex multiphase flow, are the most difficult variables to be calculated, many parameters and assumptions are required. The tubing space beneath the liquid slug which affects the tubing pressure calculations contains three separate fluid sources, gas from the casing annulus, liquid from the reservoir formation, and liquid fallback from the slug as droplets or wetting film on the wall (Brill et al., 1967). The tubing pressure calculation procedure at the operating valve is the combining values of the pressure in different regions consisting of the gas-liquid interface, gas column under liquid slug, and the pressure of the falling-back liquid (Ayatollahi et al., 2004).

1.2. Intermittent gas lift research problem

Intermittent gas lift is a complex system due to the unsteady state nature of the flow, the high number of parameters involved in the process, the interfacial instabilities between the gas and the liquid phases, the various kinds of acting forces in the system all contribute to increasing the complexity of intermittent lift process. There is no tangible effort in the open literature to study and predict the essential parameters of the intermittent process. For proper design of an efficient intermittent gas lift process, a complete description of transient flow in the intermittent process is required and the relationships between different interaction parameters involved in the system should be defined. Although the gas lift valve is the heart of any lift process, still the industry is based on the empirical correlations which have been proven to predict the gas flow rate through the injection valve with error (Hernandez 2013).

1.3. Thesis Contribution

The contribution to research is the development of a CFD model to study the liquid production rate with different injection conditions. This model is a novel model to physically describe the transient flow in intermittent lift and predict the interaction between intermittent parameters during the gas injection time.

The pilot valve, discharge coefficient correlation is developed in this study to calculate the actual gas flow rate through a 1-inch pilot valve in the petroleum industry. This correlation efficiently corrects the gas rate from the theoretical to actual flow because it is based on the numerical model that considers the change in the velocity, temperature, and pressure gradient around the valve piston.

Finally, the machine learning model developed in this research based on the field data can be used to predict the tubing pressure at the gas injection depth.

1.4. Thesis Objectives

Intermittent gas lift is considered a complex process and contains many interaction parameters that required trial and error procedures to find the best and optimum operation conditions that are good case by case. The work on the intermittent gas lift should be proceeded to find a good computer model which can accurately describe the whole intermittent cycle and the effects of interaction parameters on the system efficiency. The main objectives of this research are:

1- To construct a numerical simulation model using CFD that investigates the effect of injection time on the liquid production rate and calculates the velocity and pressure profile of the slug flow in an intermittent process.
2- Carry out a dimensionless analysis model to reduce the complexity of the system and the required computational time.
3- To develop a CFD simulation procedure for the pilot valve, based on conditions similar to those found in the industry. This procedure is used to propose a numerical correlation equation of the discharge coefficient of a 1-inch pilot valve.
4- To build an artificial machine learning model using different algorithms to predict the tubing pressure at the gas injection depth.

1.5. Thesis Structure

1. Introduction

It gives a general insight into the intermittent gas lift method, and the surrounding issues associated with this method. The chapter then highlights the main objectives of this research.

2. Literature survey

This chapter describes the intermittent gas lift process and the literature survey associated with it as well as the literature on intermittent gas lift flow, the flow parameters, and the appropriate gas lift valves.

3. CFD modeling for intermittent gas lift flow

This chapter introduces ANSYS Fluent computational fluid dynamics modeling and the applications of CFD simulation in a vertical column for two-phase fluid flow. A detailed description of the concept of the three-dimensional Fluent-VOF model setup which was used to simulate the gas-liquid flow in a vertical intermittent gas well as well as the geometry structures and the boundary conditions are also presented.

4. CFD modeling for pilot operated gas lift valve

This chapter introduces the Ansys CFX simulation for modeling the gas flow through the gas lift valve and the procedure that was followed to develop a correlation for the discharge coefficient of the 1-inch pilot valve. This chapter briefly describes the geometry, mesh, and operational conditions used to study the gas passages through the pilot valve.

5. Machine learning algorithms for predicting tubing pressure.

This chapter presents the preprocessing steps that were followed to prepare the data for machine learning models. This chapter also explains different machine learning algorithms that were used to predict the tubing pressure at the gas injection depth.

6. CFD Numerical Results, Analysis and Discussion.

This chapter presents the numerical simulation results, analysis, and discussions of the upward two-phase flow behaviors in a vertical pipe related to the intermittent gas process. This includes the different variables that influence the liquid production rate. Also, the single-phase flow of the injected gas through the pilot gas lift valve is presented.

7. Conclusions and Recommendation

This chapter shortly summarize the main conclusions can be drawn based on the result of the research shown in this thesis and pointing on further research possibilities.

8. New Scientific Achievements

This chapter shows the new scientific achievements of the research work presented in this thesis.

2. LITERATURE SURVEY

2.1. Introduction

In the long term, the ability of reservoirs to naturally produce oil will decrease as a function of time and the energy of the reservoir will not be enough to sustain the flow of oil in the well up to the surface. This will affect the bottom hole pressure and the capability to transport oil, therefore the production of oil will decrease. Artificial lift methods have been used widely in the petroleum industry to maintain or supplement oil reservoir energy. Several artificial lift methods are used in the industry to enhance the oil well productivity such as hydraulic pump, sucker rod pump, electrical submersible pump, and gas lift methods. Artificial gas lift is one method which is widely used in the oil industry to enhance the well productivity. There are several crucial requirements that petroleum engineers must be aware of to make the gas lift system successfully designed and efficiently functional. The availability of a gas source in the oil field is essential to provide the injected gas to the well. Moreover, a single point of the gas injection in well completion should be considered in the design of the gas lift. Finally, understanding the well unloading process and multi-phase flow behaviors in the vertical production string must be paid attention to ensure the stability of the gas lift process. (Forero et al., 1993).

2.2. Gas Lift Concept

Gas lift is one of the most common artificial lift methods used in the oil industry. Gas lift is often an ideal selection of artificial lift, if gas is readily available, either as a dissolved gas in the produced oil or from an outside gas source. The gas lift process is bearing a resemblance to the natural flow process of a well. In a naturally flowing well, the pressure in the fluid column is reduced as the fluid travels upwards, so the gas is expanding and it moves upwards faster, as shown in Figure 2.1 (A). On the other hand, gas lift is an extension of the natural flow, in this process, additional gas from external sources is injected to improve fluid production by increasing the gas-liquid ratio (GLR) as shown in Figure 2.1 (B).

The gas lift system has surface and subsurface equipment. The surface facilities consist of a natural gas source either external source or internal source associated with the produced crude oil from the well and separated by a separator, then dehydration unit or filters are used to dehydrate the gas and then compress it in the compressor station to a certain pressure based on the required injection pressure. Finally, the gas can be distributed through a gas injection manifold to the wellheads as shown in Figure 2.2.

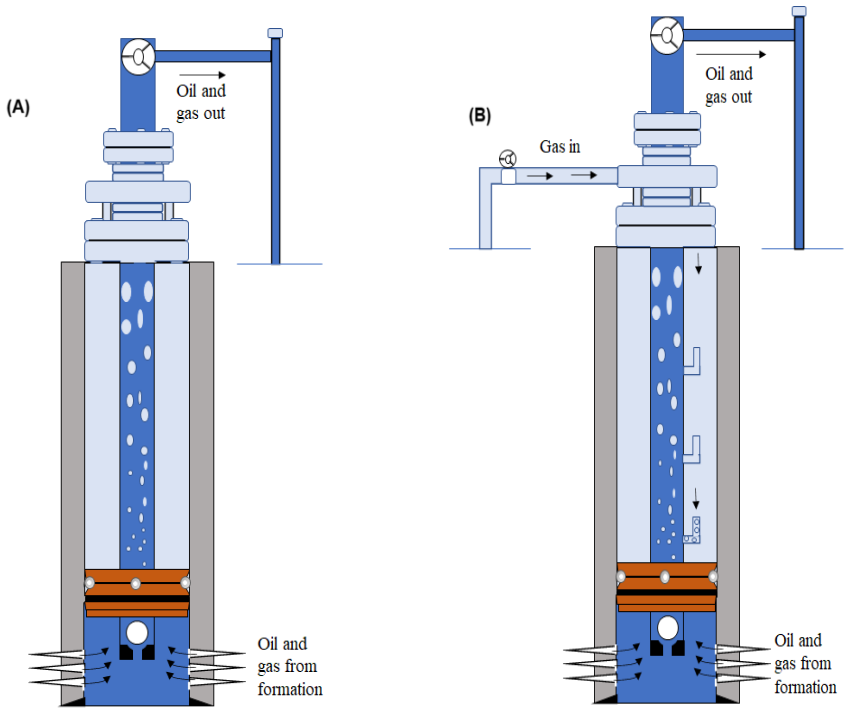

Natural flow/ Fluid column weight reduce by formation gas.

Gas lift flow/ Fluid column weight reduce by formation and injected gas.

Figure 2.1 Natural flow vs. gas lift flow (edited by the Author)

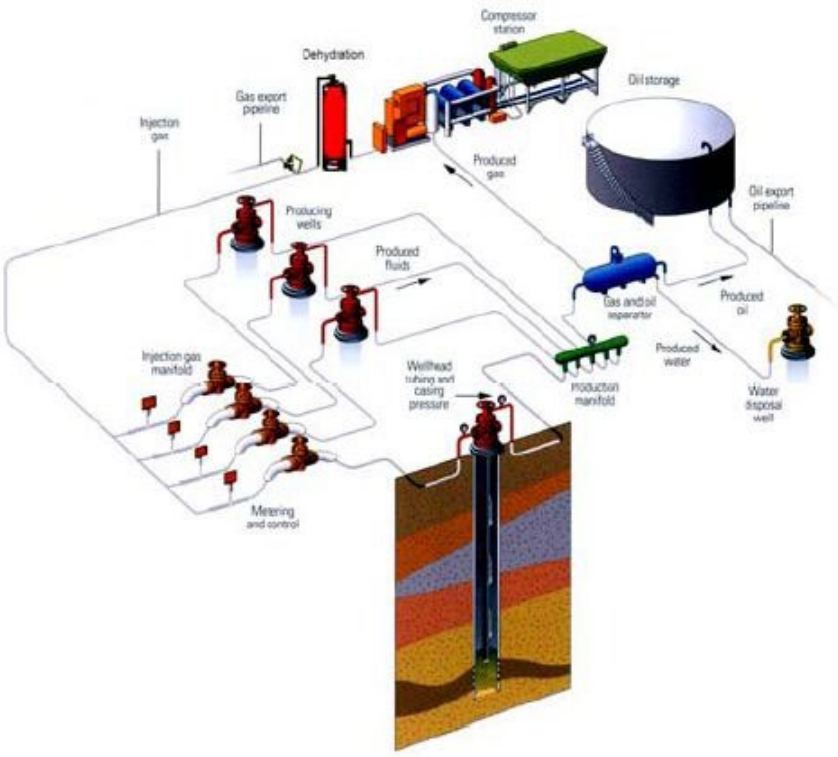

Figure 2.2 Gas lift system (Schlumberger, 1999)

Gas lift is very popular artificial lift method due to its many advantages features, the modest costs required for installation of downhole equipment and a flexible gas lift system using side pocket mandrels (SPMs) compared with the other artificial lift systems. Gas lift installations are more flexible than other mechanical lift methods. It can very easily be modified to be used in case of extremely great changes in liquid production rate. It is more tolerant to produced gas than other mechanical pumping methods. Elevated gas-liquid ratios (GLRs) usually improve the effectiveness of the gas lift method, whereas high GLRs have been found to cause problems, increase the failure frequency, and limit the drawdown achieved by mechanical lift systems (Sami and Turzo 2021).

2.3. Well Unloading

In all gas lift installations regardless of their configuration, completion fluids must be displaced from the injection string into the production conduit to enable injection gas to proceed. Therefore, multiple gas injection points are required to unload deep wells. Initially, all gas lift valves are opened and the pressure gradient in the tubing and in the annulus is the same as that of the static fluid column. The injection pressure drops in the casing as the amount of the gas passed through the valve relatively increase to the amount of the gas injected at the surface, which in turn allows the upper valve to close and the lower valve starts to unload the well and so forth, causing a single operation gas injection point. Figure 2.3 (A) shows all valves are open because of the high pressure of the kill fluid acting on them. There is no fluid production that occurs in the well due to the high pressure exerted on the well bottom. In Figure 2.3 (B), the pressure of the injection gas continuously depresses the liquid level in the annulus until the first valve (valve 1) starts to inject gas into the tubing string and invades the liquid column above the valve. In Figure 2.3 gas injection through the first valve continuously decreases the tubing and annulus pressure to a stabilized value. The annulus liquid level drops as well until the gas injection starts in valve 2. In Figure 2.3 (D), valve 1 will close as soon as the gas injection has begun through valve 2 to ensure a single injection point. In part (E) of Figure 2.3, gas injection through valve 2 decreases tubing pressure, and the liquid level in the annulus drops further until the gas starts to inject through valve 3. In Figure 2.3 (F), valve 2 will close and the objectives of the unloading process have been reached by gas injection through a single operating point. During the unloading process, at a certain point, flowing bottomhole pressure drops below the formation pressure, and liquid production from the formation to the well starts **(**API Gas lift manual, 1994**).** If the well has poor inflow performance and continuous gas injection is not economic to continuous production, intermittent gas lift is preferred for this case.

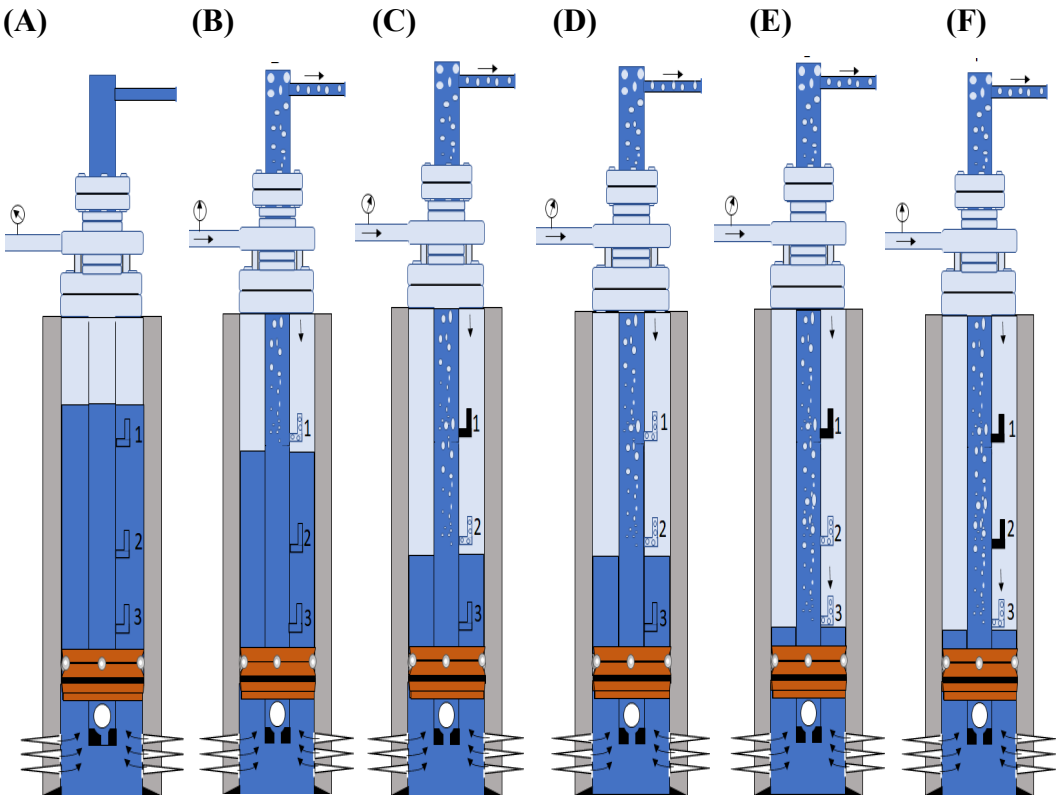

Figure 2.3 Unloading process for continuous flow gas lift installation (edited by the Author)

2.4. Types of gas lift systems used in the petroleum industry

There are two types of gas lift systems used in the petroleum industry, continuous flow, and intermittent flow. The procedure of gas lift is similar in both systems as high-pressure natural gas is injected from the surface to lift formation fluid upward, but the operation principle is completely different.

Continuous flow gas lift system

Continuous flow gas lift is very similar to the natural flow, and it is the most common gas lift method used in the industry. As the name suggests, in this technique, gas is injected continuously into the flow stream at the designed depth, usually from the casing-tubing annulus to the production pipe (Deng et al., 2019). The injected gas creates bubbles that have a "scrubbing" action on the liquids also, injection gas supplements the associated gas from the reservoir to reduce the density of the fluid column as shown in Figure 2.4. Both actions act to lower the flowing bottomhole pressure and increase the inflow from the reservoir. The flowing bottom hole pressure available will now become sufficient to move the formation fluids to the well surface. Therefore, the dead well will start to produce again with all other operating conditions remaining unchanged due to the continuous injection of lift gas from

an outside source. The basic mechanism of continuous flow gas lift is: when the liquid density decreases, the tubing pressure decreases and drop the bottom hole pressure to the point that allow the reservoir pressure to move the fluid to the surface. This mechanism ensures that the produced formation gas of the well can be fully utilized for fluid lifting. The continuous flow gas lifting process can be considered the sole type of artificial lift method that completely uses the formation's natural energy stored in the form of dissolved gas (Latif et al., 2018).

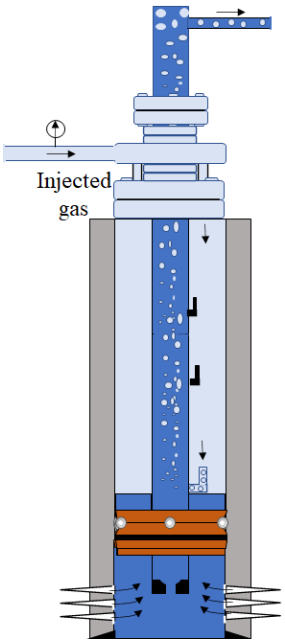

Figure 2.4 Continuous flow gas lift process (edited by the Author)

Advantages of continuous flow gas lifting:

- can produce high to extremely high liquid rates from any depth,
- successfully usable in wells with sand face due to relatively constant bottom hole pressure (open hole completion),
- the viscosity of highly viscous oils can be kept low,
- in contrast to other artificial lift methods, continuous flow gas lifting can fully utilize the available energy of the formation gas,
- flexible operation, according to its application with a wide variety of well conditions,
- controlling the gas injection at the surface is simple.

Limitations of continuous flow gas lifting:

- a sufficiently high flowing bottom hole pressure is required to lift the multiphase fluid mixture (the formation fluid and injection gas) to the surface,
- cannot be used at a very low bottom hole pressure close to the well abandonment whereas intermittent gas lift can be used in this case.

Intermittent gas lift system

When reservoir pressure declines in mature fields, and the continuous gas-lift technique becomes no longer efficient or not profitable when the bottomhole pressure drops to a certain value, at this point the well may be converted to intermittent gas-lift. It is also applied for wells with relatively high formation pressures but low productivities. Intermittent gas lift is a cyclic process that has been used widely in the petroleum industry for many years. (Sami and Turzo 2020).

The process of intermittent gas lift starts by allowing the specified amount of formation fluid to build up in the tubing string at the bottom of the well (Figure 2.5 (A)). When the height of the liquid reaches a desired value above the gas-lift valve depth, high-pressure gas is injected very quickly through the gas lift valve to push the accumulated liquid up to the surface (Figure 2.5 (B)). The energy of the flowing and expanding gas raises the liquid upward to the surface in the form of a slug or piston. During this stage, part of the liquid falls back into the gas in the form of droplets and/or liquid film on the pipe wall (Figure 2.5 (C)). The liquid fallback is due to the higher apparent velocity of the injection gas than the liquid slug velocity. When the liquid slug reaches the well head and starts to produce, more gas is injected into the tubing string through the gas lift valve as a result of the high-pressure difference between the tubing and the casing. The valve then closes and the injection gas stops flowing when the casing pressure drops to the valve closing pressure (Figure 2.5 (D)). A stabilization time occurs after the slug has been produced, and the liquid falls back from the previous cycle to the bottom of the well and becomes a part of the next cycle (Brill et al., 1967). Although the need for high-pressure gas is periodic in intermittent flow and gives it the advantage over the continuous flow gas lift, intermittent flow is not capable of producing fluid at high volume rates as continuous flow gas lift. Intermittent gas lift systems could have different configurations, systems that introduce plungers to reduce fluid fallback, and chamber lift systems to increase the initial slug volume by including a volumetric chamber-sized that allow more volume of the liquid to be accumulated in the well. Despite their apparent configuration differences, the fundamental principles for each of these intermittent gas lift system operations remain the same.

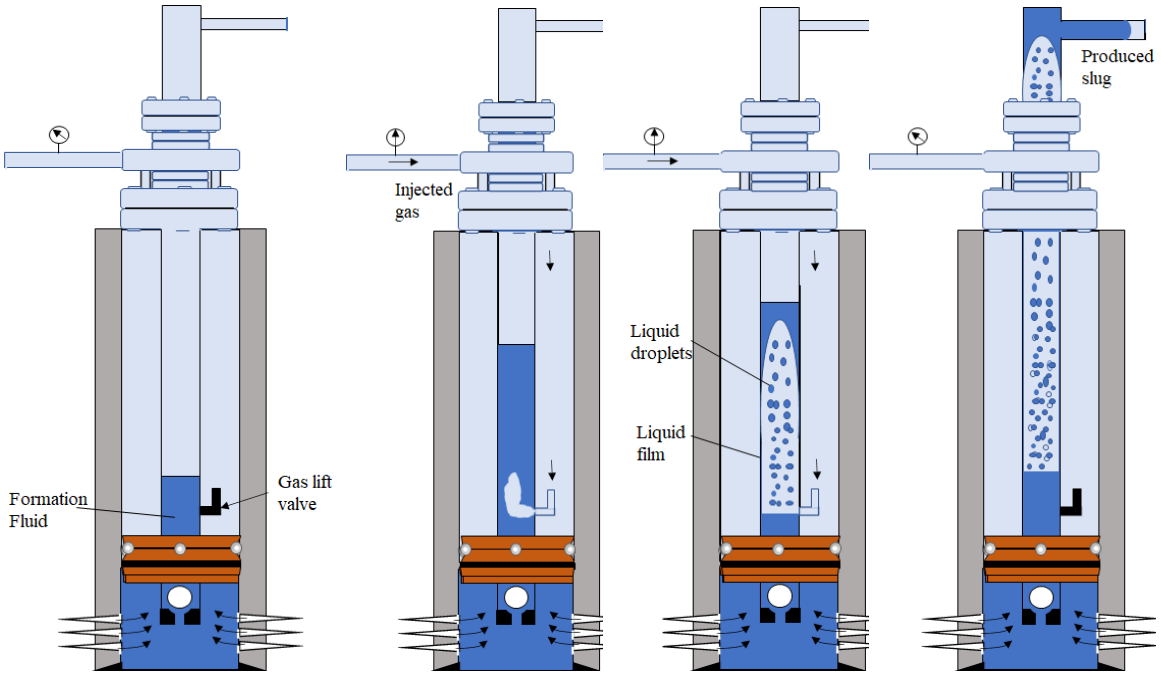

(A) Buildup of liquid slug (B) Gas is injected (C) Liquid fall back (D) Slug production

Figure 2.5 Intermittent gas lift cycle. (edited by the Author)

Advantages of intermittent gas lifting:

- relatively flexible to the changes in well inflow parameters,
- it can be used until the well's abandonment in some cases by changing the installation type from the conventional to the chamber installation,
- effectively lower costs than pumping applications.

Limitations of intermittent gas lifting:

- the energy of formation gas is not utilized for fluid lifting,
- limited liquid production rates,
- sand production problems due to high fluctuations in the flowing bottomhole pressure,
- possible overload of a rotative gas lift system due to high instantaneous gas flow requirements in the intermittent cycle.

2.5. Types of intermittent-flow gas lift installations

There are several types of well completions that can be used for intermittent gas lift wells, each of these methods can be recommended for specific operational conditions. Intermittent gas lift is used for tubing flow only and is not used for annular flow. Most installations will have a packer between the casing and the tubing and a standing valve at the bottom of the tubing. Standing valve is opened during the liquid accumulation period and

closed during the gas injection time. Although most intermittent gas lift wells' installation will show a standing valve, some wells installations with very low productivity index will not have a standing valve at the tubing (Takacs 2007).

2.5.1. Single point gas injection in closed gas lift installation

The basic operation of a single point gas injection in intermittent gas lift wells is illustrated in Figure 2.5. The well has a closed gas lift installation with a standing valve at the bottom of the tubing string. The bottom valve is usually the operating valve and all the above upper valves serve only for unloading. When gas is injected from the surface into the casing-tubing annulus, Lift gas of a relatively high pressure enters the tubing from the bottom valve at a very high flow rate creating a large gas bubble below the liquid slug. All the upper valves remain closed during this type of operation.

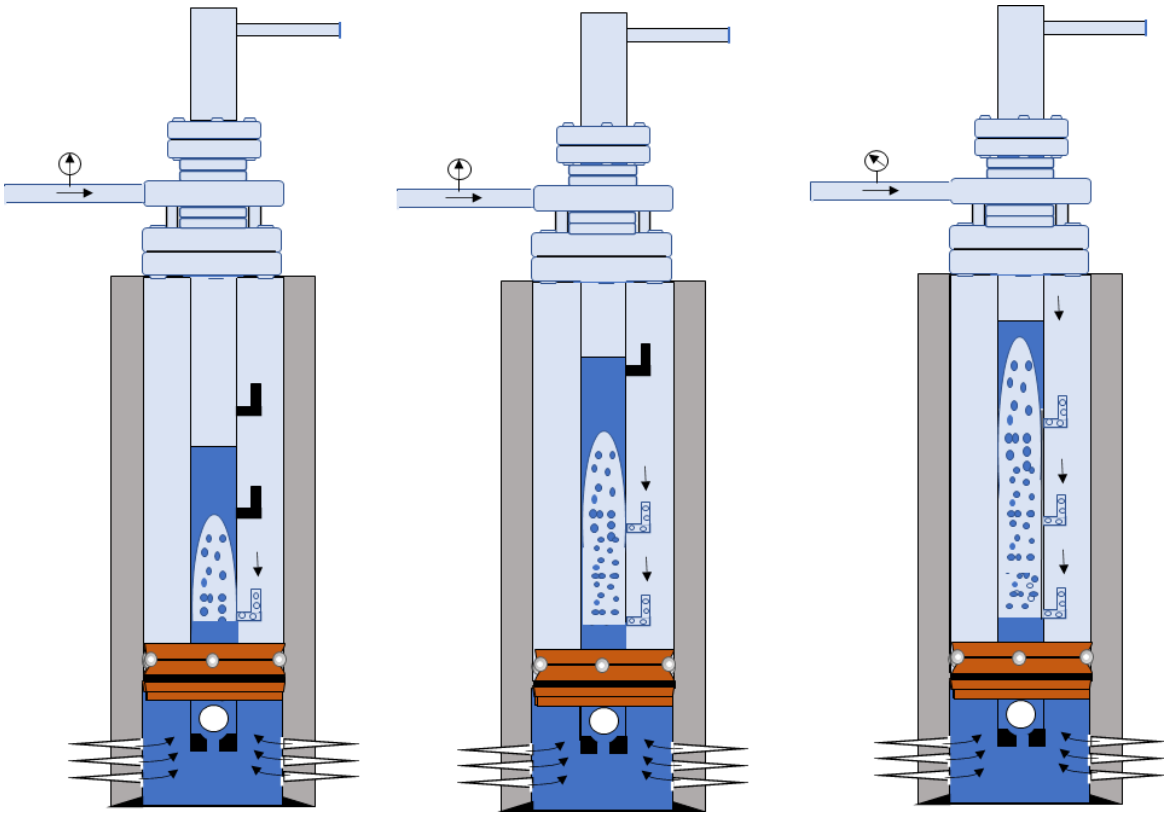

Figure 2.6 Intermittent gas lift with multipoint gas injection (edited by the Author)

2.5.2. Multipoint gas injection in closed gas lift installation

Multi-pointing gas injection is considered if surface injection pressure is low or in deep wells. In multipoint injection installation, the upper valves consecutively open when the liquid slug moves from the bottom of the well up to the surface. Gas is injected below the upwards-rising slug as it passes into the tubing as shown in Figure 2.6. This type of

installation requires the use of production pressure-operated gas lift valves to control the opening and closing pressure of the valves.

2.5.3. Chamber installations

In chamber installations, formation fluids accumulate in special chamber having substantially larger diameters than the tubing. Chamber installations are used in intermittent gas lift wells with low reservoir pressures to increase the volume of the accumulated liquid. If the same height of formation fluids is allowed to accumulate in the tubing and champers, the later will contain much greater liquid volumes than the tubing due to their larger diameter (Gasbarri et al., 1999). During the same accumulation period, the accumulated liquid volume in a chamber installation is greater than in a closed one. Bottomhole pressure is directly proportional to the liquid column height, the pattern of pressure buildup is the same in both the closed and the chamber installations. On the other hand, if the same liquid volume per cycle is allowed to accumulate, the hydrostatic pressure against the reservoir formation will be much lower in a chamber as compared to the tubing, this is due to the higher capacity and lower liquid column height. From the above discussion, chamber installations can highly improve the liquid production rate in intermittent wells with low bottomhole pressures and relatively high productivities (Hardegree et al., 2020). There are two types of chamber installations usually used in the industry, two-packer chamber installation and insert chamber installation as shown in Figure 2.7. The two-packer chamber installation comprises the space between two packers in the casing-tubing annular and the gas is injected at the upper packer from a bypass. In the insert chamber installation, the chamber is constructed from a large pipe section and run through the casing string to the bottom of the tubing with a diameter considerably less than the casing.

2.5.4. Plunger-assisted intermittent gas lift installation

Plunger installation is similar to a conventional intermittent installation with the only difference that there is a special designed plunger in the bottom of the tubing string between the gas and the liquid slug as shown in Figure 2.8. The plunger can improve the production in intermittent wells, especially in the deeper wells (Zhu et al., 2019). The difference in density between the liquid and injected gas makes the injected gas bubble below the liquid slug penetrate the liquid and cause liquid fallback. Liquid fallback is a natural phenomenon that occurs in intermittent wells that cause a reduction in the production rate, and it can also happen that gas penetration consumes the total starting slug length, and no liquid is produced at the wellhead. Plunger installation basically is a closed gas lift installation with a packer and a standing valve set close to the depth of the perforations. Gas is injected from the surface

to the bottom of the tubing string below the special plunger. Then the plunger rises along with the liquid slug and separates it from the injected gas to prevent an excessive amount of fallback to occur. The plunger falls to the bottom of the tubing after the slug reaches the wellhead, and the pressure in the tubing string is bled down (Bello et al., 2011).

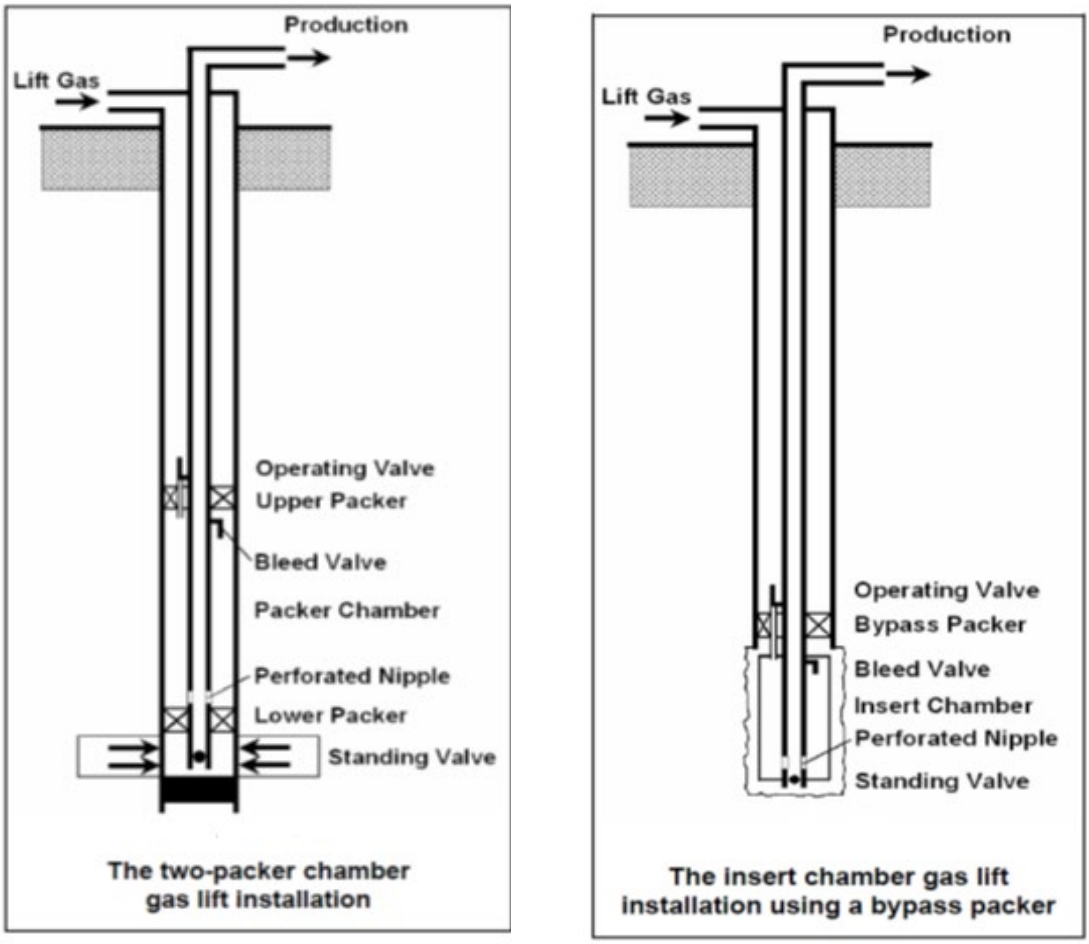

Figure 2.7 Chamber gas lift instillation (Takacs, 2007)

2.6. Multiphase flow in intermittent wells

Examination of the multiphase flow during the process of liquid slug rising in the tubing string reveals the researcher interesting. However, the unsteady nature of the intermittent process, the high number of parameters involved, the interfacial instabilities, and the different kinds of acting forces in the system restrict the development of an accurate and successful model to describe the whole intermittent cycle (Liao et al., 1995). Also, from the open literature, it can be seen, that the research and publications on intermittent gas lift, up to now are still less compared to another field. Some of the researchers studied intermittent gas lift systems using field test wells and operation conditions like real wells. Based on the

experimental results, they examined the effect of different parameters on the efficiency of the intermittent process. Also, analytical, and empirical correlations have been developed to study the entire process of slug flow based on the experimental results. Brown and Jessen carried out experiments on an instrumented well with 800 ft length, equipped with 2 in. tubing. They proposed a method of calculating the average bottomhole pressure and the time required for pressure stabilization for a gas-lift cycle (Brown and Jessen, 1962). Beadle et al. studied the effect of surface back-pressure on the continuous and intermittent flow. The results from the experiments of the field well tests showed that the average bottom hole pressure in intermittent cycle increase considerably as the surface choke size is decreased (Beadle et al., 1963). Neely et al. carried out a series of experiments in an instrumented conventional intermittent well, the results established empirical rules for the setting of the operational parameters (Neely et al.,1974). Hernandez et al. conducted experiments on intermittent gas lift wells to study the effect of liquid column length, injection pressure, crude API, formation gas-liquid ratio, and gas flow rate injected per cycle on the liquid fallback (Hernandez et al., 1999).

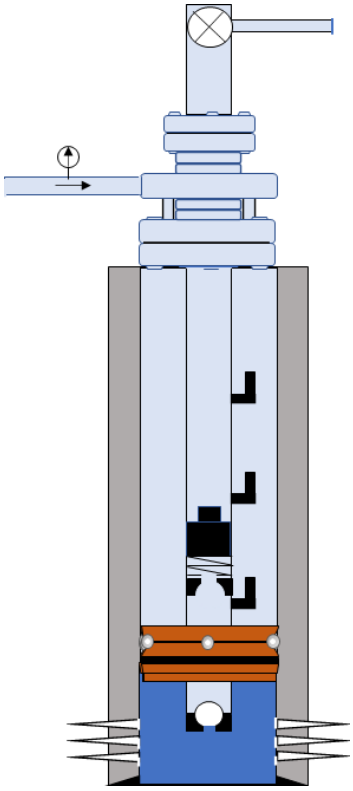

Figure 2.8 Plunger assisted intermittent gas lift. (edited by the Author)

Since the experimental work on a large scale that can represent the integrated intermittent gas lift production system is costly and complicated, some researchers tried to describe and determine the impact of different parameters on intermittent gas lift using laboratory-scale experiments. White et al. used dimensional analysis to model intermittent gas lift flow and compared the experimental results with the conceptual developed model. The proposed mathematical model was simplified by assuming that the liquid slug velocity reaches a constant value and the penetration of the gas bubble into the liquid slug is constant (White, et al.,1963). Brill et al. conducted a wide range of intermittent gas-lift tests in an experimental well to develop an empirical fallback correlation . The proposed correlation was used in a conceptual model of basic fluid flow equations and the model predictions were compared with the test data (Brill, et al., 1967) Schmidt et al. conducted a laboratory experiments to develop a hydrodynamic model for intermittent gas lift flow. The model was verified by the experiment results to study the slug velocity profile and the effect of gas injection pressure and gas injection time on the production rate (Schmidt et al., 1984). Sandoval et al. predicted the two-phase formation fluid flow behavior during the liquid accumulation period based on laboratory experiments tests (Sandoval et al., 2005). Alahmed and Bordalo conducted experiments to study the factors that influence the intermittent flow such as: gas lift valve port size, valve closing pressure, valve opening pressure, tubing diameter and injection gas amount per cycle (Alahmed and Bordalo, 2017). Other researchers developed computer programs based on mathematical models. Solesa et al. proposed a mathematical model to describe the hydrodynamic flow of intermittent gas lift. This model synthesizes the principle of unsteady state flow in a vertical tube and divided the whole intermittent system into several subsystems for a more accurate results. The results from the model are used to develop a computer program for designing and optimizing intermittent systems (Solesa et al., 1991). Hernandez et al. mathematically analyzed the downhole pressure and temperature data obtained from a combination of static and dynamic downhole surveys. The mathematical model can be used to find the liquid slug length as a function of time and the productivity index (Hernandez et al., 1998).

Some researchers developed a numerical model to study intermittent flow. Caicedo proposed new inflow performance relation (IPR) method for intermittent wells. He developed equations that related the inflow performance equation of Vogel's with field data and introduced a numerical method to solve these equations (Caicedo, 2001). Cheung and Gasbarri presented a numerical method to compute the liquid column height of the multiphase fluid accumulated in intermittent gas lift wells. Two pressure drop correlations

were modified to determine liquid column length: Hagendorn and Brown's, and a combination of Aziz's and Wallis'. Experimental data obtained from twelve wells were used to test these programmed correlations (Cheung and Gasbarri, 2002). Cedeno and Ortiz developed a computerized system called SOLAG to optimize the required gas injection rate for distribution intermittent system that help to manage thousands of wells with different production performance characteristics (Cedeno and Ortiz, 2007). Table A.1 (in Appendix A) summarizes most of the investigations on conventional intermittent gas lift.

Liao et al. developed a mechanistic model showed the potential to describe the multiphase flow in an intermittent system based on the fundamentals of physical principles. The intermittent gas-lift process is divided into four stages in the mechanistic model since the process involved in each stage change significantly. In each stage, the mass and momentum conservation equations are applied for each system component to obtain the model. The system components for each stage and the associated parameters used in the mechanistic model are as below (Liao et al., 1995):

Stage 1- Liquid Slug Rising in the Tubing:

This stage begins when the liquid slug moves upward to the surface and lasts until the top of the slug reaches the surface. In this stage, gas is injected through the gas injection choke into the tubing-casing annulus. Gas flow into the tubing through the gas-lift valve and the accumulated liquid starts rising upward. Some of the liquid slugs form a film on the tubing wall while moving to the surface. The physical system consists of a surface choke, tubing-casing annulus, gas-lift valve, gas slug, liquid slug, and the liquid fallback as film and droplets. The variables of the system include the mass flow rate of injected gas through the gas-lift valve into the tubing, position, pressure, and velocity of the gas slug, liquid fallback as a film thickness and droplet, position of the top of the liquid slug, velocity of the liquid slug and the amount of formation liquid that flows into the tubing from the reservoir.

Stage II - Liquid Slug Production at the Surface:

This stage begins when the top of the liquid slug reaches the surface and lasts until the tail of the slug reaches the well head. Due to slug shortening during the production period, the velocity of the slug increases, and the pressure of the gas column below it decreases. The injection gas through the valve will increase if it does not reach the critical flow rate. All the system variables for stage I are still valid for stage two except the top of the liquid slug is no longer a variable and is dropped out of the model system.

Stage III - Liquid Production by Entrainment:

This stage begins when the tail of the slug leaves the wellhead, and the liquid slug in the tubing no longer exists. During the bleeding period, if the gas velocity is high enough, the liquid droplets are extracted, and the phenomenon of liquid transfer will continue. Vanishing liquid slug results in an increase in the gas velocity in the gas slug due to a decrease of pressure the gas flow. Some of the liquid in the liquid film was wiped away and entrained in the gas core by the rapidly expanding gas. This entrained liquid in the gas core is produced at the surface. This stage of the entrainment production process is complicated and consequently, very difficult to model. The mass transfer must be considered between the entrained liquid and gas core. Partial differential equations are developed for modeling the liquid entrainment in the gas core and the liquid film on the tubing wall using the gas pressure, velocity, and density. Then, these gas variables are added to those variables of the liquid film to form a closed system for the model.

Stage IV: Liquid Slug Regeneration:

In this stage, the gas energy in the tubing no longer supports the gas flow with the entrained liquid. The gas flow ceases when the gas blow-down continues in the stage of liquid production by entrainment. The liquid in the film and the entrained liquid in the gas bubble fall back to join the formation liquid inflow from the reservoir to generate a new liquid column for the next intermittent cycle. The gas-lift valve opens, and the system begins a new intermittent cycle when the liquid column and the casing pressure reach specific required values.

From the previous literature studies, one can conclude that the results obtained from the experiments under specific conditions cannot be applied to another well under different operating conditions. Also, the intermittent gas lift model is complex and included overlapping parameters and many assumptions that decrease the accuracy of the calculations.

2.7. Tubing pressure at Intermittent gas injection depth

Tubing pressure at the operating gas lift valve is the most important parameter for calculating the amount of the injected gas into the tubing string as the gas passing through the gas-lift valve. They serve as the link for combining the annuls behavior with the tubing behavior. As might be expected, tubing pressures are the most difficult parameters to be determined, and the calculations procedure requires a large number of input data and assumptions. The tubing space beneath the liquid slug which affects the tubing pressure calculations during intermittent gas lift contains three separate fluid sources, gas from the

casing annulus, liquid from the reservoir formation, and liquid fallback from the slug as droplets or wetting film on the wall. The pressures in the tubing string due to entrained liquid can be assumed as a static liquid slug located at the operating valve. Also, the contribution of the pressure due to the injected gas slug below the liquid slug to the tubing pressure at the gas lift valve can be calculated by assuming a static gas column (Brill et al, 1967).

Neely at al. proposed an equation to calculate the tubing pressure during an intermittent gas lift with many assumptions. The authors neglect the friction below the liquid slug and the length of the liquid film along with the gas core (Neely et al., 1974).

Liao et al. developed a mechanistic model to predict the intermittent gas lift parameters including the tubing pressure at the gas lift valve (Liao et al 1995). The intermittent process was divided into four stages and a system of ordinary and partial differential equations was used to build the mathematical model for each of the four stages. The resulting system of equations is numerically solved. The mechanistic model was able to determine the tubing pressure at the gas lift valve during the intermittent gas lift. The model is validated using experimental data from Brill (Brill et al., 1967).

The tubing pressure calculation procedure at the operating valve is the combining values of the pressure in different regions consisting of the gas-liquid interface, the gas column under the liquid slug, and the pressure of the falling-back liquid. Ayatollahi et al. developed a new intermittent gas lift (IGL) simulator considering all aspects of the intermittent gas lift method including the temperature differences between the injected gas and the produced liquids to predict the tubing pressure at gas injection depth. The result of the simulator was compared with the experimental result from open literature. The mathematical model developed in this study showed that ignoring the heat transfer between the injected gas and the liquid slug when calculating the pressure gradient in the tubing string below the liquid slug shifts away from the model results from the experimental points and therefore, decreases the accuracy of the model (Ayatollahi et al., 2004).

Pestana et al. built a mathematical model to predict tubing pressure at gas injection depth. In this model, the intermittent gas lift cycle is divided into five main stages: gas injection from the annulus to tubing, liquid slug rises in the tubing, a liquid produced at the tubing head and enters the production line, the gas leaves the tubing and loading the well by liquid flows from the reservoir into the well. Validating the model using real well data had not been performed in order to prove the accuracy of this simulator. However, the simulator is based on literature models that showed reasonable agreement with some experimental data (Pestana et al., 2013).

It can be concluded from the above discussion that even though many researchers have attempted to study the tubing pressure at the valve depth the results can be inaccurate due to the complexity of the calculations and also it is limited to the specific operating conditions.

2.8. Pilot valve for Intermittent gas lift

In most intermittent lift wells design, gas lift valves are unbalanced, single-element, bellows-charged valves with a large port size. For these valves, time-cycle control of the injection gas at the surface is recommended. These valves may not operate satisfactorily on choke control of the injection gas.

In intermittent lift designs, double-element (bellow-charged with spring) gas lift valve is not recommended because of the higher load rate of the spring-loaded as compared to the bellows-charged gas lift valve with the same bellows and port size.

In an ideal intermittent well design, the operating valve should tend to “snap” open and provide a large port size to inject the gas throughout it so that the liquid slug can be raised in the tubing string efficiently with minimal gas slippage and liquid fallback. There are gas lift valves, so called pilot operated or pilot valve, that have been designed for intermittent gas lift operation. These valves will have a large port for gas passage and designed to operate on either time cycle or choke control of the injection gas. A properly selected pilot-operated gas lift valve will function in most wells on time cycle or choke control (Hernandez, 2013).

A pilot valve is an ideal valve for intermittent lift, the way as pilot valves operate allows its opening and closing pressures to be set at any desired value to select the right valve spread. Valve spread is the difference between a gas lift valve's opening and closing pressures. Spread is a very important parameter in the intermittent lift process since the amount of gas used for one intermittent cycle is directly related to the actual valve spread. The spread of the valve is controlled by the pilot section. At the same time, the instantaneous gas flow rate through the valve is always kept at very high values since, the main section of these valves provide the greater flow area (Hernandez et al., 2001).

The pilot valve contains two parts: a pilot and the main section as shown in Figure 2.9. The pilot section controls the operation of the main section and the cooperation of the two sections provides the required operation results. The upper part (pilot section) usually a bellows charged unbalanced valve with or without a spring, controls the opening and closing pressures of the valve and in turn controls the valve spread. The lower part (power or main section) allows a very high instantaneous injection gas flow to the production tubing. The port diameter of the main section is of constant value for a given valve design. The closing-opening section could be a nitrogen-charged or a spring loaded (Sami and Turzo, 2020).

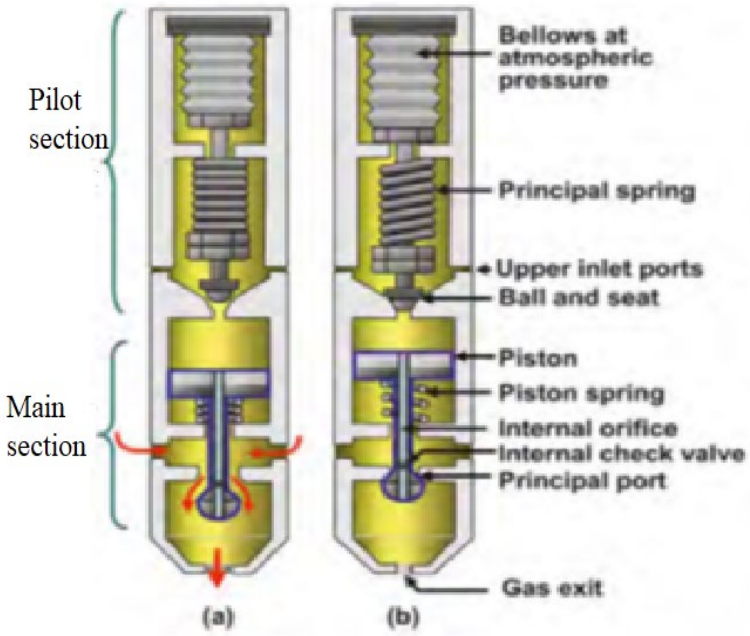

Figure 2.9 Pilot operated gas lift valve (Hernandez, 2013)

2.8.1. Pilot valve mechanism

The most important parts of the pilot section are the bellows, pilot ball, and closing element which could be a nitrogen-charged dome or spring. The production pressure acts on the pilot section by means of a bleed hole located in the main section and allows the tubing pressure to appear in the space below the pilot port. When the forces exerted by injection and production pressure are high enough to overcome the force of the dome charge pressure or the spring, the pilot section opens. The power piston of the lower part is exposed to high pressure that makes it moves down until it opens the power section, allowing the injection gas to move through the main port to the production tube.

During a normal intermittent operation, the piston remains in the lower position as long as the pilot section is opened and when the casing pressure gradually decreases; the closing condition is reached and leads to the close of the pilot section. The pilot section of the valve closes when the gas injection pressure in the casing-tubing annulus drops to the valve's closing pressure. Then the pressure at the pilot side of the piston becomes equal to the production pressure while the pressure at the main section below the piston is almost equal to the injection pressure. The piston moves upwards by the pressure beneath it so, finally, the main section of the pilot valve closes and the gas injection from the annulus to the tubing ceases (Hernandez, 2013).

The valve stem in the pilot section opens or closes the pilot port based on its axial position. The stem position is varying according to the net force on it. At the close position, the force acting by the pressure of the valve dome exerts a downward force (F_d) so, the stem tip is pushed to the port and closes the upper section. The upward force (F_u) acts to open the valve by a combination of injection and production pressures. The upper section opens when the opening forces are greater than the closing force. The pilot section will remain open until the opening force decline and become less than the closing force (Acuna et al., 1992).

The equations for the opening and closing pressures of the pilot section of a valve are the same as those for an unbalanced single-element gas lift valve.

$$F_d = P_d \cdot A_b$$

$$F_u = P_i(A_b - A_v) + P_p \cdot A_v$$

The downward and upward forces are equal when the valve is just about to open:

$$P_d \cdot A_d = P_i(A_b - A_v) + P_p \cdot A_v$$

Where F_d and F_u expressed in N. P_d is the dome charge pressure in Pa. P_i and P_p is the injection and production pressure respectively in Pa. A_b is bellow area and A_v is the port area in m^2. These equations from the balance of the force are accurate in calculating the opening pressure of a pilot section however, not very useful for the closing pressure: nitrogen charged, pilot valves close usually at a closing pressure below the one predicted by mechanic equations. The high gas flow rate through the pilot section cools the nitrogen in the dome and in turn the valve's closing pressure decreases. On the other hand, for the spring-loaded pilot section, the closing pressures are higher than the closing pressure from the mechanic equation. This is due to the effects of instantaneous very high gas flow rates through the main section once it opens. The volume of gas injected per cycle is greatly affected by the changes in the closing pressure, even if these changes seem to be very small (Milano, 1999).

2.8.2. Dynamic performance of gas lift valves

Gas lift valves are used for both well unloading and gas injection operations. A gas lift valve is usually designed to open, reclose, and pass the injection gas in response to changes in either the injection or production pressure. The pressures at which these events occur, and the rate of gas passage are vitally important to the proper unloading and subsequent lifting of a well. The dynamic performance of any gas lift valve is the relation between production pressure and gas flow rate for a given injection pressure and port size (Decker,1986). There are two models that describe the flow through the gas lift valve: orifice and throttling. Orifice flow is similar to gas flow through a fixed choke and is divided into two regions: subcritical

and critical. Subcritical flow is characterized by an increase in flow rate as the production pressure is decreased from a constant injection pressure to the critical production pressure as shown in Figure 2.10.

In the critical flow region, for further reduction in production pressure below the critical production pressure, there is no change in flow rate. The critical production pressure is the pressure at which sonic velocity is achieved at the minimum area of flow. Throttling flow resembles flow through a variable area such as a venturi device and occurs for the injection pressure less than the transition injection pressure. Throttling flow is also divided into two regions by the production pressure belonging to the maximum flow rate Pmax. Subcritical flow is similar to subcritical flow in orifice flow. It is characterized by an initial increase in flow rate as the production pressure reduces from a constant injection pressure. As production pressure is reduced below a maximum value, the injection rate linearly decreases with production pressure until the flow rate ceases at the closing production pressure (Hepguler et al.,1993).

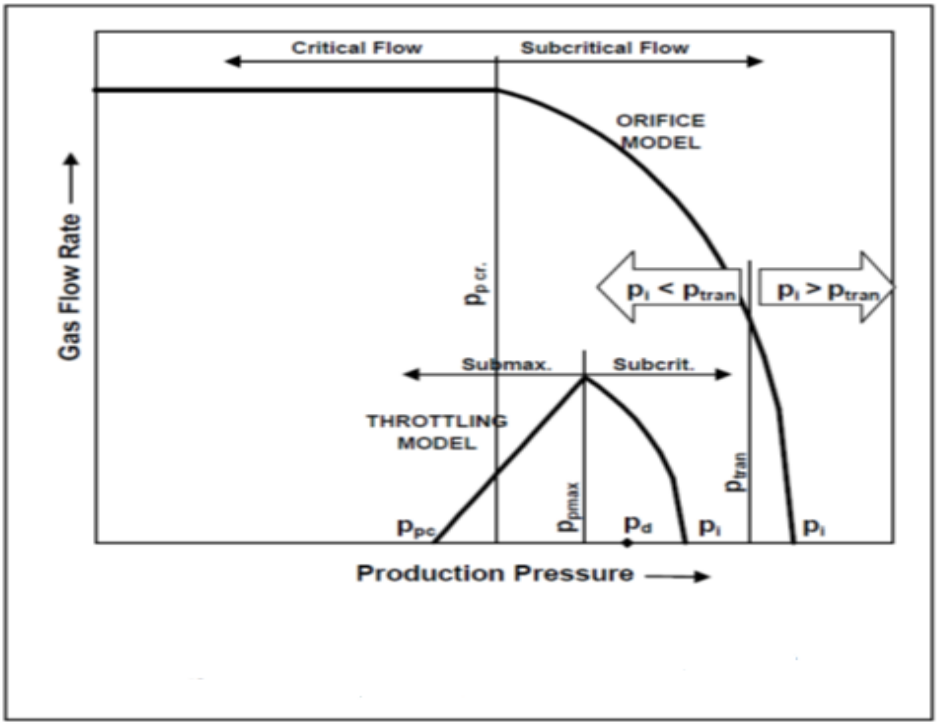

Figure 2.10. Gas lift valve performance curve (Takacs, 2007).

2.8.3. Dynamic performance of pilot valve

To design an efficient intermittent gas lift system, reliable information on the performance of all the installation components is needed. The gas lift valve is one of the critical components since it is acting as a pressure regulator and control the injection gas

flow rate for lifting the cumulated oil to the surface through the tubing string. Pilot valve exhibit only orifice flow because the injection gas flows through the power section is either fully open or closes as soon as the upper part opens or closes and cannot take intermittent positions (Hernandez et al., 2001). The performance curve of orifice flow shows two flow regions: critical and subcritical, as shown in Figure 2.11. For subcritical flow, the gas flow rate through the valve increases as the production pressure decreases while the injection pressure is held constant. Eventually, the critical flow occurs; the gas flow rate remains constant despite further decreases in the production pressure. The production pressure that separates the subcritical and critical regions is called critical production pressure. The critical production pressure depends on the injection pressure and the injection gas properties and can be calculated from the following equations:

$$P_{pcr} = c \cdot P_i$$

$$c = \left(\frac{2}{k+1}\right)^{\frac{k}{k-1}}$$

Where, P_{pcr} is the critical production pressure in Pa, k is the ratio of specific heats of the flowing gas what is unitless. c is so called critical pressure ratio, it is unitless.

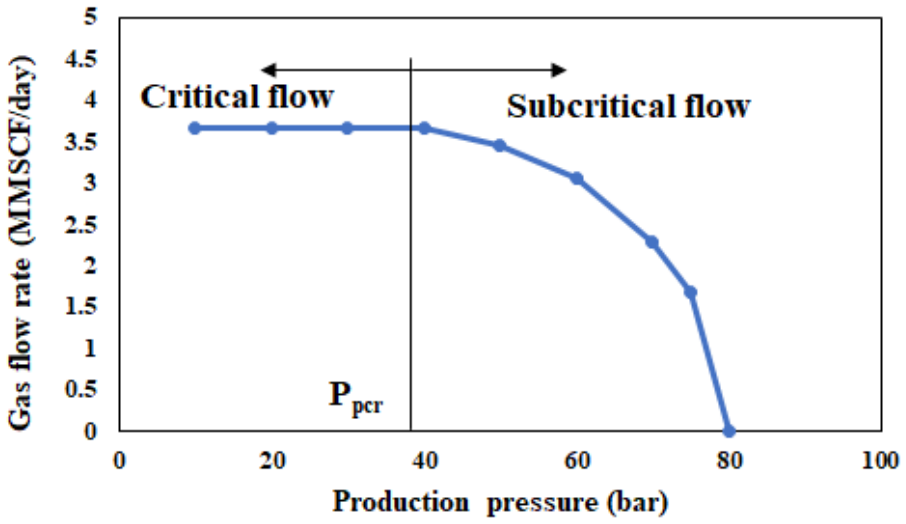

Figure 2.11. Pilot valve performance curve. (edited by the Author)

The gas passage characteristics and the performance curve of the gas lift valve are essential for any intermittent gas lift system including the pilot valve as a gas injection component. For many years, the Thornhill-Craver equation is used to calculate the flow rate through the gas lift valve. This model was originally developed in 1946 to predict the gas

flow rate through a choke with diameters ranging from 1/8-inch to 3/4-inch. For over thirty years, Thornhill-Craver model is used in the petroleum industry to predict orifice flow in gas-lift valves (Bertovic et al., 1997). The gas flow rate through chokes and restrictions is one of the interesting topics of many researchers. The numerical equations that are used to predict the flow rate through the restriction have passed through many stages of development. Thornhill-Craver model is based on the gas flow across restriction as shown in Figure 2.12.

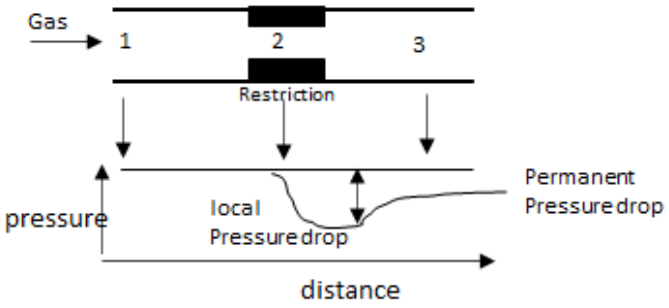

Figure 2.12 Gas flow through a restriction (Hernandez, 2013).

The equations that describe the gas flow rate in restriction had been derived from the basic equation of energy balance for compressible, adiabatic flow as below:

$$\frac{P_1}{\rho_1} + \frac{{v_{g1}}^2}{2} + u_{g1} = \frac{P_2}{\rho_2} + \frac{{v_{g2}}^2}{2} + u_{g2}$$

Where P is the pressure in Pa, ρ is the density of the gas in kg/m^3, v_g is the gas velocity in m/s and u_g is the internal energy of gas for unit mass in J. Subscripts "1" and "2" correspond to the positions "1" and "2" shown in Figure 2.12.

The final form of Thornhill-Craver equation is:

$$Q_{sc} = \frac{155.5 C_d \cdot A_v \cdot P_i \cdot \sqrt{2g\frac{k}{k-1}\cdot(r^{\frac{2}{k}} - r^{\frac{k+1}{k}})}}{\sqrt{T_v \cdot z_v \cdot \gamma_g}} \qquad (2.1)$$

$$r = \frac{P_p}{P_i}$$

Where C_d is discharge coefficient (dimensionless), A_v is effective flow area (in^2), P_i is upstream or injection pressure (psi), P_p is the downstream or production pressure (psi), g is gravitational acceleration (32.174 ft/s^2), k is ratio of specific heats (dimensionless), T_v upstream gas temperature (^{o}R), z_v is gas compressibility factor at upstream condition (dimensionless), γ_g is gas specific gravity (dimensionless).

The research at TUALP on both 1 and 1.5 inch diameter gas lift valves showed that the Thornhill-Craver model over-predicts the flow rate through a gas lift valve. A group of researchers at TUALP in 1988 modified the Thornhill-Craver model by introducing a new term called non-constant discharge coefficient C_dY to predict orifice flow in gas-lift valves. C_dY, the product of discharge coefficient and expansion factor, was normalized as a linear function of $(P_i - P_p)/(P_i \cdot k)$ in equation form (Nieberding et al.,1993):

$$C_dY = m\frac{(P_i - P_p)}{P_i \cdot k} + b$$

The final equation developed by TULAP is:

$$Q_{sc} = 1240.3 \cdot C_dY \cdot A_v \cdot \sqrt{\frac{P_i \cdot (P_i - P_p)}{T_v \cdot z_v \cdot \gamma_g}} \qquad (2.2)$$

Where m and b are constants determined by laboratory measurements. m, b and C_dY are dimensionless. Qsc is gas flow rate (Mscf/day). Over the last three decades, there have been some studies conducted in developing accurate correlations to predict the gas flow rate through a single element gas lift valve. Acuna et al. studied three types of one-inch Nitrogen charged gas lift valves from different manufacturers and found that C_dY correlations are changed with the valve's types and the port size. The study showed that the TUALP orifice model can predict the gas flow rate with high accuracy if the correct C_dY coefficient is used and the new simple procedure for the calculation of normalized discharge coefficient is introduced. (Acuna et al. 1992)

Nieberding et al. developed two semi-mechanistic models to predict throttling and orifice flow and presented a procedure to use the models in gas lift design. (Nieberding et al., 1993) Hepguler et al. developed a dynamic model for a 1.5-in nitrogen charged gas lift valve for both orifice and throttling flow. The model investigated the pressure, temperature distribution and the forces acting on the internal elements within the valve. (Hepguler et al., 1993) Faustinelli and Doty developed a new dynamic model to predict gas flow rate based on physical principles and has the advantage of describing the internal flow mechanics occurring at the ball-seat and port locations. (Faustinelli and Doty 2001)

The above publications had been developed to predict the gas flow for one-section valves and cannot be used for the pilot valve since the gas is injected mainly through the lower part of the valve. Despite the work done by the researchers to study the gas lift valve, the pilot valve has not been incorporated into the existing works except for the research by Milano in 1999 when the equation for the closing pressure of the pilot valve has been developed based on the experiment's data (Hernandez, 2013).

There is a lack of research regarding the pilot valve and a poor understanding of the physical description of compressible flow behavior within it. In order to improve intermittent gas lift installation, an accurate model is needed to calculate the gas flow rate through the pilot valve and to understand the difference between the calculated and the actual field data. In addition to inaccuracy the gas flow rate through the intermittent gas lift valve, the valves tend to close at a pressure difference from the calculated pressure using the static force balance equation. For nitrogen charged pilot valve, the high flow rate of the injection gas through the main section cools the nitrogen in the dome to overcome the increase in the gas velocity. When the temperature drops, the pressure also drops in the dome, and the valve tends to close at a pressure lower than the valve closing pressure intend, the volume of the gas injected per cycle could be larger than expected (Maria et al., 2000).

2.9. Summary

This chapter provides a detailed description of the general concept of the gas lift method for both continuous and intermittent. Literature reviews of multi-phase flow in a vertical intermittent well show the development of the research over the years. This includes the attempt to investigate intermittent gas lift stages and the flow pattern that may occur for each stage. In addition, this chapter presents a brief description of the gas flow through an intermittent gas lift valve and the problems associated with the prediction of the gas flow rate through this complex geometry. From this chapter, one can clearly see that intermittent gas lift is required more attention from the researcher to predict the parameters involved in this system. The aim of this research is to use the potential of CFD and machine learning algorithms to predict various system variables and their effects on the production rate. Also, there is a lack of research regarding the pilot valve and a poor understanding of the compressible gas flow behavior within it. In this study numerical model is proposed to determine the discharge coefficient of the valve that corrects the theoretical gas flow rate to the actual one.

3. CFD MODEL OF INTERMITTENT TWO-PHASE FLOW

3.1. Introduction

The flow behavior of multiphase flow in intermittent gas lift systems is the priority of the petroleum companies for designing any intermittent system. One of the methods used widely to understand and optimize the multiphase fluid flow behaviors is CFD (Cengel and Cimbala, 2014).

This chapter presents the use of ANSYS Fluent-CFD to simulate the multiphase flow in the intermittent gas lift process. This research will investigate the effect of different system parameters on the efficiency of the production rate and the physical explanation behind it. A novel dimensionless analysis technique will be also introduced to simplify the study. A tubing string of 18 m length with 0.076 m internal diameter was designed in this research to study the effect of injection pressure on the slug velocity and in turn on the liquid production rate and liquid fallback. In addition, the dimensionless analysis using CFD is used to study the effects of slug length, port size, and injection pressure on the production rate.

3.2. Overview of Computational Fluid Dynamics (CFD)

The CFD model is one branch of fluid mechanics that depends on the numerical solution and data structures to analyze and solve the complex problems that may be involved in fluid flows. In CFD, computers are used to perform the mathematical calculations required to simulate the fluid flow and the interaction between the components of the multiphase fluid such as liquids and gases with surfaces of the flow stream defined by boundary conditions. Better solutions can be achieved with a high-speed supercomputer and are usually required to solve the largest and most complex problems. All the governing equations are based on the Navier-Stokes equations for the CFD model. CFD simulation of a given problem can obtain details about the flow characteristics such as shear stress, velocity, pressure profiles, and flow pattern that experiments results cannot achieve. Numerical methods can predict the fluid flow behavior of different scenarios and conditions before the attempt of building any experiment, moreover, there are certain parameters that can be calculated by these methods that cannot be measured in the experiments. The CFD software also allows the user to change the system variables such as the pipe size, pressure, temperature, and velocity without the need for new equipment setup. Nowadays, a CFD model has been widely applied to perform the multiphase flow study of different types. A computation model is applied in most engineering fields including research to optimize gas-lift systems using CFD. Still,

unfortunately, these studies are not dealing with the unique conditions found in the intermittent gas lift process and on such a large scale.

In CFD, the Finite Volume Method (FVM) technique is commonly used to divide the computational domain into small control volumes where the variable is located at the center of the volume. Over each control volume, FVM integrates the partial differential form of the governing equations to ensure the conservation in the cells and globally in the domain. This method allows the use of unstructured mesh or grids, which has the potential to decrease computational time. Two methods are presented for the variable to be centralized: cell-centered, and vertex centered. In cell-centered, approximate values at certain positions are obtained by interpolation methods since the discretized equations include the values for the cell faces. The accuracy of the simulation is affected by the stability, and convergence rate. The control volumes are built around each mesh vertex, in the vertex-centered method and several mesh elements form the control volume. The discretization is solved within each element, then the properties are distributed to the corresponding control volume (Stenmark, 2013).

3.3. Multi-phase Numerical Modelling Approaches

Studying a multiphase flow in the pipe is a challenging part of any research due to its complexity and limitations. The procedure of multiphase flow models uses to describe and predict the fluid flow is time-consuming and the capacity of the computer might not be sufficient. To overcome these difficulties, the scientists have developed two main types of modeling; Eulerian-Lagrange and Eulerian-Eulerian that can be applied to different multiphase flow applications.

3.3.1. Euler-Lagrange Model

In this method, Lagrangeian is tracking an object to determine its properties. The Euler-Lagrange method is used if a fluid particle is needed to be followed at each point in the domain. The fluid properties are then determined as the fluid particles move around. The characteristics of this method do not require any specific boundary layer and it can track fluid movement, location, and direction wherever it moves. In summary, the method can be used to obtain information about the flow by simply following an object's movement (Stenmark, 2013).

3.3.2. Euler-Euler Model

This method determines fluid properties as a function of time and space with the assumption of continuous phases are involved in the domain. Multi-fluid- Eulerian models are appropriate for two-phase gas-liquid flows since the two phases can be treated as a

continuum. Consider a container with fluid particles flowing in and out of it, the Multi-fluid-Eulerian method can observe and track the particles inside the container. On the other hand, outside the container, the method is not able to follow the fluid particles.

The overall flow of dispersed phases is an interesting area, every individual particle in a dispersed flow can also be tracked using this model with the high-volume fraction in order to describe the dispersed phase as a continuum. For each phase, a set of conservation equations is solved independently, and the model coupled pressure and interphase coefficients need to be also modeled. It is up to the user which model to include for their simulation and should have a knowledge of it. Different flow patterns can be solved by a number of models, and this is all based on empirical evidence and developed from other open literature.

Another Eulerian method is the mixture model where the phases are treated as interpenetrating continua. In the mixture model, the equations are based on the flow mixture properties, such as mixture velocity or mixture viscosity. This method can also solve the mixture momentum equation and can be used for the dispersed phases without relative velocities to model a homogeneous multiphase flow (Stenmark, 2013).

The volume of fluid (VOF) model is used where the location of the boundary between two or more immiscible fluids is a point of interest. Throughout the domain, momentum equations and the volume fraction of each fluid in each cell are calculated. A single set of momentum equations is solved and tracking the volume fraction of each of the fluids in the domain. The variables of the phases are presumed to be shared between the phases and the transport equations solve the mixture properties. The VOF model is suitable for flows with sharp interfaces, so it is used to track the interface between two or more phases. (Stenmark, 2013).

3.4. CFD applications for multi-phase flow

Intermittent gas-lift flow is a transient flow, when the gas is injected into the tubing the liquid is raised by the large bubble of the injected gas as a liquid slug. Some of the liquid is fall into the gas phase as a small bubble and/or liquid film. Then, the flow is transferred to the annular flow as soon as the liquid slug core is produced at the well surface. From these facts, the transient-turbulence model will be used in intermittent slug flow regimes. The common approaches for modeling two-phase flow in the gas-lift systems are the Eulerian-Eulerian, Eulerian-Lagrange, and direct numerical solution (DNS) (Dakshinamoorthy et al., 2013). In the Eulerian-Lagrangian approach, the discrete bubble model is used to track all the particles or bubbles in the gas phase individually. This approach required high

computational cost and time. The Euler-Euler model is commonly used to model the gas lift system and there are various models of it that can be used, such as the mixture model, the Volume of Fluid (VOF) model, and the Euler model.

There are two types of flow usually take place with two-phase fluid flow in a pipeline, Laminar and Turbulent flow. Turbulent flow is more difficult to be solved than laminar flow. The field in turbulent flow is always unsteady and random, eddies and vortical structures take place where turbulent swirls occur in three dimensions. Turbulence models are used to solve turbulent flow problems. The CFD simulation needs a fine and a good-quality grid to resolve the unsteady state three-dimensional turbulent swirls. In addition to the mass and momentum equations, turbulent models have transport equations that must be solved to enhance the mixing and diffusion of turbulent flow. (Çengel and Cimbala, 2014).

There is no standard model for a turbulent gas-liquid flow, (DNS, LES, k − ε, k − ω, etc.) model specifically used for this case. The turbulence model that is widely used in the numerical simulation for two-phase flow in a vertical pipe is the two-transport equation model: the k − ε model where k is the kinetic energy and ε is the turbulent dissipation. This model is usually preferred over the others to predict the liquid flow regime and gas hold-up due to its lower computational time, and it provides valid results with the simplest algorithm (Behbahani et al., 2012, Sattar et al., 2013, Pourtousi et al., 2015).

For the continuous bubbly phase, the standard k − ε model is used, while a zero-equation turbulence model is applied for the disperse phase. These two turbulence models perform better under higher superficial gas velocity when the bubble coalescence and break-up occur, in this case, the k − ε model is used for simulating 3D gas-liquid flow (Pourtousi et al., 2015). The turbulent equations are solved simultaneously with the mass and momentum equations. However, the parameters are not necessarily to be known, and instead, it is used for specifying turbulence intensity and turbulent hydraulic diameter. Furthermore, two additional boundary conditions will be added to the turbulence properties at inlets and outlets by the two new equations. Most of the research uses the standard k − ε model, especially when the Reynolds number is low for the turbulence simulation to capture the flow properties inside the pipe (Çengel and Cimbala, 2014).

Taha and Cui investigated the motion of single Taylor bubbles in vertical tubes using CFD to assess the bubble movement, a complete description of the bubble propagation in both stagnant and flowing liquids was studied. The commercial CFD-Fluent with the volume of fluid (VOF) model was used to compute the shape, velocity magnitude, and velocity distribution of the slug flow and the result from the simulation was compared with the

published experimental. Taylor bubbles were found to have a cylindrical body shape with a spherical nose and fluctuating tail. (Taha and Cui, 2005)

Behbahani et al. employed a multi-phase Euler-Euler model with the turbulent standard $k - \varepsilon$ model to predict the bubbly flow of air-water in a vertical pipe with a length of 80 times of diameter. The proposed model was validated with the result from a direct numerical solution (DNS) and experimental data. The authors used experimental studies from open literature to validate the CFD model. The multiphase flow is assumed to be one continuous phase and one or more dispersed phases, incompressible flow with no mass transfer in the well. The proposed model was also used to simulate gas lift in an oil well of 20 m height, 73 mm diameter tubing, and 8 mm valve port diameter. Four gas superficial velocities (0.05, 0.1, 0.2, 0.3 m/s) were modeled for each size of gas bubble of four different sizes (2, 3, 4.5, 5.5 mm). The model results were plotted and compared with eight other correlations from the previous researchers for the bubble flow regime. (Behbahani et al., 2012)

Dakshinamoorthy et al. presented a model for studying all flow regimes (bubbly, slug, annular, etc.) in a section of a vertical pipe with a length of 30 times the diameter. Multi-phase flow approach of Euler-Euler coupled with the multi-fluid VOF model was implemented using CFD and compared with experimental results. Gas holdup, flow instability, and pressure drop are predicted for a different flow regime and compared with the available data. The authors concluded that the CFD model can predict the flow regimes with high accuracy and give a better understanding of the complex flow behavior of the gas-liquid flow. (Dakshinamoorthy et al., 2013)

Wardle and Weller implemented a hybrid multiphase method to predict the flow in liquid-liquid extraction devices based on the combination of an Euler-Euler multifluid approach coupled with sharp interface capturing using the Volume of Fluid (VOF) model. CFD model developed in this study provided the necessary models to predict liquid-liquid interfacial area and consequently capturing of the dispersed phase droplet size distribution in stage-wise liquid-liquid extraction devices. The solver capability is demonstrated through various flow examples including three-phase, liquid-liquid-air simulations in which dispersed phase modeling is used for the liquid-liquid interactions and a sharp interface is maintained between each liquid and air phase. (Wardle and Weller, 2013)

Garcia et al. simulate the motion of the Taylor bubble in slug flow using CFD commercial software. A numerical database had been generated to develop a relationship between the bubble velocity as a function of fluid properties, flow conditions, and pipe geometry. Dimensionless numbers are used to simplify the simulation and describe Taylor

bubble movement such as the Froude number, Reynolds number, Morton number, and Eötvös number. The results showed that Taylor bubble velocity did not affected by the bubble length in an inclined pipe. Furthermore, the model suggested that the Taylor bubble velocity is reduced if there is no lubricating liquid film between the wall and the bubble in the inclined pipe. (Garcia et al., 2015)

Parsi et al. employed CFD model for multiphase flow in relatively larger diameter pipes (76 mm I.D.) for slug and churn flows in horizontal and vertical pipes. CFD results were validated with experimental results obtained with a Wire Mesh Sensor (WMS) and showed qualitatively and quantitatively match with the experimental data. VOF model was significantly capable of capturing two-phase distributions even at very high gas and liquid flow rates. (Parsi et al., 2015)

Dabirian et al. analyzed gas-liquid flow patterns in a horizontal pipe utilizing CFD simulation and compare the results with experimental data. Investigation of turbulent flow structures had been presented such as liquid height, liquid holdup, wall shear stress, and velocity profiles. CFD simulation had the potential to be utilized for facility design and scale-up processes in the petroleum industry. (Dabirian et al., 2015)

Emmerson et al. used CFD to predict realistic forcing functions on pipe bends in the slug flow regime typically seen in subsea flowlines, manifolds, and jumpers. This force could be used to investigate stress and fatigue in complex combinations of bends and tees. A novel approach of a quasi-three-dimensional CFD model is utilized to determine the inlet boundary conditions for a horizontal slug flow for subsequent force prediction. The CFD results of this approach are compared with physical tests of slug flow and slug flow correlations to validate the model accuracy. Moreover, CFD improved horizontal slug flow inlet boundary conditions compared to simplistic approaches based on correlations such as defining time-varying square waves. (Emmerson et al., 2015)

Abdulkadir et al. presented CFD studies of slug flow in a vertical riser of 67 mm internal diameter with air and silicone oil as the simulated fluids. The model results were compared with experimental data on different methods of introducing fluid into the riser. In this study, the effect of different liquid and gas superficial velocities on the model accuracy was studied. The velocities of liquid and gas of 0.05 and 0.344 m/s were introduced respectively and did not yield a difference between the CFD and experiment result at steady-state flow. The authors concluded that the flow was considered fully developed at a length of 60 times pipe diameters. (Abdulkadir et al., 2015)

Tocci et al. presented a CFD model for the multiphase flow of gas and liquid through vertical pipe sections. The authors employed two different multiphase flow approaches namely the Volume of Fluid (VOF) and the two-fluid model methods to study the two-phase flow in a vertical pipe. VOF is typically used for capturing the liquid-gas interfaces, while the Euler-Euler model approach is used for dispersed phases. This study combined these two models in a hybrid model and validated the proposed model with two representative test cases. This hybrid method has the potential to predict the flow since the VOF part track a sharp interface between segregated flow structures (for example, a liquid film that is separated from the gas core in annular flow), and the two-fluid model (Euler-Euler) represents properly the dispersed regions (for example, bubbly flow or the liquid slug body that has entrained gas bubbles). From the above explanation, a hybrid solver is a promising approach without a priori knowledge of the flow pattern, for predicting two-phase fluid flows in pipes. (Tocci et al., 2017)

Hussein et al. employed CFD simulation to model the churn flow in a vertical pipe with a 3-inch diameter. The gas flow near the critical gas flow rate for different liquid flow rates. In this research, the two-fluid Eulerian model along with the turbulent model of the RNG (Re-Normalization Group) k-ε model was used to study the behavior of the flow in a two-dimensional computational domain. Air and water were used as the two working fluids. The model results were validated with the experimental data and showed a good agreement. Along with the formation of interfacial waves, the details of velocity, shear stress, and pressure profile were observed. (Hussein et al.,2019)

Table A.2. (Appendix A), illustrated a summary of the research characteristics for multi-phase flow.

3.5. Numerical Simulation Methodology for Intermittent Gas Lift

3.5.1. Introduction

In the intermittent gas-lift system the flow is transient, and the fluid flow behavior is extremely complex. In order to design and simulate the fluid behaviors in an intermittent gas-lift system, the user needs to have good knowledge of both a multiphase flow and CFD background. This technique is widely used in the industry to inject high-pressure gas to artificially lift reservoir fluid to the surface. In simple terms, the principle of intermittent gas-lift is that the gas is injected down into the tubing string through the annulus-tubing space to lift the accumulated reservoir fluid up to the well surface. The gas forms a large bubble beneath the liquid slug and part of the liquid is fall down as a liquid film on the pipe

wall or as small droplets in the gas bubble. When the liquid slug reaches the surface, the injected gas ceases to flow, and the gas blows down. Generally, the gas-lift process is outstanding flexibility, especially for offshore oil wells with wide ranges of depth. Also, minimal maintenance costs are required. To achieve the optimum intermittent design and efficient operation conditions, the interaction between the operating parameters must be understood.

CFD models had developed as a powerful tool to simulate the operating parameters in a continuous gas-lift system in different scenarios. However, CFD simulation for studying intermittent gas lift has not been developed yet. The CFD software is a promising numerical model for an intermittent gas lift since it enables the user to couple a multiphase model with a turbulence model to capture a real-world intermittent gas-lift. This research focuses on physically understanding the two-phase flow behaviors in the vertical column of intermittent gas-lift systems using a numerical method. This will give more details about the upward movement of the gas bubble and liquid slug in this system. The effect of different parameters on the liquid production rate will be studied and these results obtained from numerical simulation methods will be compared with experimental results from open literature. Therefore, it was important to learn about different multi-fluid modeling methods to capture the transient-two-phase flow behaviors in such a system. This section will present the simulation of three dimensions tubing string with the gas lift valve for gas injection as well as the numerical solution setup. There will be a brief description of the commercial CFD program, ANSYS (Analysis System).

3.5.2. Fluent

Computational Fluid Dynamics Fluent is a software produced by ANSYS. Fluent software is widely used for modeling fluid flow, and it contains a comprehensive suite to be used for other related engineering applications. CFD-Fluent has the potential to model a wide range of multiphase and single-phase flow phenomena. Applications of liquids and gas mixtures, turbulence, heat transfer and the transient flow phenomena are solved by Ansys-fluent. In general conservation equations for mass and momentum are solved by Fluent software and if the flow involves turbulence, an additional equation for viscous and transport equation will be solved. Fluent base on finite volume method (FVM) discretization technique in dividing the computational domain and solving the governing equations. It has the flexibility to allow the user to use segregated and coupled solution methods. In the FVM method, the domain is divided into small control volumes where the choice of discretization technique will also dictate the results in other multiphase models. Furthermore, Fluent

contains a number of models that can be solved to model the interfacial momentum forces such as the equations of drag, lift, and wall forces (Stenmark, 2013).

3.5.3. Numerical CFD Modelling Stages

There are three main stages for a typical CFD modelling process: pre-processing, solving, and post-processing. These stages are performed using software components like: pre-processor, solver and post processor.

Pre-processor:

1. Create the 3D geometry model of the fluid domain on ANSYS Design Modeler.
2. Create a quality mesh on ANSYS meshing tool and name the boundary of the model.

Solver:

3. Solve the numerical problem after settings the physics and the boundary conditions on Fluent by using appropriate turbulence model and multiphase model.
4. Implement the mesh independency test.
5. Monitor the convergence of the model.

Post-processor:

5. Visualize and analyze the CFD results on CFD-Post.

6 Validate the model using the experimental results.

Figure 3.1 describe the CFD method that will be used in this research.

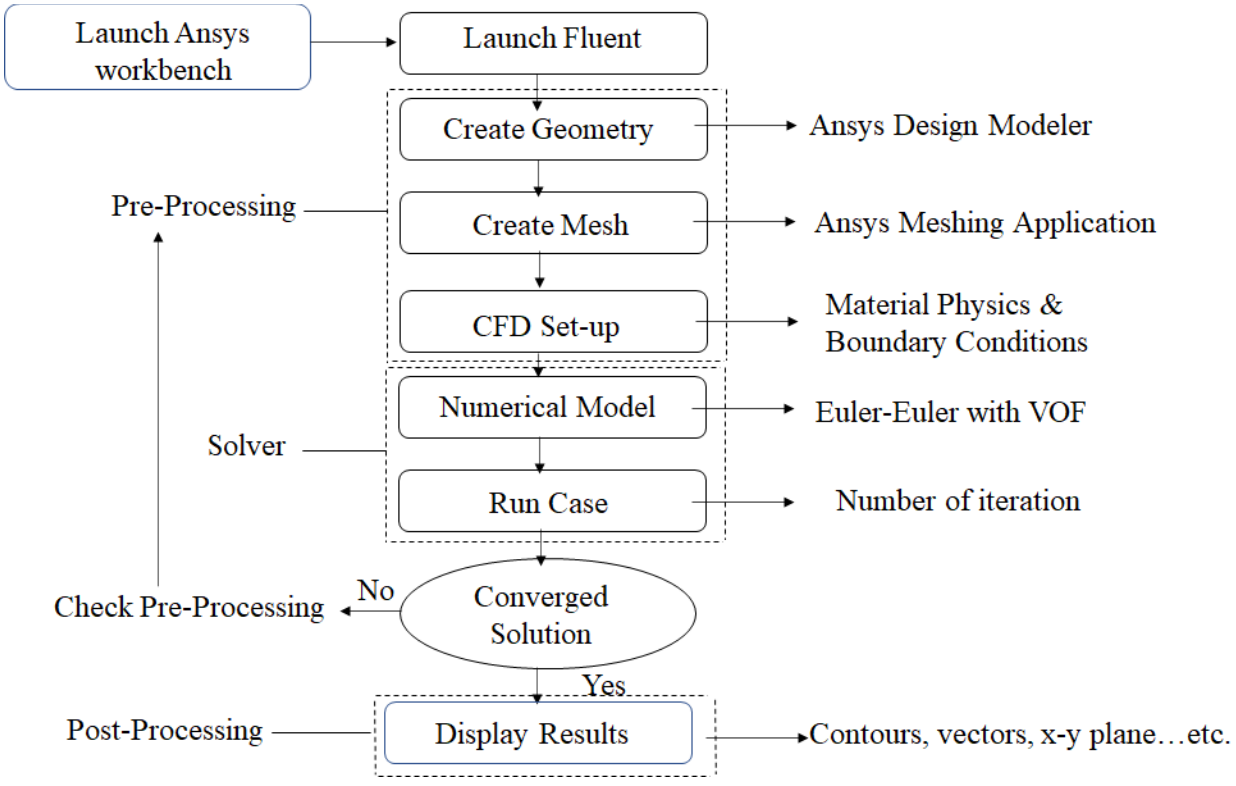

Figure 3.1. CFD simulation flow chart. (edited by the Author)

3.5.4. CFD Governing Equations

CFD- Fluent software (Ansys 19) is used in this paper to simulate the movement of the gas bubble and liquid slug in a vertical tube. In CFD- Fluent, the control volume method—sometimes referred to as the finite volume method is applied to solve the transport equations. One should understand the transport mechanism before choosing a multiphase model to capture the flow regime properly. Intermittent gas lift is a transient process in which liquid moves like a slug, and some of the liquid falls back as liquid film and/or small droplet. Tracking the interface between the liquid slug and the gas bubble is important in this type of flow. Multiphase flow can be numerically calculated in the CFD simulator using either Euler- Lagrange approach or the Euler-Euler approach. In the present study, the volume of the fluid VOF multiphase model is used, which is a type of Euler-Euler approach. VOF model is a surface tracking technique, and it is usually used to model more than two immiscible fluids, where the interface position is important. The movement of a large bubble in a liquid and the tracking of any liquid-gas interface is typical of VOF model applications. Tracking the interfaces between the phases is achieved by solving a continuity equation for the volume fractions of the modeling phases. The continuity equation for the (q) phase, has the following form:

$$\frac{1}{\rho_q}[\frac{\partial}{\partial t}(\alpha_q\rho_q) + \nabla(\alpha_q\rho_q\vec{v}_q)] = S_{\alpha_q} + \sum_{p=1}^{n}(\dot{m}_{pq} - \dot{m}_{qp})$$

Where $\dot{m}_{pq}$, $\dot{m}_{qp}$ are mass transfer from phase *p* to *q* and *q* to *p* respectively (kg/s), ρ_q is density of phase *q* (kg/m^3), α_q volume fraction of phase q (dimensionless), $\vec{v}_q$ is the velocity of phase *q* (m/s), S_{α_q} is external mass source entering phase *q* (kg/sec/m^3), *t* is time (sec).

In the VOF model, a single momentum equation is solved over the domain so that, the velocity field is shared among the phases. Based on the volume fractions of all phases through the mixture properties of density and viscosity, the momentum equation is solved as follows:

$$\frac{\partial}{\partial t}(\rho\cdot\vec{v}) + \nabla(\rho\cdot\vec{v}\vec{v}) = -\nabla p + \nabla[\mu(\nabla\vec{v} + \nabla\vec{v}^T)] + \rho\cdot\vec{g} + \vec{F}$$

$$\overrightarrow{v} = \frac{1}{\rho}\sum_{q=1}^{n}\alpha_q\cdot\rho_q\cdot\vec{v}_q$$

$$\mu = \sum\alpha_q\cdot\mu_q$$

$$\rho = \sum \alpha_q \cdot \rho_q$$

$$\sum_{q=1}^{n} \alpha_q = 1$$

Where μ_q is the dynamic viscosity of phase q (Pas), ρ is mixture density (kg/m^3), $\vec{v}$ is mixture velocity vector (m/s), μ is mixture dynamic viscosity (Pas).

The impacts of surface tension along the interface between the phases can also be included in the VOF model. Surface tension is a result of attractive forces between different molecules of fluid. If an air bubble is moving in a liquid phase, the net force of a molecule within the entire bubble body is zero, however, at the bubble surface, the net force is radially inward, and the surface is contracted. This is caused by the effect of radial force on the entire spherical surface which increases the pressure on the concave part of the bubble. The surface tension creates an equilibrium between the intermolecular attractive force and the outward pressure gradient force towards the surface. The surface tension model of continuum surface force (CSF) is applied in Ansys Fluent. To include surface tension in the VOF model calculations, a source term is added to the momentum equation. If only two phases are present in a cell, a source term can be expressed as a volume force equation and can be written as below (Ansys Fluent 12.0):

$$F_{vol} = \sigma_{ij} \frac{\rho \cdot k_i \nabla \alpha_i}{\frac{1}{2}(\rho_i + \rho_j)}$$

Where:

$$k = \nabla \cdot \hat{n}$$

$$\hat{n} = \frac{n}{|n|}$$

$$n = \nabla \alpha_q$$

$$k_i = -k_j \text{ and } \nabla \alpha_i = -\nabla \alpha_j$$

Where F_{vol} is volume force (N), σ_{ij} is surface tension coefficient between phase i and j (N/m), k is curvature (m), $\hat{n}$ is unit normal (dimensionless), n is surface normal at the interface (dimensionless), ρ_i and ρ_j are the density of the phase i and j (kg/m^3).

The calculation of surface tension impacts is more accurate on hexahedral, and quadrilateral meshes than on triangular and tetrahedral meshes (Ansys Fluent 12.0). Therefore, where surface tension effects are important, the geometry should mesh with quadrilaterals or hexahedra mesh. Since the flow is turbulent under gas lift conditions, the

standard k – ε viscose model is used with the RNG (Renormalize group) for turbulent modeling.

3.5.5. Scenarios of CFD Simulation

In this research two scenarios of intermittent gas lift have been studied and compared with experiment results. The geometry size and the solution set up in each case are the same as those of the experimental conditions in order to validate the CFD model. Table 3.1 shows the summary of different variables for the two cases.

3.5.5.1. Case One

In this study, CFD simulation will develop for a tubing string with a length long enough (236D) to capture the flow regime and the feature characteristic of intermittent gas lift flow. Air will be used as the injection gas to lift the accumulated oil in the tubing string to the well surface. The goals of this study are to physically describe and investigate the slug flow during intermittent gas lift within the production string and to calculate the slug velocity at different injection pressure with high accuracy. The effect of injection time and injection pressure on the fraction of liquid production is also studied. The results from the numerical model developed in the present study are verified with experimental data from the literature.

Table 3.1. Parameters for intermittent gas lift cases (edited by the Author)

Parameters	Tubing size	port size	Injected Gas	Liquid Slug	Injection pressure
Case 1	0.076 m (3 in)	0.025 m (1 in)	Air	Oil	2.7&3.5 bar (40&50 psig)
Case 2	0.051&0.060 m (2&2.375 in.)	0.013 m (0.5 in)	Natural gas	Water	2&3 times Pt (tbg. press.)

3.5.5.1.1. Domain and Grid Generation for Case One

The geometry used in this study represents a tubing string with a length of 18 m and a diameter of 0.076 m. The gas is injected from an inlet orifice with a diameter of 0.025 m representing the port size of the gas lift valve. The geometry was created using ANSYS Design Modeler 19, and the mesh was constructed using the ANSYS meshing tool. Hexahedral computation mesh was created with enough mesh resolution near the wall as shown in Figure 3.2 to capture the liquid film flow near the tubing wall. The number of

nodes and elements are 1217758 and 1104000 respectively with skewness of 0.075 and quality of 0.98. To compare the CFD results obtained from this study with experimental results from the literature, the geometry and the liquid properties are similar to that used in the literature (Schmidt et al., 1984).

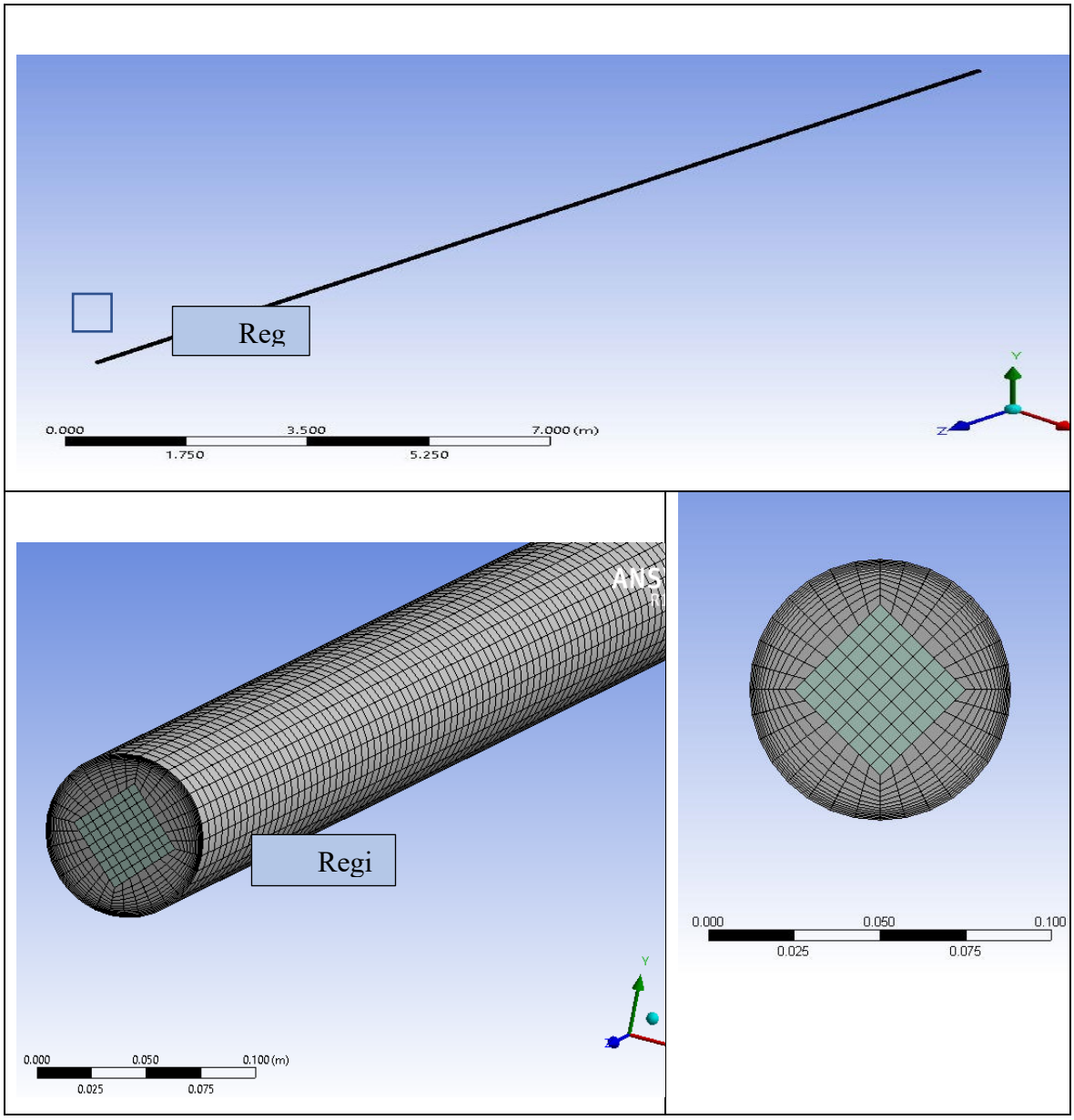

Figure 3.2. The structured mesh used for intermittent gas lift (Case 1). (edited by the Author)

3.5.5.1.2. Setup and Boundary Conditions of Case One

In intermittent gas wells, the liquid accumulates in the tubing string to a certain level before the gas is injected. To represent the real intermittent gas lift process, at zero time of simulation, the designed tube is patched with oil to 9 m, and the remaining part patched with air. The pressure inlet and pressure outlet are set at the boundary condition. Two different

values of injection gas are used in this study 40 psi (2.7 bar) and 50 psi (3.4 bar) and the gas injection stops when the tail of the liquid slug or the head of the gas bubble reaches the tubing surface to represent the same conditions used in the literature (Schmidt et al., 1984). A three-dimensional transient model using a pressure-based solver with a time step of 0.001sec is performed.

3.5.5.2. Case Two

Three-dimensions tubing strings with two diameters were used in this study. Natural gas with a specific gravity of 0.7 is used as an injection gas to lift the accumulated liquid in the tubing (saltwater in this study) to the surface. The goals of this study are to build a dimensionless analysis numerical model that can be used to calculate the liquid production percent as a function of different operations conditions with high accuracy. The results from the model developed in this study are compared with experimental data from works of literature to validate the simulation data.

3.5.5.2.1. Domain and Grid Generation for Case Two

The geometry used in this study represents a tube string with two different diameters of 2 inches (0.05 m) and 2.375 inches (0.06 m). Figure 3.3 shows the details of the domain parts used in this study to simulate the intermittent gas lift process. To represent the real intermittent gas lift process, at zero time of simulation, the designed tube is patched with liquid to a certain level and the remaining part patched with gas. The gas is injected from an inlet orifice with a diameter of 0.5 in (12.7 mm) representing the port size of the gas lift valve. The geometry was created using ANSYS Design Modeler 19, and the mesh was constructed using the ANSYS Meshing tool. Hexahedral computation mesh was created with enough mesh resolution near the wall as shown in Figure 3.4 to capture the liquid film flow near the pipe wall. The mesh is considered high quality with skewness equivalent to 0 and orthogonal quality equivalent to 1. The mesh independence study is conducted as shown in Figure 3.5 to establish the accuracy of the CFD solution and reduce the simulation time without affecting the calculation accuracy. Table 3.2. shows the mesh statistics and quality.

Table 3.2. Mesh statistics and quality for tubing string geometry. (edited by the Author)

Mesh	No. of element	Skewness	Element quality
$2^3/_8$-inch tubing	153722	0.085	0.99
2-inch tubing	148700	0.073	0.93

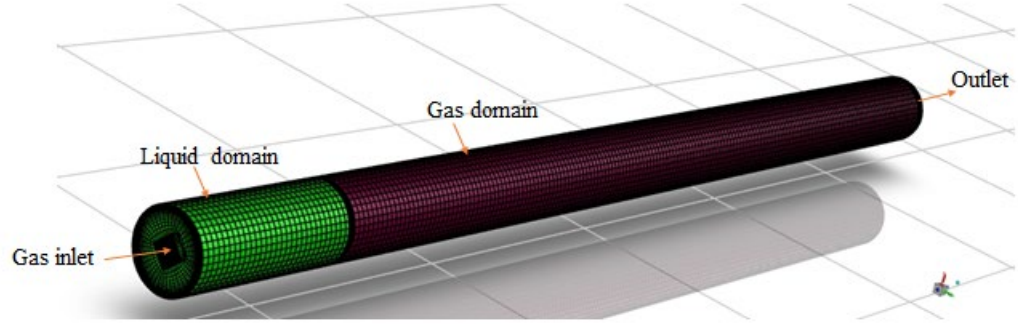

Figure 3.3. The different domain parts used to simulate the intermittent gas lift process. (edited by the Author)

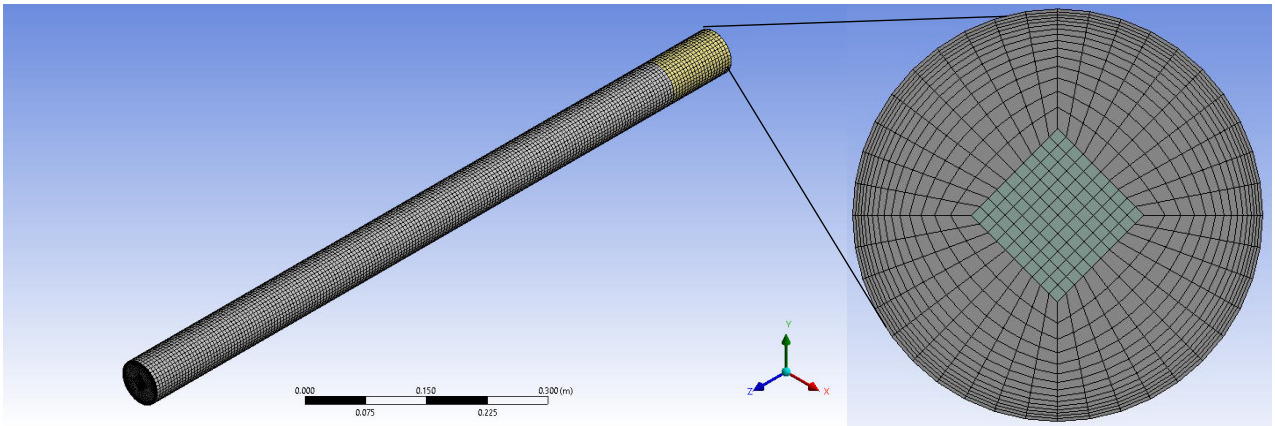

Figure 3.4. The structured mesh used for intermittent gas lift (Case 2) (edited by the Author)

3.5.5.2.2. Setup and boundary conditions of case two

The pressure inlet and pressure outlet are set at the boundary condition. Pressure inlet and pressure outlet boundary conditions are used. A three-dimensional transient model using a pressure-based solver with a time step of 0.001 is performed and the solution data file is automatically saved at a defined point during the simulation. In the industry, the gas injection is ceased when the liquid slug reaches the well surface so, the user defined function is written to set the pressure inlet based on the liquid volume fraction in the tubing outlet (Appendix B).

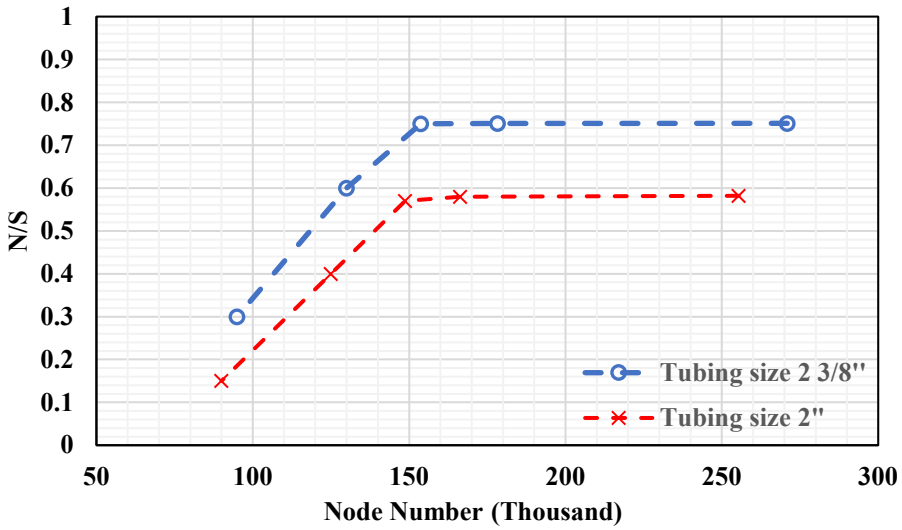

Figure 3.5. Mesh independence study for dimensionless analysis. (edited by the Author)

A user-defined function (UDF) is a function in C programming language that can be dynamically loaded to the Ansys-Fluent solver to identify the variables or enhance its standard features. UDFs are defined using DEFINE macros supplied by Ansys-Fluent and these functions are coded using predefined macros and functions to access the Fluent solver data and perform other tasks. UDFs files can be either interpreted or compiled in Fluent. In the interpreted method, the UDF source files are interpreted and loaded directly to the solver at runtime in a single-step process. While in the compiled method the source files are not directly loaded to Fluent, First, a shared object code library is built and then loaded, into Fluent (Ansys Fluent UDF manual, 2011).

3.5.6. CFD solution set-up

The multiphase model of VOF is selected with an implicit numerical solution scheme. During computation, the k – ε turbulence model with enhanced wall function as a near-wall treatment model was selected. The value of Y+ was kept around 1 to capture the velocity gradient precisely. Figure D.1 (Appendix D) shows the visual representation of the Y+ value over the wall of the simulated tube. The simple algorithm scheme is used in this study to solve Navier-Stokes equations and the spatial discretization methods are as follows: least-squares cell-based for gradient, Presto for pressure, second-order upwind for momentum, first-order upwind for volume fraction, and bounded second-order implicit for translate formulation. The residual value of 10^{-5} for different parameters is used to study the solution's

convergence of the CFD model. Figure D.2 (Appendix D) shows the surface monitors for the velocity and mass flow rate have been plotted to understand the number of iterations necessary to reach the final CFD solution.

4. CFD SIMULATION OF PILOT OPERATED INTERMITTENT GAS LIFT VALVE

4.1. Introduction

There is a lack of research regarding the pilot valve and a poor understanding of the physical description of compressible flow behavior within it. In order to improve intermittent gas lift installation, an accurate model is needed to calculate the gas flow rate through the pilot valve and to understand the difference between the calculated and the actual field data. The gas flow rate calculations through intermittent gas lift valve is inaccurate and also the valve tends to close at pressure difference from the calculated pressure from the static force equation. In the last decade, CFD model has been extensively applied to perform single and multiphase flow studies in most engineering fields. Thus, in this chapter, CFD simulation is used to analyze the flow details and characteristics through the pilot valve. The CFD study of the pilot valve investigates the internal pressure, velocity, and temperature distribution within the pilot valve that cannot be predicted in experiments and mathematical models. A general equation for the nonconstant discharge coefficient will be developed for a 1-inch pilot valve.

4.2. Ansys-CFX

Ansys CFX is a general-purpose, high-performance, software program that has been applied for more than 20 years to solve various ranging of fluid flow problems. Companies around the world have trusted the Ansys CFX technique as a reliable solution and powerful CFD simulation tool. CFX is accessible to both designers' engineers with general engineering knowledge and specialists in fluid dynamics who require in-depth model control and options. The robustness of the CFX model is by combining both the advanced solver technology with a modern user interface and an adaptive architecture. CFX uses a Finite Volume Method with a vertex-centered approach to solving the transport equations.

4.3. CFD for Flow in Restriction

Measuring the mass flow rate of a fluid running through a restriction or a valve is a recurrent need in several industrial processing including the petroleum industry. In restriction, a physical barrier is inserted perpendicular to the tube axis which leads to a reduction in a fluid flowing area thus, causing a local fluid to accelerate and therefore a pressure drops. For an idealized incompressible flow, the pressure drop can be directly related to the mass flow rate of the flowing fluid. However, inertial, and viscous effects need

to be considered, which can be accomplished by introducing a correction factor, namely the discharge coefficient (C_d) (Imada et al., 2013).

Discharge coefficient C_d is the ratio of actual mass flow rate to the ideal mass flow rate. The discharge coefficient is a unique value for each type of valve. It represents the effects of boundary layers in the viscous region of the flow, the effect of the structure of the geometry, and also the physical properties of the gas.

$$C_d = \frac{\dot{m}\ actual}{\dot{m}\ ideal}$$

Where $\dot{m}\ actual$ and $\dot{m}\ ideal$ are actual and ideal mass flow rate (kg/sec)

In the last years, CFD tools are widely used in modeling and analyzing the flow through restriction.

Li et al. combined Finite Element Analysis (FEA) with CFD to develop a procedure for evaluating the performance of the Surface-Controlled Subsurface Safety Valve (SCSSV). Full-scale physical experiments were carried out to validate the model and it showed that CFD is proved to be a cost and time-efficient practice. After the validation of FEA/CFD models with flow testing results, the changes in the valve performance as a response to the flow parameters or safety valve configuration can then be predicted using the proposed FEA/CFD models. Actual testing may be required to confirm the results of FEA/CFD or may be totally avoided. (Li et al., 2005)

Imada et al. applied a finite volume-based method in Ansys-Fluent to simulate incompressible flows through orifice plates and long radius nozzles in the Reynolds range between 15,000 − 500,000. Pressure-velocity coupling equation is solved via the Pressure Implicit with Splitting of Operators (PISO) algorithm. Pressure and velocities are resolved through a staggered mesh and all other flow parameters are interpolated via the Second-order Upwind method. Two turbulence models - Realizable k − ϵ and Shear Stress Transport (SST) k − ω are used to simulate the gas flow. The calculated values of discharge coefficients from CFD were compared with the ISO Standard equation for the discharge coefficient of the orifice and show a good agreement. (Imada et al., 2013)

Gharaibah and Zhang used 3D CFD choke valve simulations to explore the erosion issues associated with the subsea choke valve. Numerical experiments were carried out on various choke and subsea production systems to examine these issues and provide the best optimization practices. Various configurations of the choke upstream pipes and bends were investigated to explore the geometrical effect on the sand particle concentration. The flow and erosion rates of the investigated configurations are compared with real experiments data.

Depending on the configuration of the upstream piping, high localized erosion rates may occur due to asymmetrical jetting flow entering the choke. It was concluded from CFD and experiment results that the material loss in the choke and the piping system is significantly affected by the location of the choke valve in the production system, the choke module configuration, and the production conditions. The authors recommended using the CFD model to optimize the choke module configuration and reduce the damage problem of sand jetting. (Gharaibah and Zhang, 2015)

In the study of flow metering, it is believed that flow physics, such as the location of the maximum velocity (the vena contracta point), pressure profile, and characteristic length and velocity scales in orifice flow, are interesting topics for academic researchers and engineers. Tukiman et al. carried out a CFD simulation to predict the flow pattern in the orifice flow meter. The results of the numerical simulations were discussed in terms of velocity profile and pressure profile. The location of vena-contracta was estimated from CFD simulations. It was concluded that the CFD technique can be used as an alternative tool and cost-effective technique for estimating discharge coefficient empirically and replacing the method of the experiment. While experiments may be too expensive, complex, or time-consuming, CFD would candidate as a promising tool for the design and use of such valves in all the industrial situations that are common in the oil and gas fields. (Tukiman et al., 2017)

Bagaskara and Moelyadi determined the discharge coefficient of the sonic nozzle using the computational fluid dynamics method and considering the roughness of the wall. It was observed that the CFD results show better agreement with the experimental data compared to the analytical result. The inlet pressure boundary condition is selected in accordance with the experimental data to investigate the effect of the Reynolds number on the discharge coefficient. To ensure critical flow at the throat area and to avoid shock formation in the divergent parts of the nozzle, back pressure was lowered sufficiently. (Bagaskara and Moelyadi, 2018)

Poletto et al. implemented computational fluid dynamics coupled with a discrete element method (CFD-DEM) numerical approach to study the tendency of solids scale deposition on the surfaces of sliding-sleeve valves (SSV). The main aim of this study was to determine potential scaling spots on the SSV walls and to analyze the influence of particle size distribution over the scaling process. This work is the initial effort of the research to model complex tasks such as the hydrodynamic aspects of scale formation in wellbore arrangement and production facilities. (Poletto et al. 2020)

Kabir et al. conducted comprehensive experiments and simulation studies to determine the optimum combination of seat and ball for a gas lift valve. The experiments cover a wide range of ball and seat sizes combined to cover the industrial conditions. For a 5/16-inch port seat, the combination of seat and ball showed an improvement of more than 27% over the current industry practice, and this improvement is expected to be more for larger port seats. The CFD model was validated using experimental results for the actual gas lift valve. It showed a good matching with the expected maximum error of not more than 5%. (Kabir et al. 2020)

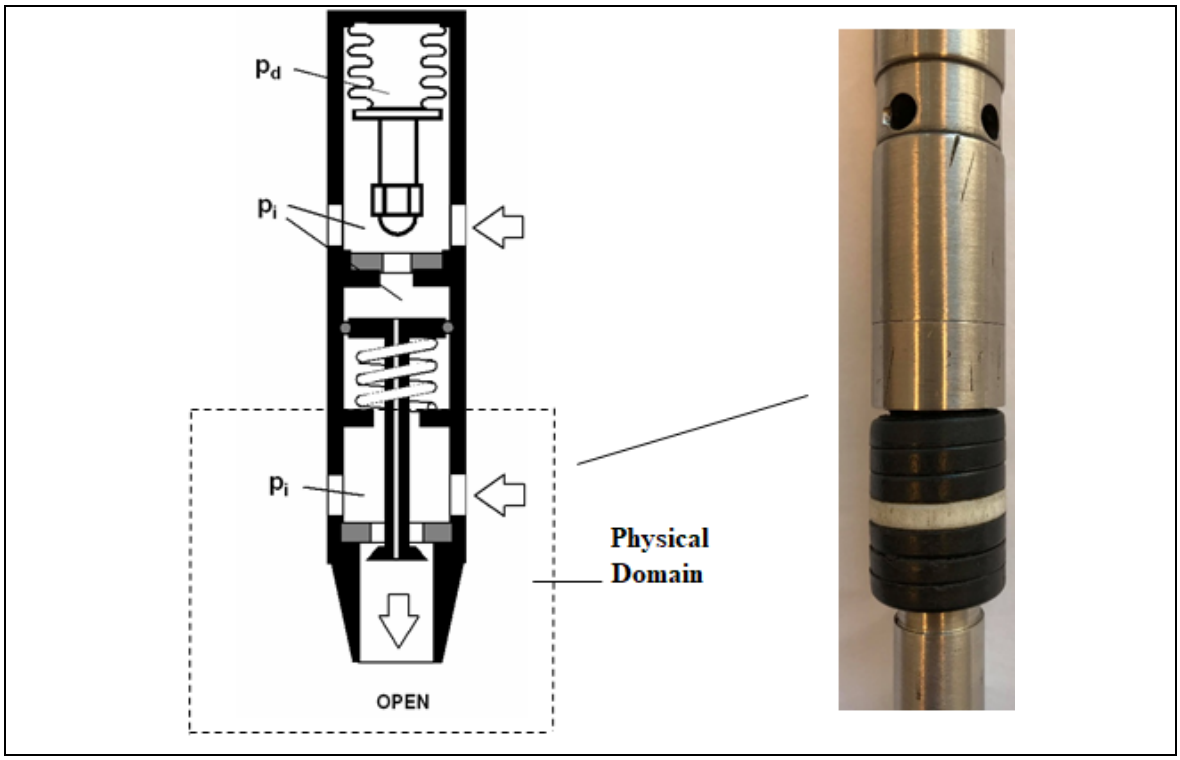

Figure 4.1. Physical pilot valve domain for CFD simulation (Takacs, 2007)

4.4. Domain and Grid Generation

The domain considered in this study is shown in Figure 4.1. The important part to be simulated is the power part, since the injected gas flows through this section to the production tubing and it is responsible for the gas flow rate. To simplify the geometry, the following assumptions are made.

(a) The gas flow through the bleed hole has not been modeled, in fact, the gas flow through the bleed hole is not that significant compared to the total gas flow rate.

(b) The inlet boundary condition is located on the wall that separates the piston seal ring and the gas entrance to the main part.

The internal space where the gas flow takes place in the investigated part is designed using ANSYS Design Modeler 19. The space available for the gas to flow constitutes the flow space for CFD calculations. Since the CFD calculations require filling the space with interconnected mesh. The mesh was constructed using the ANSYS Meshing tool and the final mesh structure is shown in Figure 4.2.

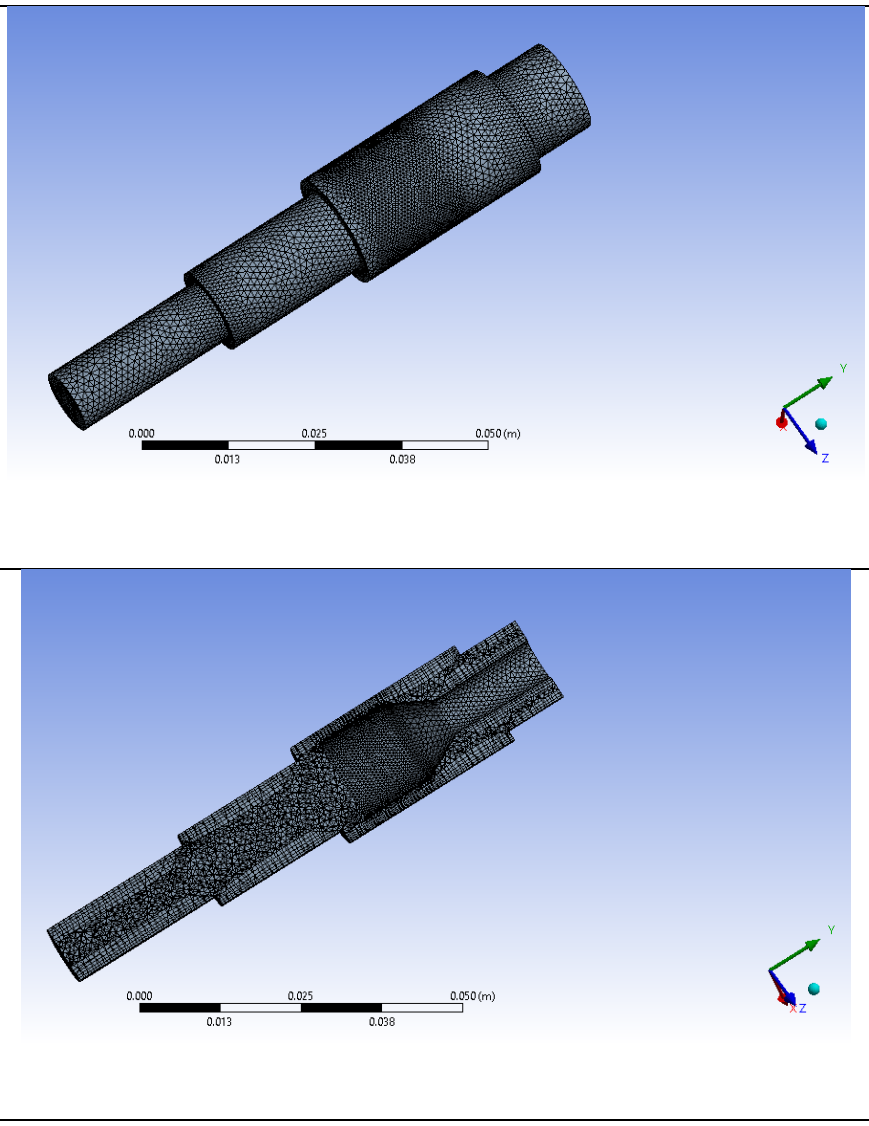

Figure 4.2. (a) Final mesh structure of pilot valve flow space. (b) Vertical cross section plane (edited by the Author)

4.5. Numerical Solution

CFD- CFX software (Ansys 19) is used in this study to simulate the flow of injection gas through the main part of the pilot valve. Methane is used as an injection gas for all the simulation conditions. In CFX, the control volume method—finite volume method is used to solve the transport equations. In this method, the domain is subdivided into control volumes and then the differential governing equations are integrated for each control

volume. The set of equations solved by CFD is the unsteady Navier-Stokes equations in their conservation form. The governing equations are described below (Turzo and Takacs, 2009):

$$\frac{\partial \vec{v}}{\partial t} + div(\vec{v}.\vec{v}) = \vec{g} - \frac{1}{\rho} grad\ p + \vec{v}\Delta\vec{v} + \frac{\mu+\xi}{\rho}\ grad\ div\ \vec{v} \quad \text{(Navier Stokes)}$$

$$\frac{\partial \rho}{\partial t} + div(\rho\vec{v}) = 0 \quad \text{(Mass conservation)}$$

$$\frac{\partial}{\partial t}\left(\frac{v^2}{2} + h\right)\rho + div\left[\left(\frac{v^2}{2} + h\right)\rho \cdot \vec{v} - \lambda\nabla T\right] = \frac{\partial p}{\partial t} \quad \text{(Energy conservation)}$$

$$\rho = \rho\ (p, T) \quad \text{(Equation of State)}$$

$$h = h\ (p, T) \quad \text{(Change in Enthalpy)}$$

Where $\vec{v}$ is the velocity vector (m/s), t is time (sec), $\vec{g}$ is acceleration of gravity vector (m/s^2), r is density (kg/m^3), p is pressure (Pa), μ and ξ is dynamic and bulk viscosity (Pas), h is enthalpy (J), T is temperature (^{o}K), λ is heat transfer coefficient (W/m^2/K).

4.6. Optimization of CFD Results

4.6.1. Mesh Independence Study

Prior to performing CFD simulation, the mesh independence study is conducted, to establish the accuracy of the solution and reduce the simulation run time without affecting the calculation accuracy. Thus, seven mesh types from coarse to dense were generated to ensure that the CFD results were sufficiently grid independent**.** The gas flow rate is calculated for different meshes as shown in Figure 4.3. The figure shows that as the number of the mesh increases the gas flow rate also increases until it reaches a constant value. The optimal number of elements is found to be 111740 cells; beyond this value, the gas flow rate shows no change with the number of elements.

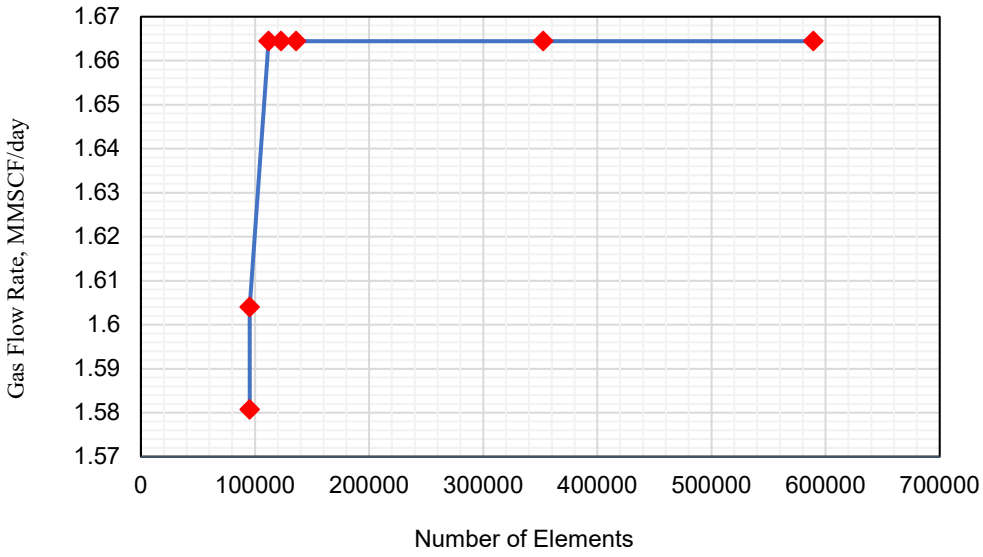

Figure 4.3. Mesh independence study for pilot valve. (edited by the Author)

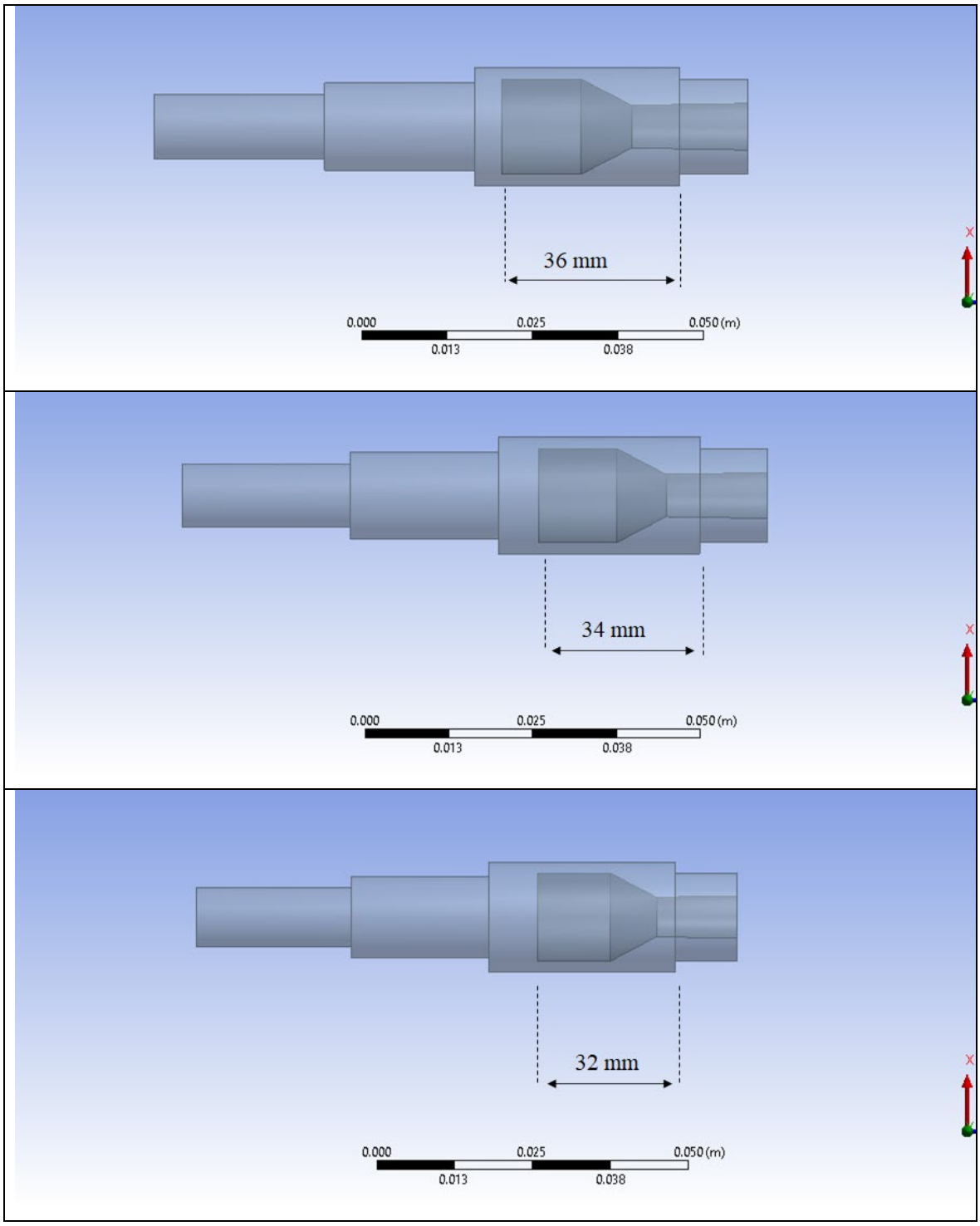

Figure 4.4. Different piston travel geometry for pilot valve (edited by the Author)

4.6.2. Effect of Power Piston Travel

The effect of the distance that the power piston travels inside the power section of the pilot valve on the gas flow rate had been studied. In the normal intermittent process, the piston is supposed to move down into the power section as soon as the valve is opened based on the adjusted piston spring force. In case of any technical problem in the piston spring, the movement of the piston is restricted. Thus, this study had been conducted to show the effect

of this movement on the gas flow rate. Three different travels measured from the boundary wall to the end of the piston had been studied as shown in Figure 4.4. For each piston travel, the gas flow rate is measured as follows:

- The boundary condition of the pressure, temperature, and gas properties is set at the power section inlet and outlet.
- The CFD simulation is run for each condition until the convergence is reached and

For each piston travel, the gas flow rate through the valve is measured for different production pressure.

The results show that the piston travels of 32, 34, and 36 mm have no significant effect on the gas flow through the pilot valve for different production pressure as can be seen from Figure 4.5.

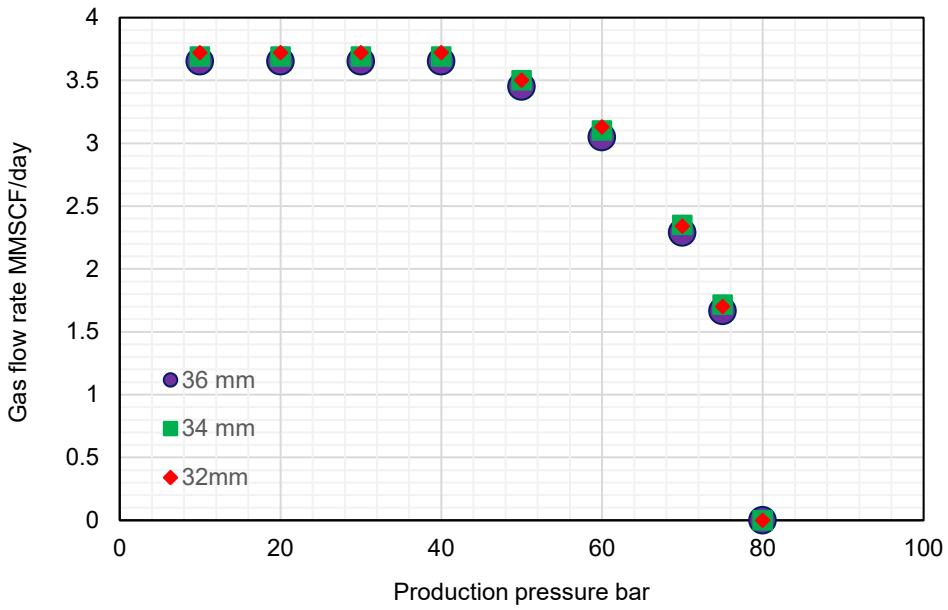

Figure 4.5. Effect of piston travel on the gas flow rate (edited by the Author)

5. MACHINE LEARNING ALGORITHMS FOR PREDICTING TUBING PRESSURE

5.1. Introduction

Calculating tubing pressures at the operating intermittent gas lift valve are the most important parameters in determining the mass flow rate of injection gas as well as calculating the oil production rate per cycle. Tubing pressure is the connection parameter that combines casing annuls behavior with the tubing string behavior. These pressures, in such complex multiphase flow, are the most difficult variable to be calculated, it is required a large number of parameters and assumptions. Artificial Intelligence is a potential technology that recently provided a reliable result for big data analysis. A Machine Learning algorithm is a promising tool of artificial intelligence that helps humans understand complex problems and used potentially in predicting and capturing non-linear complex behaviors. The ability of machine learning prediction improves by learning from more databases over time. In this chapter, three different machine learning algorithms will be used in order to predict the tubing pressure at the injected gas depth in intermittent gas lift wells. Real data from the Algyo field in Hungary will be used to build and evaluate the model.

5.2. Machine Learning Overview

Machine learning is an application of artificial intelligence that focused on building software applications by automatically learning and improving from experience without being explicitly programmed. In machine learning, computer programs are developed based on massive access data and use it to learn for themselves. The machine learning process begins by learning from observations or records, such as examples, direct experience, or instruction. Based on the examples that the user provides, the machine learns the patterns of the data and makes better decisions in the future to predict the new data. The primary concept of machine learning is to allow the computers to automatically learn without human intervention or assistance and accordingly adjust proper actions.

A major difference between humans and computers is that a human tends to automatically improve their way of handling a problem. The human brain learns from previous mistakes and tries to avoid them by looking for new approaches to solve the problem. Traditional software application does not look at the target required results of their tasks and therefore would not improve their behavior. Advance machine learning algorithms address this problem associated with traditional computer applications and create computer

programs that are able to learn from previous data and experience to improve their performances (Artun, 2020, Yang et al., 2020).

Machine learning algorithms are often grouped based on desired output: (Mohammed et al., 2017)

- **Supervised machine learning algorithms:** The algorithms build a function that relates input data to desired outputs. It applies what has been learned from the available data with labeled examples to predict future events. The machine algorithm produces an inferred function after analyzing a known training dataset and this system after sufficient training can be used later to make predictions about the output values of any new input dataset. During the training stage, the output from the learning algorithm is compared with the correct one and find the errors to modify the model accordingly.
- **Unsupervised machine learning algorithms:** Unsupervised learning are used when the dataset available to train the model is neither classified nor labeled. Hence, it studies how to build a function to describe a hidden structure in the unlabeled data. The system doesn't map an input to the right output. Instead, it examines the structure of the dataset and draws inferences that describe the hidden pattern from unlabeled data.
- **Semi-supervised machine learning algorithms**: Semi supervised learning combines both supervised and unsupervised learning. Both labeled and unlabeled data are used for training the algorithms, typically a small amount of data is labeled, and a large amount is unlabeled. This method considerably improves the learning accuracy of the system.
- **Reinforcement machine learning algorithms:** Reinforcement is a learning method in which an agent interacts with its environment by producing actions. Every action has some impact on the environment, and in turn, the environment provides feedback to the learning algorithm based on the action and discovers errors or rewards. The most relevant characteristics of reinforcement learning are trial and error, search, and delayed reward. In this method, machine agents automatically determine the ideal behavior within a specific task to maximize its performance.

In the engineering field, most of the machine learning applications are for labeled data, this chapter will focus on supervised machine learning. The term supervised learning

indicates that the system learns with the help of something, typically a labeled training dataset. Two groups or categories of algorithms come under supervised learning. They are:

1. Regression
2. Classification

Regression and Classification algorithms are supervised machine learning that is used for predicting future data by learning and analyzing the labeled datasets. Each one is used for different machine learning scenarios. Regression algorithms are used to predict continuous numbers such as pressure values, production rate, and oil price. While classification algorithms are used to predict the discrete values such as True or False, types of valves, and types of artificial methods (Ayyadevara, 2018).

5.3. Machine Learning Applications for Gas Lift

Artificial Intelligence is a fascinating field in generating smart or intelligent solutions to complex problems by combining human intelligence and computing power. In the recent few years, machine learning algorithms have been widely used in the petroleum industry to solve complex problems and predict the important parameters that are difficult to be estimated with traditional computer programs. The mean reason for using these algorithms is to provide a solution that is simple, easy to use, and universally applicable. Machine learning models have been applied to different areas in petroleum engineering such as reservoir, petrophysics, and production. Due to the high demand for petroleum products and low production rate, artificial lift methods are used to balance the supply and demand ratio. The gas lift process is a promising aspect regarding increasing the oil production rate. This encourages the researcher to always search for innovative technologies to overcome the difficulties and improve the gas lift system.

A model that can predict oil flow rates, gives a great advantage to the production engineers to optimize the gas lift well performance in real-time. Accordingly, much research has been carried out to implement machine learning algorithms to develop a simple, robust, and universally applicable model to optimize gas lift well production rate.

Ranjan et al. presented a single artificial neural network ANN method to predict two important gas lift parameters. The two parameters are the maximum gas injection rate and maximum oil production rate. Nodal analyses, gas lift databases, and gas lift monitoring systems are applied in this study to optimize the production rate. Various ANN models were trained and tested by varying the number of neurons in each layer, learning rate, training type, epoch, and minimum error. The ANN model proposed in this study showed better

accuracy and performance in optimizing the gas lift rate compared to previous traditional methods. (Ranjan et al., 2015)

Odedele and Ibrahim developed an approach to design a hybrid Particle Swarm Optimization Fuzzy Support Vector Machines (PSOFuzzySVM). This method is used to predict the performance of the gas lift well and to optimize the production in a reservoir. The performance of a production well is a function of several variables. The authors discussed the determination of optimal parameters for a continuous flow gas lift installation such as injection pressure, gas-liquid ratio, compressor horsepower, and injection rate which yields the maximum oil production rate using the particle swarm optimization approach. (Odedele and Ibrahim 2016)

Khan et al. adapted computational intelligence algorithms (CI), to predict oil flow rate in artificial wells. The authors utilized multiple computational intelligence methods, which have not been used previously in this area, namely, Artificial Neuro Fuzzy Inference Systems, Support Vector Machines along with Artificial Neural Network. The results showed that machine learning techniques successfully performed better than all the other empirical correlations in the literature to predict oil rate in an artificial lift gas well. (Khan et al. 2018)

Khan et al. utilized machine learning (ML) algorithms to predict oil production rate in artificial gas lift wells. A correlation is developed based on ML to accurately provide a usable equation to be applied to any field for future predictions. Various algorithms are implemented along with the development of Artificial Neural Network, namely, Artificial Neuro Fuzzy Inference Systems (ANFIS), and Support Vector Machines (SVM). (Khan et al., 2019)

When the well is decided to be converted into an artificial lift to enhance productivity, the method selection procedure performed by humans involves iterating several design parameters. The selection method required the decision-making with unbiased, repeatable, and reliable. However, a human decision is limited and cannot capture the mistake of the previous design to improve the new one also the lack of look back in the past well performances are the limits of humans. Therefore Ounsakul et al. applied the supervised machine learning method to improve the artificial lift selection process. This intelligent approach of using supervised machine learning can minimize the cost of artificial lift wells which incorporate the past performances and lessons learned from previous installations. The authors adopted a simple and accurate model for artificial lift selection and wells

performance assessment. The model is continuously modified by adding the performance of new wells for further model training. (Ounsakul et al. 2019)

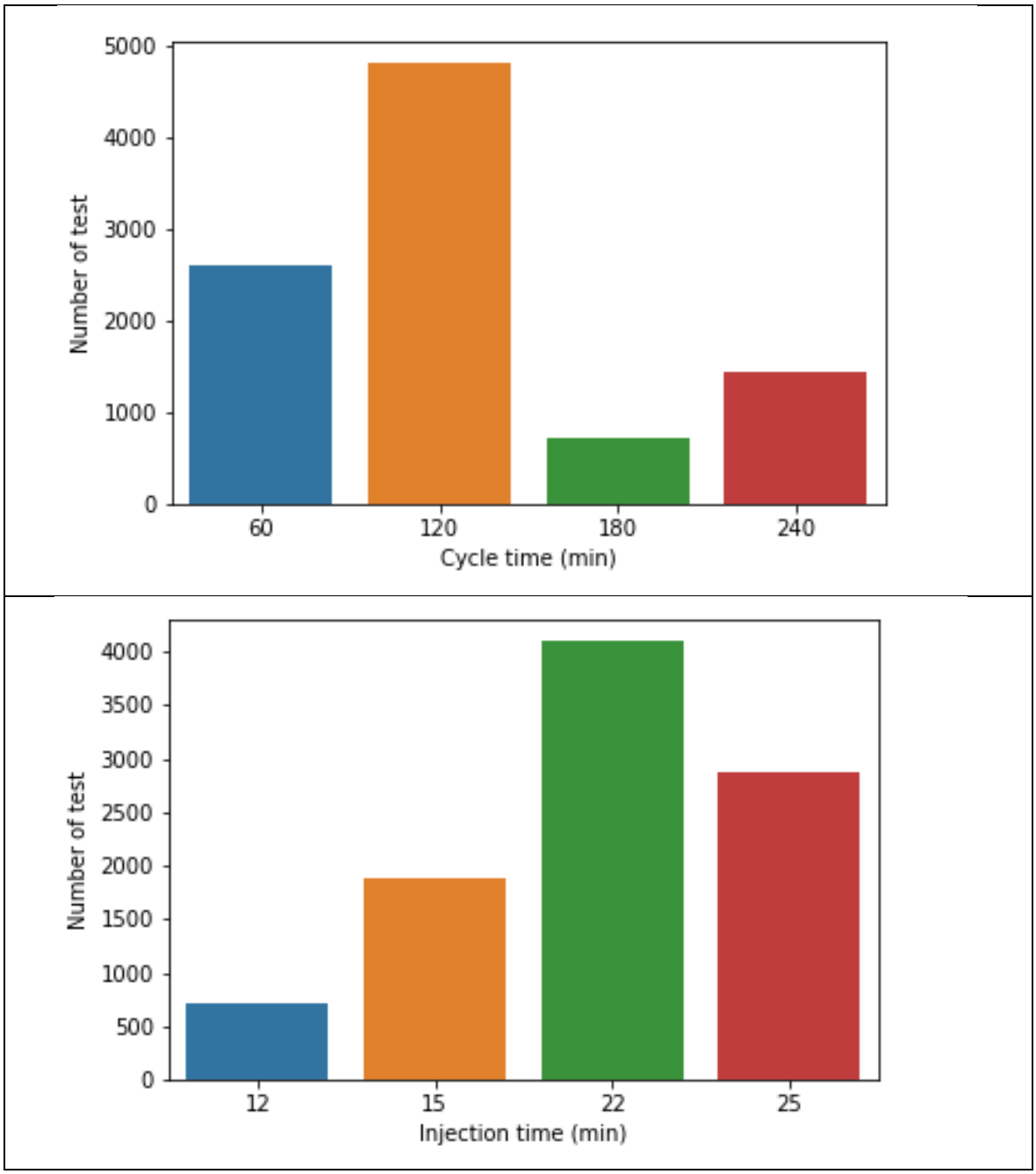

Figure 5.1. Number of intermittent test data with different a) cycle time, b) gas injection time. (edited by the Author)

Al Selaiti et al. developed a data-driven approach using Artificial Intelligence (AI) machine learning (ML) methodologies to find the optimal operating parameters for gas-lift wells. The proposed ML approach is built to instantaneously predict multiphase flow rates, gas-oil ratio, and water cut. Data at the surface are collected using a real-time sensor to build the ML model. Machine learning models can be adapted for the gas lift wells to meet the

minimum data availability expectations such as wellhead pressure, flow line pressure, and choke position. (Al Selaiti et al. 2020)

5.4. Data Acquisition and Description

A total of 9594 intermittent gas lift test data were obtained from Algyo oil wells located in the southern part of Hungary. These wells are artificially flowing using an intermittent gas lift process. During the measurements, several characteristic production parameters of the intermittent gas lifting production cycle were continuously measured and recorded. 11 different data types are available, well head pressure (Pt@s), well head temperature (Tt@s), casing surface pressure (Pc@s), casing surface temperature (Tc@s), tubing temperature at the valve depth (Tt@v), depth of injection gas (depth), oil density, tubing diameter, time of the intermittent cycle time of gas injection and tubing pressure at the valve depth (Pt@v). Table C.1 (Appendix C). lists some of the data points used for tubing pressure prediction modeling. The available dataset for training the model contains can be distinguished into 4 different intermittent cycle times and 4 different gas injection times. Figure 5.1 shows the size of each cycle time and injection time prior to pre-processing.

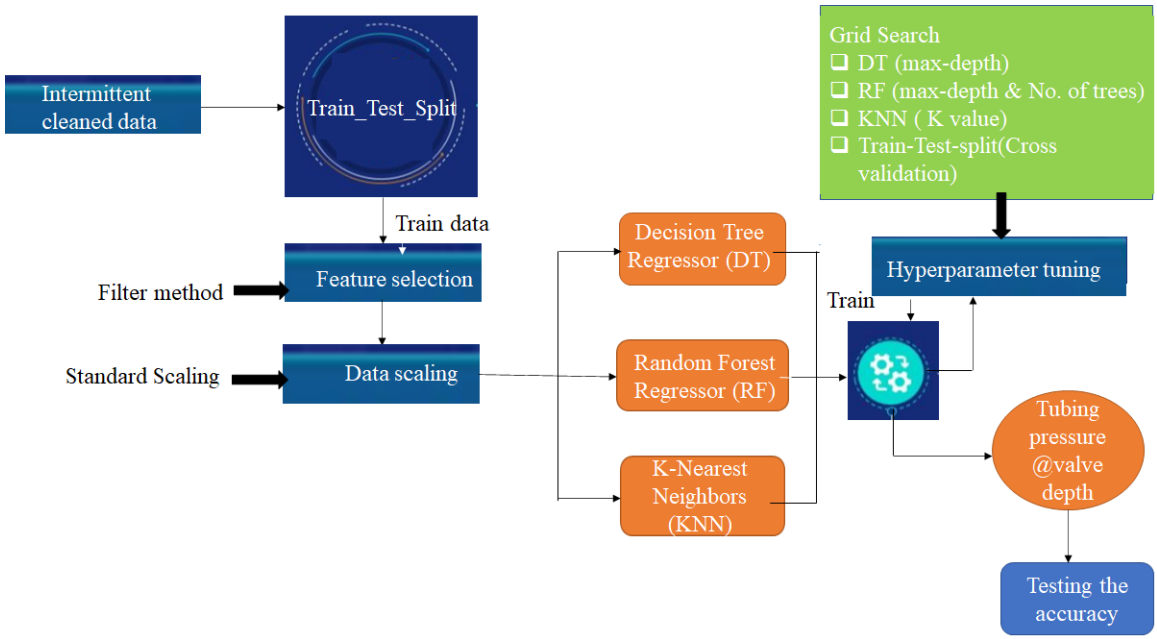

Figure 5.2. Flowchart of Machine learning models procedure. (edited by the Author)

5.5. Data analysis and Preprocessing

Data analysis and preprocessing were performed carefully in this study since the prediction performance of any machine learning model are highly dependent on the quality of the data. Figure 5.2 shows a summary of data preprocessing and model training used in this research. After the data is collected from the Algyo oil wells, the first step to preparing

the data for machine learning models is data preprocessing. Data preprocessing is the most important part of machine learning projects, it takes about 80% of the whole modeling procedure. I prepared the data for machine learning models as follows:

5.5.1. Data Cleaning:

Data cleaning refers to identifying and correcting errors in the dataset that may negatively impact a predictive model. For this data, the cleaning is down as fellow:

- Remove null values in the rows.
- Remove duplicate rows.
- Remove any inconsistency and redundancy in the data.

5.5.2. Train-Test-Split:

The train-test split technique is used to evaluate the performance of machine learning algorithms when the models are used to make predictions on data not used to train the model. Split the data into two subsets, one set is used to build and train the model and the second part is used to validate the model. A total of 9594 test data were divided randomly into two sets with a proportion of 70:30. The set with 70% of the dataset (6715 data points) was used for training the selected models, and the other set with 30% of the dataset (2879 data points) was used to test the prediction capabilities of the trained models. A complete statistical description of the selected data used in the training and testing of the model is given in Table C.2 (Appendix C).

5.5.3. Feature Selection:

Feature selection is the process of automatically selecting those features which contribute most to the prediction variable or output. Since there are 10 input attributes in a dataset, it is important to select the right amount of them because too many attributes for training the model result in time-consuming and overfitting. The first most imperative step taken in the process of data analysis of this study was to plot the attributes correlation matrix as shown in Figure 5.3. The correlation range between (-1 to +1), if the correlation is greater than zero that is mean that the two variables are positively correlated whereas correlation less than zero means negative correlations between the variables. It can be seen from this data exploration that some input parameters have a strong positive or negative correlation with each other and with the tubing pressure at injection valve depth (Pt@v).

The filter method is selected in this study to reduce the number of input data. A high correlation between the variables is often a useful property, if two variables are highly correlated, we can predict one from the other. If two parameters are highly correlated among

themselves, they provide redundant information in predict the target output. In this case, the second variable does not add additional information to the model, so removing it can help to reduce the dimensionality, and essentially, the target can be predicted more accurately with just one of these redundant variables. The correlation between each input parameter was calculated using Pearson's correlation coefficient method. The filter process based on correlated parameters reduces the number of elements from 105534 to 67158. Accordingly, the following parameters were finalized to be used as the input:

- Well head pressure (Pt@s),
- Well head temperature (Tt@s),
- Casing surface pressure (Pc@s),
- Tubing temperature at the valve depth (Tt@v),
- Time of the intermittent cycle (cycle time), and
- Time of gas injection (injection time)

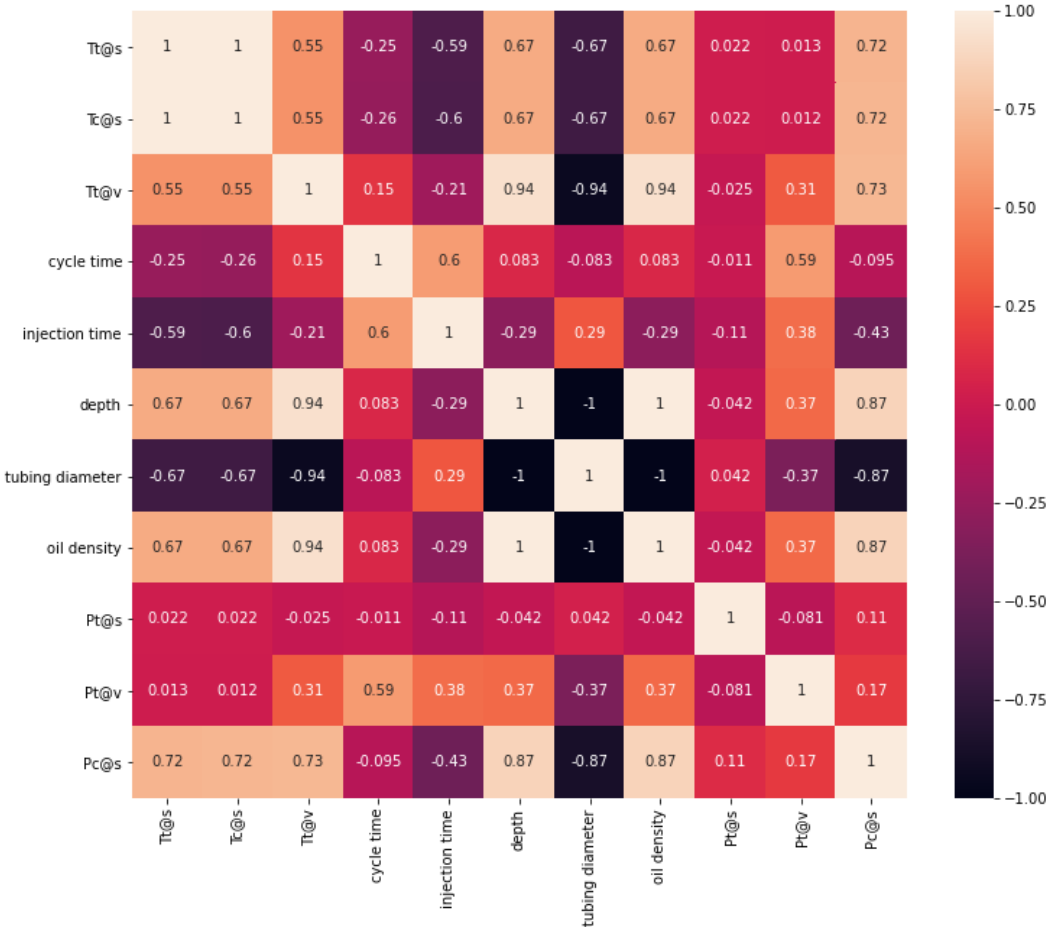

Figure 5.3 Correlation plot of all attributes in intermittent dataset. (edited by the Author)

5.5.4. Data Scaling:

Data scaling is performed in this study during the data pre-processing to handle the highly varying units and values of the data. This technique is used to standardize the independent input variables of the dataset in a fixed range. If feature scaling is not done, the machine learning algorithm tends to consider the weight of the greater values, higher than the smaller values regardless of the variable's unit. There are two methods for data scaling, the MinMax method, and standard scaling. The standard scaling method is used widely to scale the data by converting the dataset from normal distribution to a standard one. Standard distribution is the distribution of the data with a mean of zero and a standard deviation of one. To scale the data, each point in the dataset subtracts from the mean and divided by the standard deviation.

5.6. Machine Learning Algorithms

Three different machine learning algorithms namely, Decision Tree (DT), Random Forest (RF), and K-Nearest-Neighbors (KNN) are used in order to predict the tubing pressure at the gas injection depth in intermittent gas lift wells. Field data from the Algyo field in Hungary is used to build and evaluate the model.

5.6.1. Decision Tree Regressor (DT)

The Decision tree regressor (DT) is used for the output problem with continuous numbers or values. It observes all the independent variables in the entire dataset and trains a model in the structure of a tree to predict meaningful output in the future. The DT includes the following components as shown in Figure 5.4:

- Root node: This node represents the beginning of the tree and gets divided into two or more homogeneous sets.
- Splitting: A process of dividing a node into sub-nodes based on a rule or decision.
- Decision Node: represents an attribute or feature splits into further sub-nodes.
- Leaf/Terminal node: The final outcome in a decision tree.
- Branch/Sub-tree: A subsection of an entire tree.

When splitting the root node, the original dataset, we first need to determine the attribute based on which the first split has to be made. In this model for example whether to split with well head pressure, cycle time, depth…etc. Information Gain term is used to split the DT. Information gain measures the reduction in entropy (uncertainty) after a specific split of a dataset. The root node is considered as the place where maximum uncertainty exists then,

the intelligent split occurs in the direction of decreasing the uncertainty. Thus, the choice of the split should be based on which attributes decrease uncertainty the most.

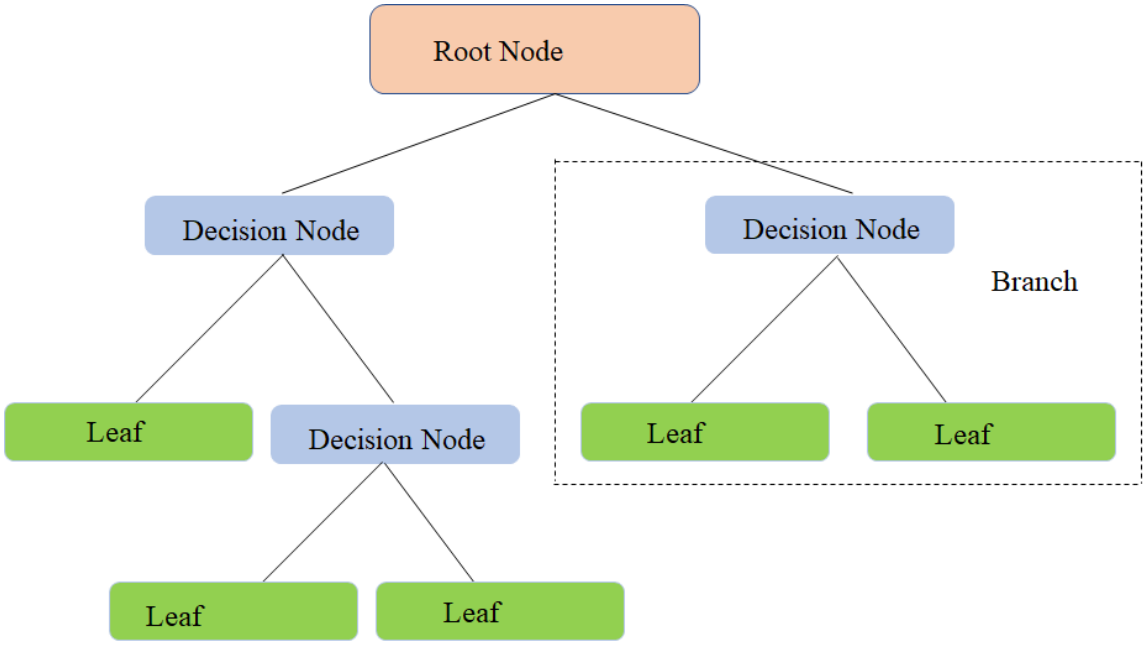

Figure 5.4. Components of Decision Tree (edited by the Author)

5.6.2. Random Forest Regressor

A random forest regressor (RF) randomly selects observations from the data set to build multiple decision trees and then gets the output prediction value from each of them and finally selects the best solution by means of averaging as shown in Figure 5.5. Decision trees can be overfitted by the training data in some cases and also having correlated variables may result in the incorrect feature being selected for splitting the root node. Random forest overcomes those challenges by building multiple decision trees, where each decision tree works on a sample of the data. Random forest adopts the bagging approach in selecting the samples for the DT models. Bagging is short for bootstrap aggregating which refers to randomly selecting a sample (few rows) from the original dataset and taking the average of predictions output from all the decision trees models that are built on the sample of the dataset. The predictions in this way are less likely to be biased due to a few outlier cases.

5.6.3. K-Nearest -Neighbors Regressor

K-Nearest -Neighbors regressor (KNN) method is a non-parametric algorithm, it does not make any assumptions about the distribution of data. It approximates the association between independent input parameters and the continuous dependent outcome by averaging the observations in the same neighborhood. This means that the new data is assigned a value

based on averaging the nearest samples based on the K value, for example, if K is three then the new data prediction is the average of the nearest three samples and if K is five, then the new data prediction is the average of the five nearest samples and so on.

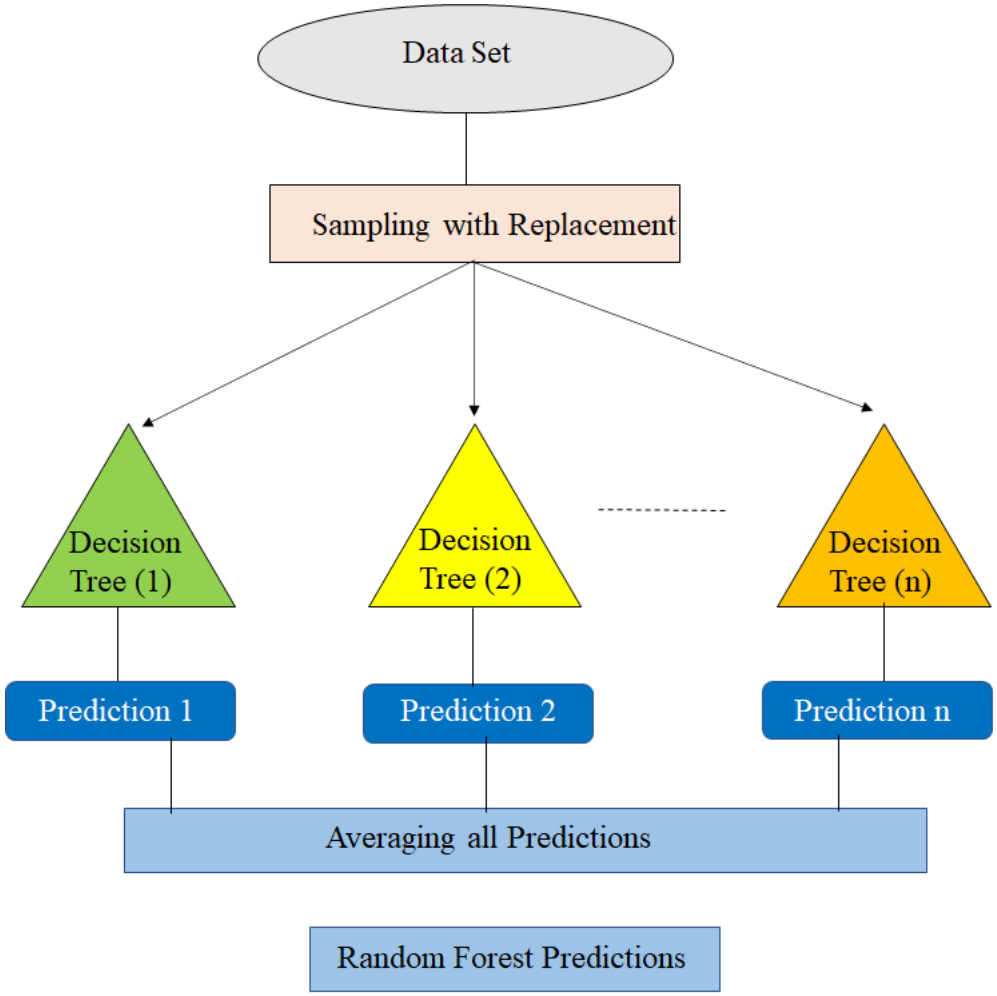

Figure 5.5. Random Forest model flowchart. (edited by the Author)

5.7. Grid Search for Models Tuning

Each machine learning model has multiple parameters that are not trained by the training set. These hyperparameters are particularly important in any machine learning project because they control the accuracy of the model. Therefore, the hyperparameters should be configured before the model is trained and the optimum parameters are provided later to the selected model. The tuning parameter for the decision tree is the maximum depth of the tree so, this parameter is tuned by selecting different values of the depth. The deeper the tree means the more splits it has, and it captures more information about the data.

Parameters to tune in a Random Forest are the sampling method and the number of features to be taken for each tree. The sampling method (bootstrap) can be with replacement

or without replacement. In each tree in the Random Forest, the number of features can be taken as all the features to train the model or the square root of the features.

The size of the neighborhood (K) in KNN needs to be set in order to select the size that minimizes the mean-squared error. Different K values are selected as tunning parameters.

Grid-search is used to find the optimal hyperparameters of a model which results in the most 'accurate' predictions. To select the optimum hyperparameters, each model is trained and evaluated for different sets of parameters to select the optimum one. The cross-validation technique is used to split the data for the train and test. In this technique, the dataset is divided into K-folds, and the model is trained in K-1 folds and tested in 1 K as shown in Figure 5.6**.** By iteration through the train/test comparison several times, a better estimation of the model performance is achieved. This check that the model is not performing differently after being trained on differently labeled data. The result of hyper parameters is shown in Table 5.1.

Table 5.1. Optimum Machine learning models parameters (edited by the Author)

Model	score	Best parameters
Decision Tree	0.99982	Max-depth=50
Random forest	0.99987	Bootstrap=True, max feature= auto
K-Nearest Neighbors	0.99920	K=2

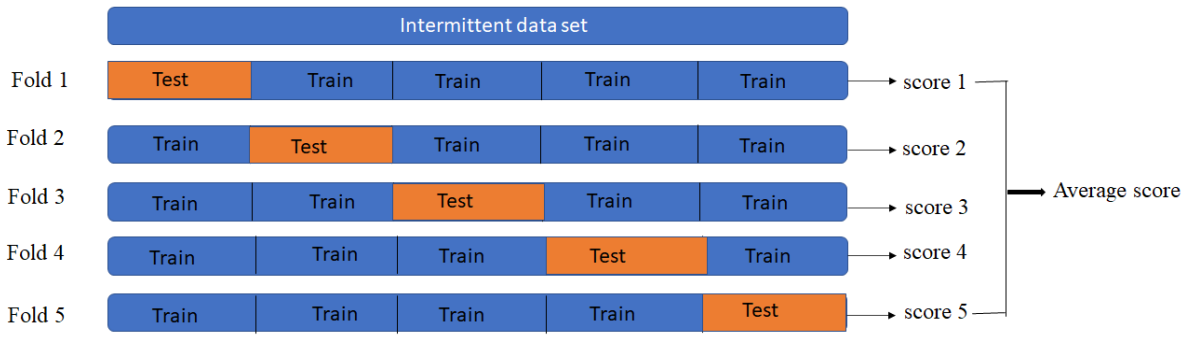

Figure 5.6. Cross validation of machine learning models using 5 K-Folds. (edited by the Author)

6. RESULTS AND DISCUSSION

6.1. Description of Intermittent Gas Lift Dynamics

The CFD simulation results are analyzed for two different injection pressures 40 & 50 psig. The contour of the oil volume fraction factor is plotted for various times and locations along the pipe to describe the transient nature of intermittent gas lift flow, as shown in Figure D.3 (Appendix D). At the initial time, the liquid length inside the tube is 9 m, and the remaining length of the tube is filled with air. The gas is injected at high pressure below the accumulated liquid column through the intermittent gas lift valve to push the liquid as a slug upward to the surface. The high-pressure gas travel at an apparent velocity greater than the liquid slug velocity resulting in penetrating the liquid slug. Due to this penetration, a part of the liquid falls back into the gas phase as a droplet and as a liquid film on the pipe wall. As the injection time increase, the expanded injection gas pushes the liquid film to the well head, and the thickness of the film decrease with the time.

Figure D.4 (Appendix D) shows vertical and horizontal cross-section planes at the same depth and same injection time to study the effects of the injection pressure on the liquid film thickness. As can be seen from the figure that the thickness of the liquid film decreases with increases in the gas injection pressure from 40 psig to 50 psig. The physical characteristics of the intermittent process cycle show good compatibility with the description of the intermittent gas lift process from the literature (Brill et al., 1967; Ortiz and Lagoven, 1990; Liao et al., 1995).

6.2. Study the Slug Velocity Profile with Gas Injected Time

The slug velocity with the gas injection time is shown in Figure 6.1 A for two different injection pressures (40 psig and 50 psig). The results from the CFD model are compared with the results from the literature in Figure 6.1 B to validate the simulation accuracy. The results of the developed model show a good agreement with the literature. From the figure, one can describe the slug velocity characteristics as follow:

1. At the initial period of gas injection, the slug is rapidly accelerated.
2. Then, the slug velocity reaches almost a constant value.
3. Finally, the slug is rapidly accelerating again when the liquid is produced at the surface.

As the injection pressure increase from 40 psig to 50 psig the slug velocity increase and this is due to the expansion of the gas injected under the slug which causes the slug to rise to the surface rapidly. Also, when the pressure of the injection gas increase, the time required

for pushing the slug to the surface is decreased. In the present study, the injection time required for the slug to reach the surface is 1.44 seconds, for a gas pressure of 40 psig and 1.2 seconds for a gas pressure of 50 psig.

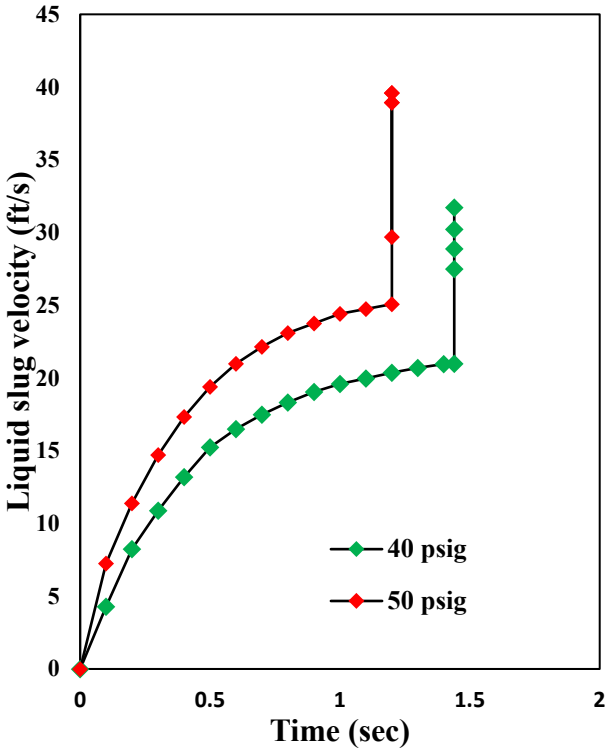

(A) (edited by the Author)

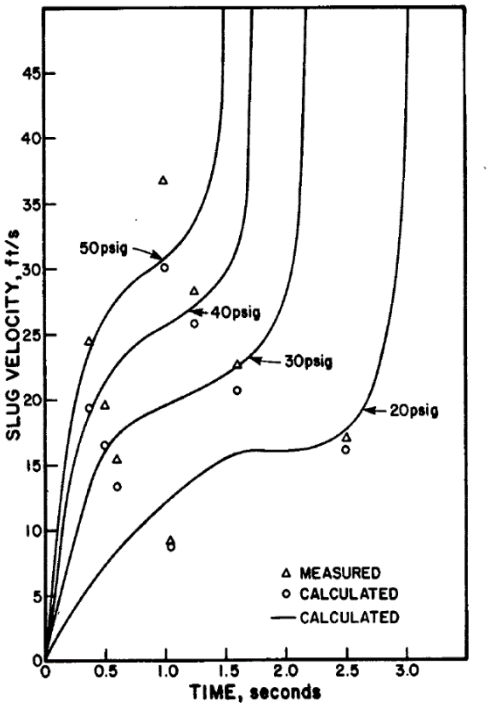

(B) (Schmidt et al., 1984.)

Figure 6.1. Liquid slug velocity vs. injection time, (A) The CFD results developed in this study (Case 1) (B) (Schmidt et al., 1984.)

6.3. Study the Liquid production with Gas Injection Time.

The liquid recovery with injection time is obtained from two different gas injection pressures. Figure 6.2 A shows the fraction of liquid produced from the slug core is about 0.366 (36.6% of the total liquid) for injection pressure of 40 psig and about 0.392 (39.2 % of the total liquid) for injection pressure of 50 psig. It is observed that when the injection pressure increases the liquid production increase. Also, when the injection time increases, the liquid production increase because of the liquid produced from the film. From the figure, it can be seen that the larger portion of production is coming from the liquid (after flow). In Figure 6.2 B, the liquid production fraction is compared with the liquid fraction from the literature to validate the results of the developed model.

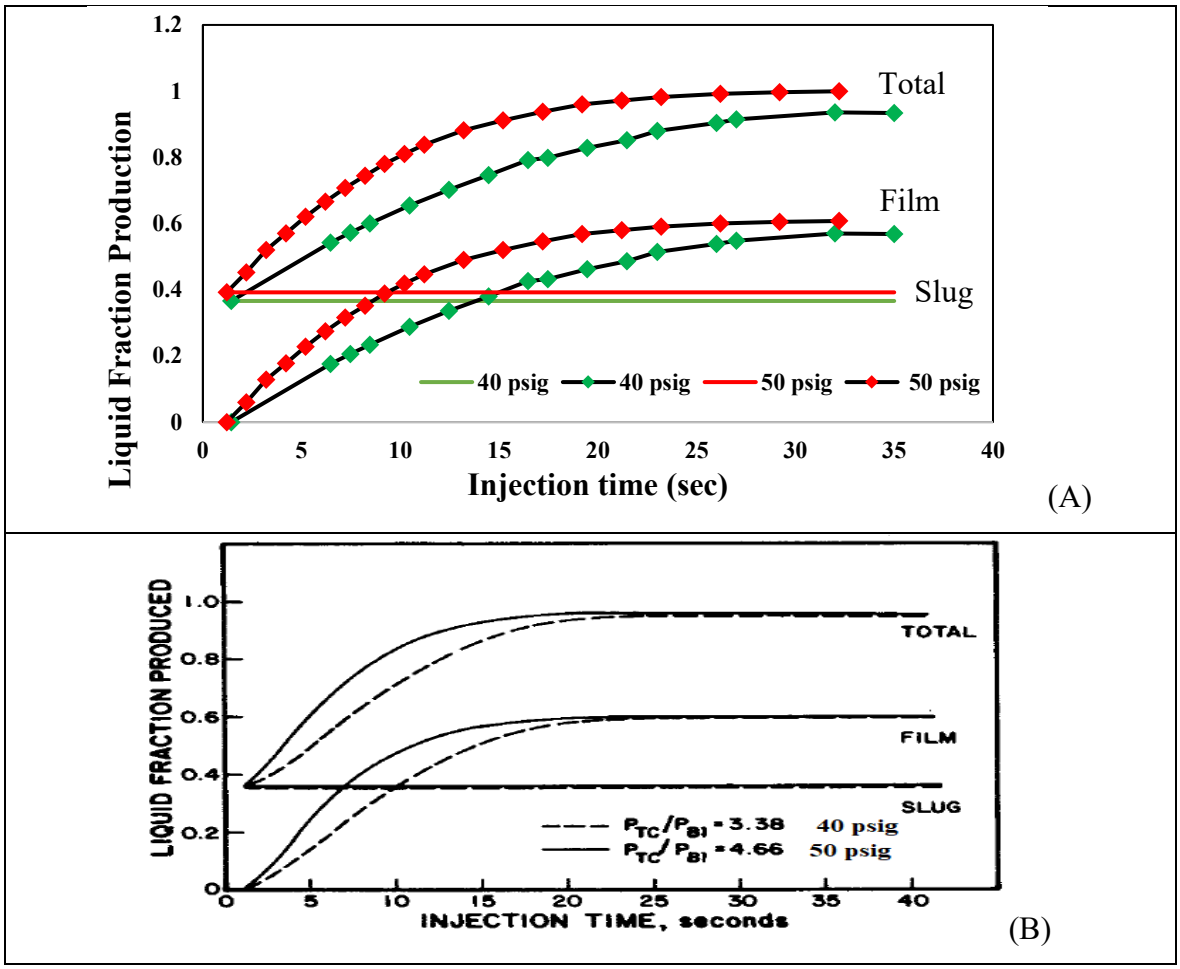

Figure 6.2. Liquid production vs. injection time: (A) The CFD results developed in this study (Case 1) (edited by the Author) (B) (Schmidt et al., 1984.)

The oil volume fraction at the tubing outlet changes with gas injection time and gas injection pressures. At the initial time of simulation, the oil holds up in the tubing outlet is zero. Then, when the gas is injected, the liquid slug is raised in the tubing up to the surface. The oil fraction starts to increase rapidly to (100% oil) when the core of the slug reaches the tubing outlet. Then, the slug starts to produce at the surface. As soon as the head of the gas bubble reaches the surface, the oil volume fraction starts to decrease rapidly, but it does not reach zero due to the liquid film. As discussed before when the injection pressure increases the thickness of the liquid film decrease and this can be observed in the liquid hold-up charts. Figure D.5 (Appendix D)

6.4. Dimensionless Analysis for Liquid Production Rate

The effect of different parameters on the amount of liquid production percent during an intermittent cycle has been studied. The initial variables of injection pressure, tubing pressure, submergence length, and valve depth are related to the liquid production fraction for a certain tubing size and valve diameter. To minimize the number of variables and the

complexity of the system, the dimensionless ratios rather than the actual values are used to study the system. The dimensionless ratios of the Pi/Pt (injection pressure/tubing pressure) and the S/D (submergence: initial liquid length in the tube/ injection depth) are related to the dimensionless production ratio N/S (production/submergence). Figure D.6 (Appendix D) shows the vertical cross-section plane of different geometry used in this study at the initial time of the simulation.

The gas is injected at a certain gas flow rate under the accumulated liquid through the gas lift valve and the injection gas is ceased when the liquid slug reaches the surface of the tubing string. The slug continues to produce as far as the expansion energy of the gas beneath it is sufficient to produce the entire slug. During the slug production period, part of the liquid is falling back as liquid film near the wall or/and liquid droplet due to the high slippage velocity of the gas. Figure D.7 (Appendix D) shows an example of the velocity vector of the liquid fall back. The liquid film is moving down along the tube wall according to the gravity direction and the liquid fall back and accumulates again in the bottom of the tube to join the new cycle.

The liquid produced in the cycle can be calculated from the initial liquid slug volume minus the liquid falling back into the tube. The dimensionless production ratio N/S is plotted versus the dimensionless submergence depth ratio S/D as shown in Figure 6.3 for the tubing size of 2.375 in. and 2 in. The results are compared with the production chart of White et al. to validate the CFD model. (White et al., 1963) It can be concluded that in a certain submergence ratio, the recovery percent increases as the injection pressure increases.

Figure D.8 (Appendix D) shows an example of the slug proceeding for two different injection pressures at the same injection time, tubing size, and initial submergence height. It can be concluded that as the injection pressure increases, the slug velocity increases and reach the surface faster so that, the liquid production would be increased. As the submergence height increases, the production percent also increases at given injection pressure. The currently developed model shows a good agreement with the literature data.

Studying the pressure profile during the intermittent gas lift cycle is an interesting topic in the oil industry that received special attention from the researchers for the efficiency and proper design of the system (Shahaboddin et al., 2005). The pressure gradient along the pipe length at different injection times can be plotted using CFD simulation and a sample of the pressure gradient is shown in Figure D.9 (Appendix D).

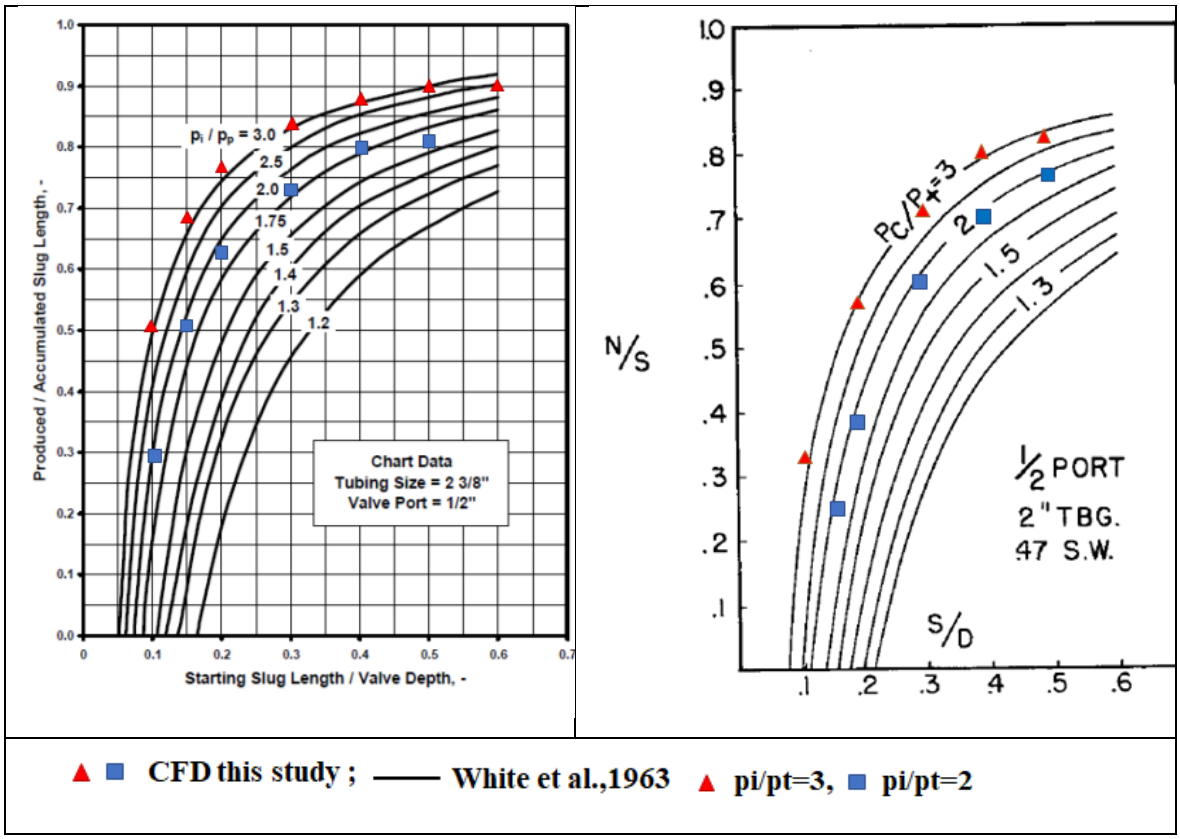

Figure 6.3. Liquid production percent for two different injection pressure and tubing size (CFD Case 2). (edited by the Author)

The pressure change with time for a certain position inside the tube can also be plotted using CFD simulation and a sample of the pressure profile is shown in Figure D.10 (Appendix D). To describe how the pressure changes at a certain position in the tube with the slug movement progress, an example is described in Figure 6.4. Before the gas is injected into the tubing, the pressure at any point along the pipe is equal to the hydrostatic pressure. When the gas is injected into the tube, the pressure began to increase inside the tube until the gas bubble is reached the studied position (Figure 6.4 a). Then the pressure remains constant at that position because of the effect of liquid film near the wall. The pressure inside the tube starts to decrease as soon as the gas injection stops when the liquid slug reaches the tube surface (Figure 6.4 b).

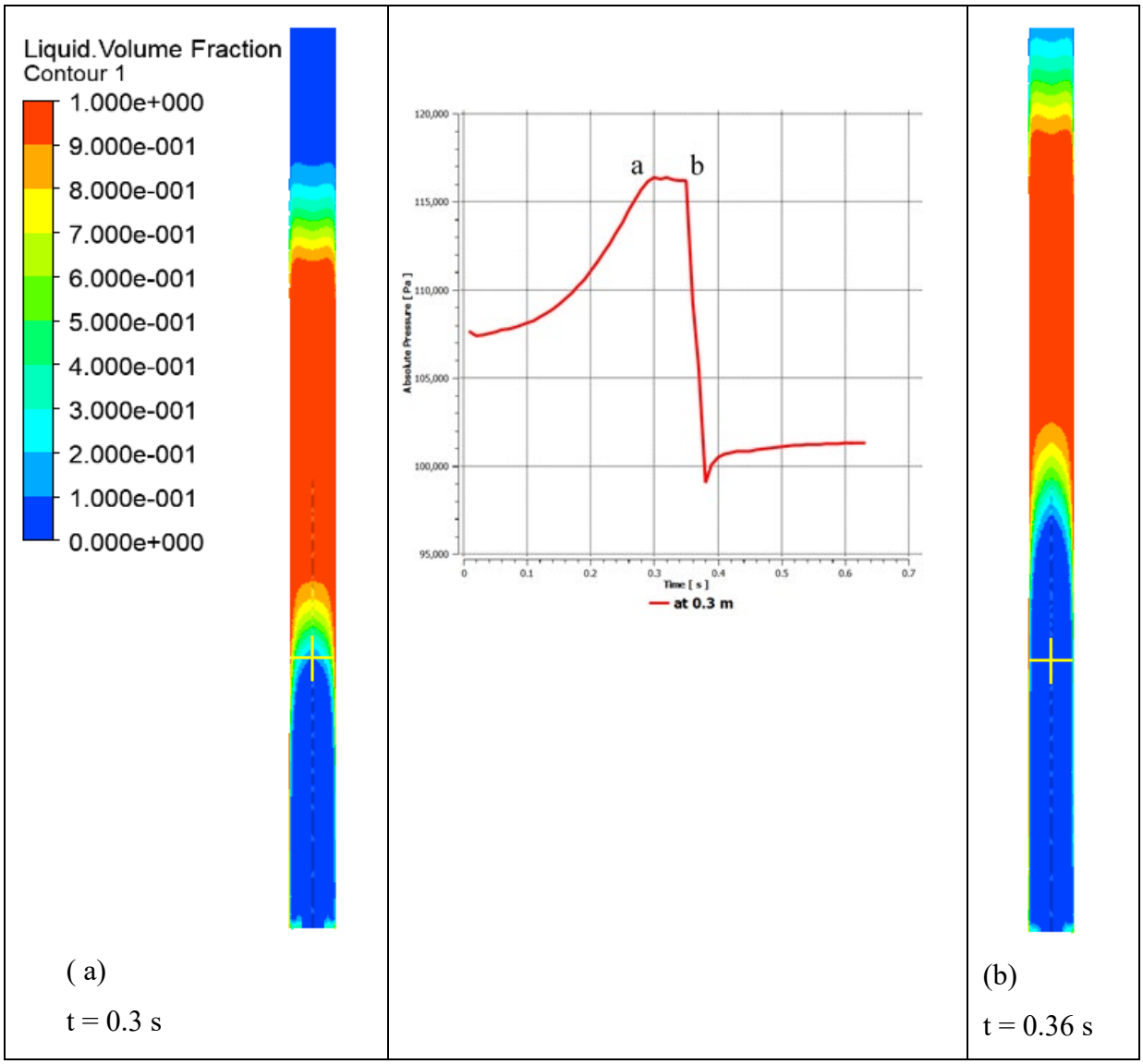

Figure 6.4. Tubing pressure with injection time at 0.3 m (tubing size 2 in. and Pi/Pt=3). (edited by the Author)

6.5. Gas Injection Through Intermittent Pilot Valve

6.5.1. Study of Velocity Field

The velocity contour is plotted using CFD results for different conditions. One example of a vertical cross-section plane of the velocity contour is shown in Figure E.1 (Appendix E). The velocity tends to increase in the area around the power piston due to fluid acceleration. The throat corresponds to the gap around the power piston and shows a high-velocity gradient that cannot be predicted during experiments and mathematical models. Similar observations have been noticed for different operating conditions.

6.5.2. Study of Mach Number

Mach number is a dimensionless quantity that represents the ratio of flow velocity to the local speed of the sound. Figure E.2 (Appendix E). shows an example of the Mach number contour results for the simulated space flow. Mach number corresponds to compressible flow increase near the throat area as a result of fluid acceleration.

6.5.3. Study of Pressure Field

The pressure contour of an elongated plane is plotted, and one example is shown in Figure E.3 (Appendix E). It can be noticed that the pressure is reduced in the throat area around the power piston. The explanation of this behavior is the inverse relationship between the pressure and the velocity, as the fluid accelerates in the throat, also the pressure drops. The area around the power piston shows a high-pressure gradient.

6.5.4. Study of Temperature Field

Bernoulli's law for the steady-state flow with no heat and work added to the system can be stated as follows:

$$\dot{m}\left(u + \frac{p}{\rho} + \frac{v^2}{2} + gz\right) = const.$$

Where $\dot{m}$ is mass flow rate (kg/s), u is internal energy (J), p is pressure (Pa), ρ is density (kg/m^3), v is velocity (m/s), g is acceleration gravity (m/s^2) and z is elevation (m).

Bernoulli's principle states that an increase in the speed of a fluid occurs simultaneously with a decrease in pressure or a decrease in the potential energy. By neglecting potential energy, relating density to temperature and pressure from a perfect gas law, and internal energy to the temperature, it can be included that the temperature would be changed to overcome the velocity change. Figure E.4 (Appendix E). shows an example of the temperature contour results. It can be seen that the temperature drops near the throat area (about a 2% reduction) as a result of the velocity increase. For nitrogen charged pilot valve, the high flow rate of the injection gas through the main section cools the nitrogen in the dome to overcome the increase in the gas velocity. When the temperature drops, the pressure also drops, and the valve tends to close at a pressure lower than the valve closing pressure intend, the volume of the gas injected per cycle could be larger than expected.

6.5.5. Modeling of Gas Flow Rate Through the Pilot Valve

The valve performance curve describes the dynamic behavior of the pilot valve and represents the gas flow rate through the valve for different injection and production pressure. The gas flow rate is calculated for different conditions using CFD simulation as shown in

Figure 6.5. Table F.1 (Appendix F) illustrates the gas flow rate results for different operation conditions used in this study.

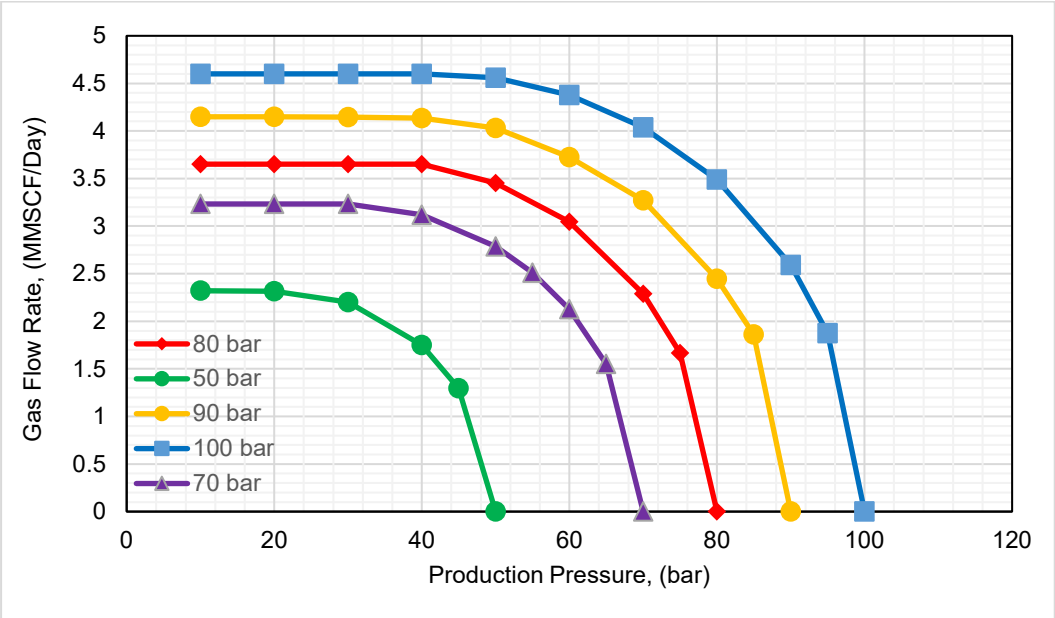

Figure 6.5. Pilot valve performance curve from CFD model. (edited by the Author)

The orifice flow equation for flow through a restriction in different forms is derived from the Thornhill-Craver model (equation 2.1). This equation can be used to calculate the gas flow rate through a gas lift valve as long as the discharge coefficient is known for the studied valve.

The discharge coefficient is a ratio between what actually will pass through an opening and what ideally can pass. On the other hand, since the flowing fluid in this geometry is gas, the expansion coefficient has to be considered. Based on the gas flow rate data collected at TUALP, a group of researchers developed an equation to predict the gas flow rate in the gas lift valve by introducing the non-constant discharge coefficient (equation 2.2). C_dY is linearly related to the pressure ratio. Using CFD results the following procedure steps are used to develop a general equation of the non-constant discharge coefficient of a 1-inch pilot valve that can be used for further calculations without using the CFD model:

1. Gas rate is calculated from CFD simulation for different conditions. Table F.2 (Appendix F) illustrates the input data used to calculate the C_dY.
2. C_dY is back calculated using equation 2.2 for different values of gas flow rates.
3. C_dY is plotted against as shown in Figure 6.6.
4. A general equation for C_dY is obtained using linear regression.

$$C_d Y = m\frac{(P_i - P_p)}{P_i \cdot k} + b$$

Where;

m= -0.217; b= 0.3229

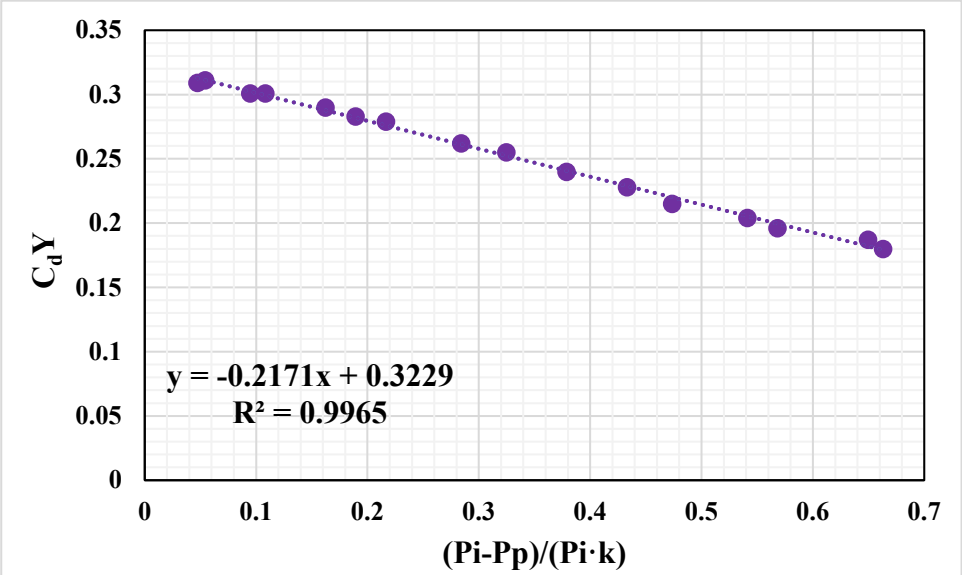

Figure 6.6. $C_d Y$ correlation of 1-inch pilot valve (edited by the Author)

Figure 6.7 shows an example of the CFD results in the present study that has been compared with the Thornhill equation using a constant value of discharge coefficient and with the TUALP equation using the non-constant discharge coefficient equation. The constant value of the discharge coefficient shows over predicts the gas flow rate through the pilot valve and the difference increases with increases in the flow rate.

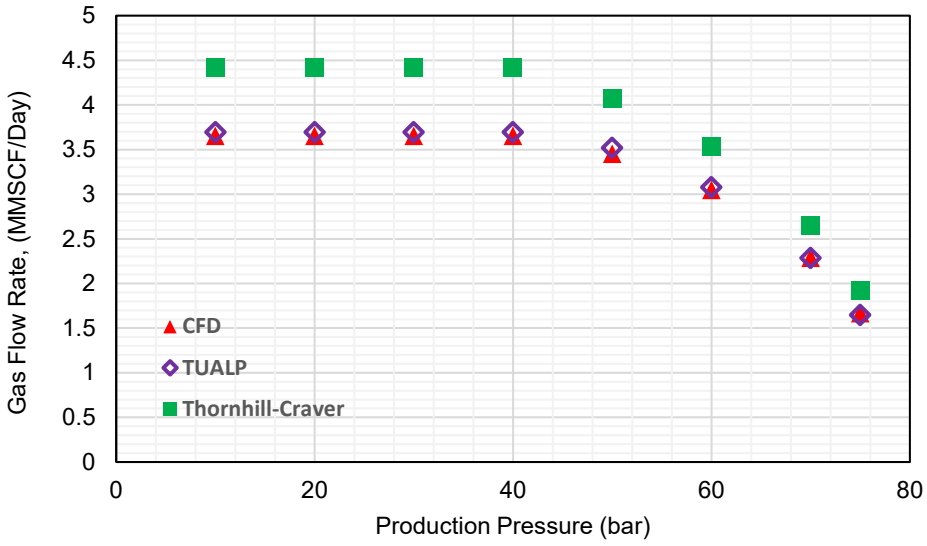

Figure 6.7. Comparison of CFD results with orifice equation. (edited by the Author)

6.6. Prediction of Tubing Pressure Using Machine Learning Algorithms

After the data preprocessing steps, the selected machine learning models were built on the training dataset. The evaluation of each algorithm was essential to ensure the quality of the employed model. The models are fit to the training dataset and then used to predict the tubing pressure for the training and testing dataset. A graphical description of the results is presented in Figure 6.8. which shows a comparison between the actual tubing pressure and ML model predicted values for both the training and testing data and also the figure displays the correlation of determination (R^2) for each model. Although there is a small variance in the prediction accuracy for the ML models, it can be seen that the tubing pressure can be predicted with high accuracy using the three selected machine learning algorithms.

The comparison between all the ML methods which were used in this study is based on minimum root mean square error (RMSE) and the highest coefficient of determination. Table C.3 (Appendix C) shows the RMSE and the R^2 values of the three models for both the training and testing datasets. This comparison clearly shows the power of the ML models in predicting tubing pressure during the intermittent process in our case. Figure 6.9 and Figure 6.10 show the comparison between the machine learning models based on RMSE and R^2 respectively.

The residual for each ML method is studied as shown in Figure 6.11. From the values of the RMSE, R^2, and the residual, it can be concluded that the decision tree model performs better than the others model in the prediction of the tubing pressure from the training data set, whereas the Random Forest model performs better than the others in the prediction of the testing dataset. The KNN model gives the highest RMSE, lowest R^2, and highest residual range than the other models.

Root of Mean Square Error = $\sqrt{\frac{\sum_i^N (predicted\ Pt@v - actual\ Pt@v)^2}{N(Number\ of\ data)}}$

Coefficient of determination $R^2 = 1 - \frac{\sum_i^N (actual\ Pt@v - predicted\ Pt@v)^2}{\sum_i^N (actual\ Pt@v - mean\ Pt@v)^2}$

$mean\ Pt@v = \frac{\sum_i^N actual\ Pt@v}{N(Number\ of\ data)}$ The residual = actual Pt@v - predicted Pt@v

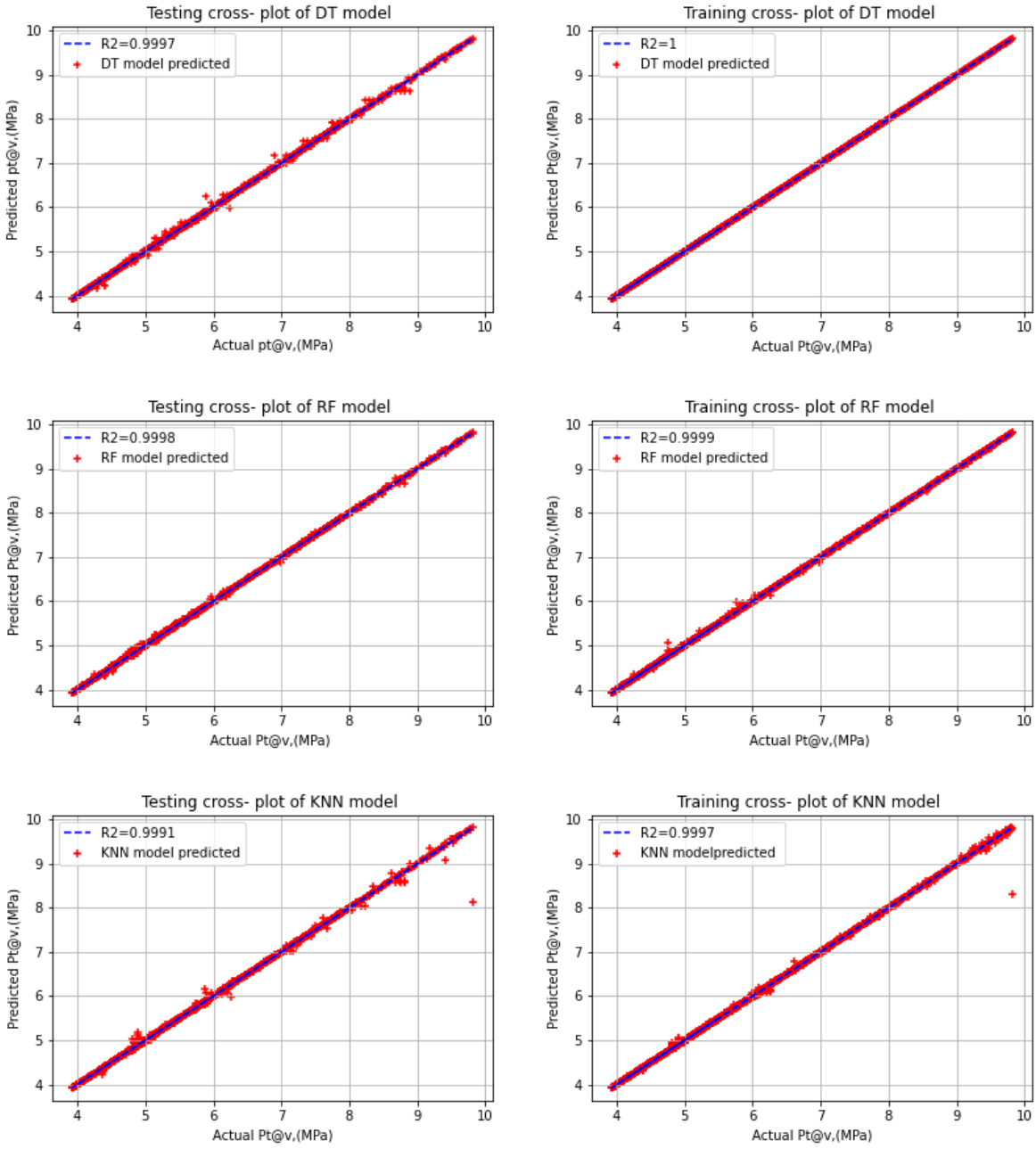

Figure 6.8—Cross-Plot between Actual and Predicted tubing pressure at the valve depth. (edited by the Author)

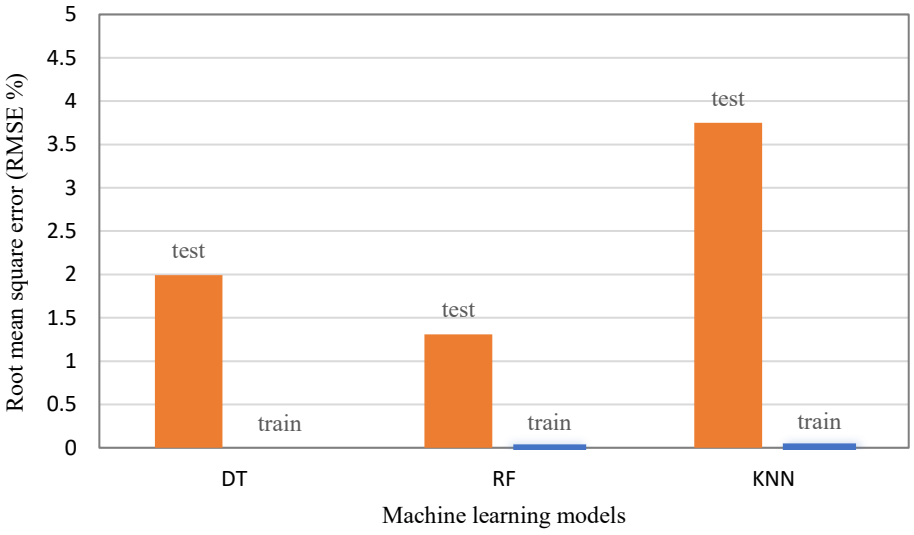

Figure 6.9. Root Mean Square Error for the developed machine learning models. (edited by the Author)

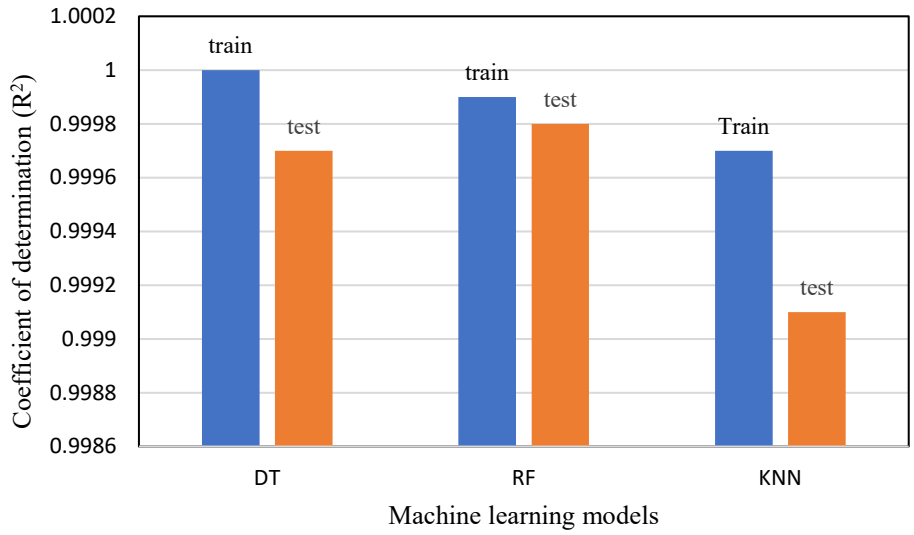

Figure 6.10. Coefficient of determination for the developed machine learning models. (edited by the Author)

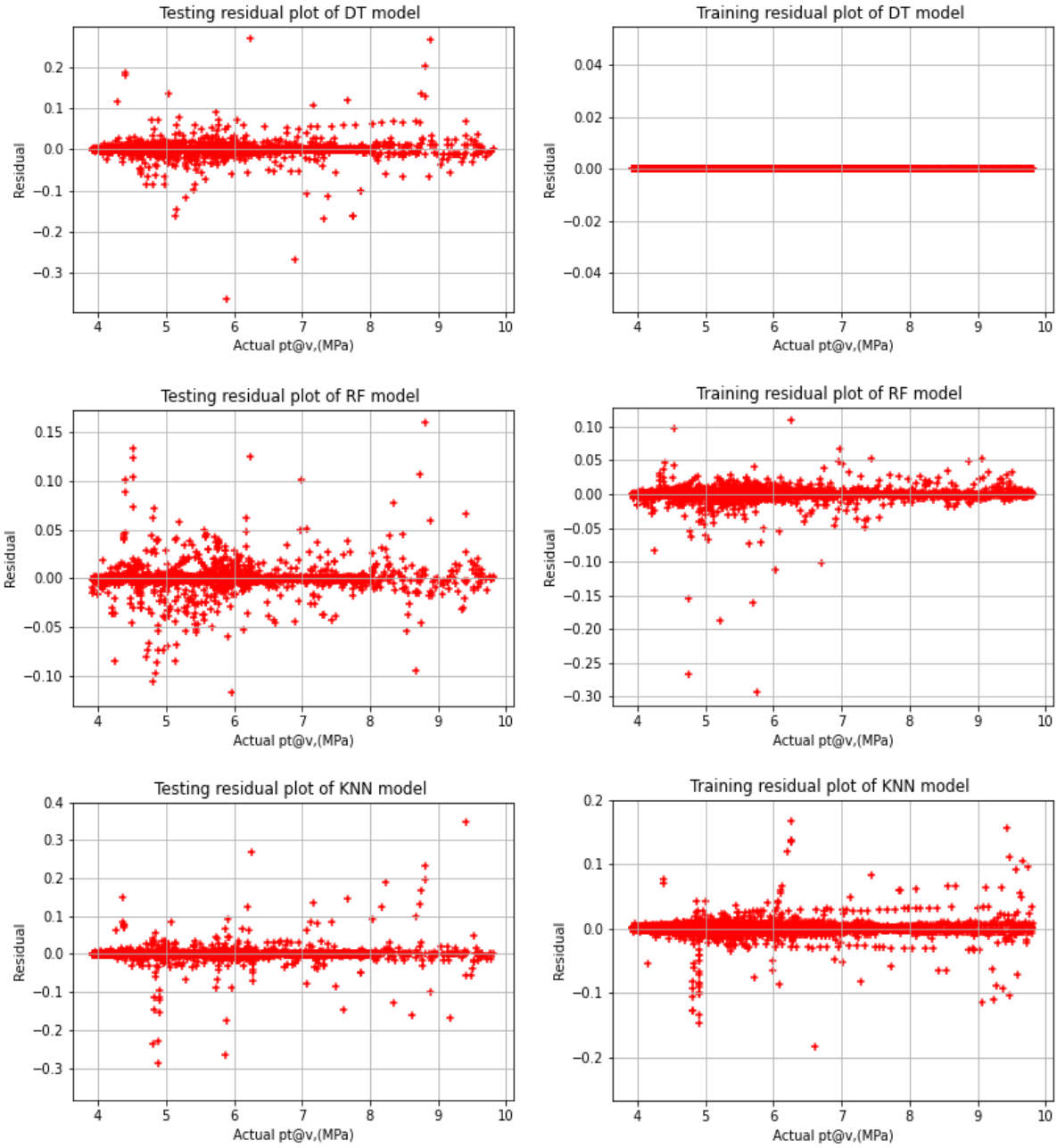

Figure 6.11— Cross plot between Actual tubing pressure at the valve depth and residual from ML models. (edited by the Author)

7. CONCLUSIONS AND RECOMENDATION

7.1. Conclusions

Intermittent gas lift is a complicated process that involves many interaction parameters making the modeling and studying of the process associated with many assumptions that reduce the accuracy of the models.

The computation fluid dynamic model is developed to investigate the transient flow behavior of the intermittent gas lift process. The multiphase VOF model with k – ε and RNG viscose model is used to model the multiphase flow. The results from the developed numerical model show a good match with the experimental results in the literature. The results show that the new model can be successfully applied to simulate the intermittent gas lift process with high accuracy. The velocity profile is studied for two different gas injection pressure and shows three regions; rapid acceleration at the initial time of gas injection and then the almost constant velocity until the liquid slug reaches the tubing surface and finally the rapid acceleration again when the liquid starts to produce. The liquid production fraction is increased with the injection time as a result of entrained liquid production in the gas core.

A computation fluid dynamic model is presented in this research to physically describe the intermittent process and study the effect of different parameters on the dynamic behavior of the system. One of the most useful tools for the study of complex systems in fluid mechanics is reducing the system to a dynamically similar model. Grouping the well parameters into dimensionless ratios have the advantage of minimizing the complexity of the system and the time required for the simulation.

The percent of the liquid product is related to the injection pressure and the submergence depth at given tubing and valve size. The results obtained from the simulation are compared with the experimental results from open literature to validate the model accuracy. The production rate increases with the increase of tubing size, length of the initial liquid in the tubing, and injection pressure. There is no significant change in the production rate could be observed when the submergence length increases higher than 50% of the gas injection depth at the same other operation conditions because the liquid fall back increases and the pressure below the liquid slug are not sufficient to lift the liquid to the surface. It is obvious that the production increase as the injection pressure increases. CFD simulation shows the potential to predict the production ratio with high accuracy and can be used in the future for further development in the research related to complex systems same as intermittent gas lift. By using the CFD model it can be physically described the slug flow inside the tube and the

interaction parameters involved in the system. The pressure profile can be easily obtained for different locations and conditions along the production tube.

The computation fluid dynamic model of the compressible flow through the pilot gas lift valve has been developed in this study of typical field operating conditions. Results show that it is feasible to simulate fluid dynamics and heat transfer for complex geometry like pilot gas lift valves using the CFD model. The region around the power piston in the valve played a crucial effect on the gas flow rate since it has developed a large pressure, temperature, and velocity gradient. The pilot valve performance curve is plotted for different operating conditions. Thornhill equation shows over prediction of gas flow rate due to the constant value of discharge coefficient. From CFD calculation the general equation of non-constant discharge coefficient has been developed for a 1-inch pilot valve which can be used for further calculations in the industry without using CFD simulation. The model developed in this paper shows that CFD is a promising numerical method to calculate the actual gas flow rate and the discharge coefficient for the pilot gas lift valve.

Tubing pressure is the most important parameter to be predicted during the intermittent gas lift process. Machine Learning techniques can accurately predict tubing pressure at the injection depth in intermittent gas lift wells. Among the three machine-learning models developed, DT and RF stood the most optimum with R^2 of 0.9997 and 0.9998, RMSE of 1.99, and 1.31% for the testing data, respectively.

7.2. Further research possibilities

The author's recommendations for possible future research are:

- The CFD simulation developed in this study can be modified by applying field data with different conditions.
- CFD modeling of the pilot valve can be extended by carrying out laboratory experiments on gas flow rate through the valve and validating the CFD results.
- Develop a correlation that correlates the liquid fall back with the operating conditions based on CFD simulation.
- Machine learning model can be used to predict intermittent production rate by collecting production data from industry.

8. NEW SCIENTIFIC ACHIVEMENTS

8.1. Thesis #1

Developed a computational fluid dynamics model for intermittent gas lift systems, this simulation is a proven program for predicting intermittent gas lift characteristics and the transient flow parameters that are changing with time and position in the coordinate system. This model is applied for a long tubing string with a length of 236 times the diameter which is not yet reported in the open literature.

The velocity profile of the liquid slug is calculated using CFD simulation for two different gas injection pressures. Also, the pressure profile inside the tubing string is calculated for different positions with the gas injection time. These calculations using the developed CFD model show good agreement with the experiment results.

8.2. Thesis #2

The dimensionless analysis procedure is developed in this research by organizing the well parameters into dimensionless ratios to reduce the complexity of the system and the required computational time. The initial variables of injection pressure, tubing pressure, submergence length, and valve depth are related to the liquid production fraction for certain tubing sizes and valve diameters using CFD.

8.3. Thesis #3

A novel approach using computational fluid dynamics simulation was performed to develop a dynamic model for the gas passage performance of a 1-in., nitrogen-charged, pilot gas-lift valve. Dynamic performance curves were obtained by using methane as an injection gas with flow rates reaching up to 4.5 MMscf/day (127 em^3/day). This study investigates the effect of internal pressure, velocity, and temperature distribution within the pilot valve that cannot be predicted in the experiments and mathematical models during the flow-performance studies.

8.4. Thesis #4

A successive procedure is introduced to develop a general equation of the nonconstant discharge coefficient for a 1-inch pilot valve to be used for further calculation in the industry without using the CFD model. The developed model calculates the nonconstant discharge coefficient taking into account the pressure, temperature, and velocity gradient around the piston. This model reduces the complexity of the data required to calculate the discharge coefficient.

8.5. Thesis #5

Machine learning (ML) algorithms are utilized to develop an artificial intelligence model that can accurately predict tubing pressure in intermittent gas lift wells. Intelligent algorithms built on the field data from Algyo wells in Hungary, provide a solution that is easy to use and universally applicable to calculate such a complex parameter in the industry. This model is capable of predicting the tubing pressure at the gas lift valve with high accuracy (~ 99%).

Filter method of feature selection is used to find the most variables that affect the tubing pressure at the gas lift valve. By using this method, the number of input variables is reduced from ten to six. It is found that temperature at the casing surface, injection depth, oil density, and tubing diameter are not necessary to be included in the machine learning algorithm since they are highly correlated with other input parameters.

9. LIST OF AUTHOR'S PUBLICATIONS RELATED TO THIS THESIS.

Sami N.A. and Turzo Z. (2020): Computational fluid dynamic (CFD) simulation of pilot operated intermittent gas lift valve, Journal of Petroleum Research. 5(3), 254-264.

Sami N.A. and Turzo Z. (2020): Computational fluid dynamic (CFD) modelling of transient flow in the intermittent gas lift, Journal of Petroleum Research. 5(2), 144-153.

Sami N.A. and Turzo Z. (2020): Tracking sequence of oil well production with artificial gas-lift installations. Műszaki Földtudományi Közlemények, 89(2), 83–91.

Sami N.A. and Turzo Z. (2021): CFD Modeling of Dynamic Flow Behavior of Intermittent Gas Lift Components. Journal Petroleum and Coal, 63(1), 106-115.

Sami N.A. and Dhorgham A. (2021): Forecasting multiphase flowing bottom-hole pressure of vertical oil wells using three machine learning techniques, Journal of Petroleum Research**,** 5(3)**,** 417-422.

Sami N.A. (2022): Application of machine learning algorithms to predict tubing pressure in intermittent gas lift wells, Journal of Petroleum Research, 7(2), 246-252.

10.REFERENCES

Abdulkadir M., Hernandez V., Lo S., Lowndes I.S. and Azzopardi B.J. (2015): Comparison of experimental and computational fluid dynamics (CFD) studies of slug flow in a vertical riser. Exp. Therm. Fluid Sci. 68, 468-483.

Acuna, H.G., Schmidt, Z.X. and Doty, D.R. (1992): Modeling of gas rate through 1-in Nitrogen charged gas lift valve. SPE Annual Technical Conference and Exhibition, Washington, D.C. October 1992.

Al Selaiti I., Mata C., Saputelli L., Badmaev D., Alatrach Y., Rubio E., Mohan R. and Quijada D. (2020): Robust Data Driven Well Performance Optimization Assisted by Machine Learning Techniques for Natural Flowing and Gas-Lift Wells in Abu Dhabi. SPE Annual Technical Conference & Exhibition. USA, October 19. 2020.

Alahmed N. and Bordalo S.N. (2017): Experimental study of the dynamic and stability of intermittent gas lift in a laboratory scale model. Presented at the Latin America and Caribbean Mature Fields Symposium, Salvador, Bahia, Brazil. March 2017.

Ansys Fluent 12.0 Theory Guide-16.3 Volume of Fluid, http://www.afs.enea.it/project/ neptunius/ docs/fluent/html/th/node297.htm, downloaded September 20, 2020.

Ansys Fluent 12.0 UDF Manual, https://www.afs.enea.it/project/neptunius/docs/fluent/ html/udf/main_pre.htm, Downloaded September 20, 2020.

API Gas Lift Manual. Book 6 of the Vocational Training Series, (American Petroleum Institute, 1994.)

Artun E. (2020): Performance assessment and forecasting of cyclic gas injection into a hydraulically fractured well using data analytics and machine learning. J. Pet. Sci. Eng. 195, 107768.

Ayatollahi, S., Narimani, M. and Moshfeghian, M. (2004) : Intermittent gas lift in Aghajari oil field, a mathematical study. J. Pet. Sci. Eng. 42, 245–255.

Ayyadevara V. K. (2018): Pro Machine Learning Algorithms, A Hands-On Approach to Implementing Algorithms in Python and R. (Apress, 2018).

Bagaskara A. and Moelyadi M. A.(2018): CFD Based Prediction of Discharge Coefficient of Sonic Nozzle with Surface Roughness, Journal of Physics: Conference Series, 1005, 012010.

Beadle G., Harlan J. and Brown K.E. (1963): Evaluation of Surface Back - Pressure for Continuous - And Intermittent - Flow Gas Lift. SPE-442-PA. 15 (3), 243-251.

Behbahani, M., Edrisi, M., Rashidi, F. and Amani, E. (2012): Tuning a multi-fluid model for gas lift simulations in wells. Chemical Engineering Research and Design, 90, 471-486.

Bello O., Falcone G., J. and Scott S. (2011): Performance Evaluation of a Plunger Assisted Intermittent Gas Lift System. SPE Production and Operations Symposium, Oklahoma, USA, 27–29 March 2011.

Bertovic D., Doty D., Blais R. and Schmidt Z. (1997): Calculating accurate gas lift flow rate incorporating temperature effects. SPE Production Operations Symposium, Oklahoma, 9-11 March 1997.

Binod, K.S., Himadri C., Pradipta, B.M. and Tapas, G. (2014): Dynamic simulation of a pressure regulating and shut-off valve. Comp. Fluids. 101, 233-240.

Bilal L, McKenzie KS, Rodgers WM., Stephenson GB. and Wildman SL. (2018): Life-of-well gas lift installations for unconventional resources. SPE Artificial Lift Conference and Exhibition - Americas, The Woodlands, Texas, USA, August 2018.

Brill, J.P., Doerr, T.C. and Brown, K.E. (1967): An analytical description of liquid slug flow in small-diameter vertical conduits. SPE-1526-PA. 19 (3), 419-432.

Brown, K. and Jessen, F. (1962): Evaluation of valve port size, surface chokes and fluid fall-back in intermittent gas-lift installations. SPE-179-PA. 14 (3), 315-322.

Hardegree C. N., B. A. Gerrard1 , S. L. Wildman, and K. S. McKenzie (2020): Chamber Gas Lift in Horizontals. SPE Production & Operations 35 (01), 018–025.

Caicedo, S. (2001): Estimating IPR curves in intermittent gas lift wells from standard production tests. SPE Latin American and Caribbean Petroleum Engineering Conference, Buenos Aires, Argentina, 25–28 March 2001.

Cedeno, M. and Ortiz, J.L. (2007): SOLAG: An intelligent gas lift optimization system for continuous and intermittent gas lift. SPE-26972.

Çengel Y. A. and Cimbala J. M. (2014): Fluid mechanics fundamentals and applications. , (McGraw-Hill Higher Education, 2014).

Chacin, J.E. (1994): Selection of optimum intermittent lift scheme for gas lift well. University of Tulsa Centennial Petroleum Engineering Symposium, Tulsa, Oklahoma, August 1994. SPE-27986-MS

Cheung, S.C.M. and Gasbarri, S. (2002): A methodology to determine the liquid column height of intermittent gas lift well. Canadian International Petroleum Conference, Calgary, Alberta, June 2002. PETSOC-2002-111

Dabirian, R., Mansouri, A., Mohan, R. and Shoham, O. (2015): CFD simulation of turbulent flow structure in stratified gas/liquid flow and validation with experimental data. SPE Annual Technical Conference and Exhibition, Houston, Texas, USA, September 2015. SPE-174964-MS

Dai, Y., Dakshinamoorthy, D. and Agrawal, M. (2013): CFD modeling of bubbly, slug and annular flow regimes in vertical pipelines. Offshore Technology Conference, Houston, Texas, USA, May 2013. OTC-24245-MS

Deng F. O. L., Lawal F. O., Davani E. and Davani C. (2019): Hypervolume-Based Multiobjective Optimization for Gas Lift Systems, SPE, Oklahoma, USA, April 9-10, 2019.

Emmerson P., M Lewis, N Barton. Improving boundary conditions for multiphase CFD predictions of slug flow induced forces. 17th International Conference on Multiphase Production Technology, Cannes, France, June 2015. BHR-2015-C3

Fathi E. (2017): Gas Lift System. Pet. and Petro. Chem. Eng. J. ; 1 (4), 000121.

Faustinelli, J.G. and Doty, D.R. (2001): Dynamic Flow Performance Modeling of a Gas-Lift Valve. SPE Latin American and Caribbean Petroleum Engineering Conference, Buenos Aires, Argentina, March 2001. SPE-69406-MS

Forero, G., Mcfadyen, K., Turner, R., Waring, B. and Steenken, E. (1993): Artificial lift manual. (Hague, 1993)

Takacs G. (2007):, Gas lifting course manual, (University of Miskolc, 2007).

Garcia, E.L., Buongiorno, J., Al-Safran, E. and Lakehal, D. (2015): Development of new CFD based unified closure relation for Taylor bubble velocity in two phase slug flow in

pipe. 17th International Conference on Multiphase Technology 2015 (June 2015), pp. 93-107.

Gharaibah E. and Zhang Y. (2015): Flow Assurance Aspects and Optimization of Subsea Choke Valve – Sand Management and Erosion. SPE Offshore Technology Conference Brasil, Rio de Janeiro, Brazil, 27–29 October 2015.

Hepguler, G., Schmidt, Z., Blais R. N.and Doty, D.R. (1993): Dynamic model of gas-lift valve performance. Journal of Petroleum Technology. 45(6), 576-583.

Hernandez, A. (2013): Fundamentals of gas lift engineering, well design and troubleshooting. Elsevier, Amsterdam.

Hernandez, A., Garcia, G., Concho, M.A., Garcia, R. and Navarro, U. (1998): Downhole Pressure and Temperature Survey Analysis for Wells on Intermittent Gas Lift . International Petroleum Conference and Exhibition of Mexico, March 3–5, 1998

Paper Number: SPE-39853-MS

Hernandez, A., Gasbarri, S., Machado, M., Marcano, L., Manzanilla, R. and Guevara, J. (1999): Field-scale research on intermittent gas lift. SPE Mid-Continent Operations Symposium, Oklahoma City, Oklahoma, March 1999. SPE-52124-MS

Hernandez A., Perez C., Villalobos B., Romero A.and Wildman S. (2001): New Gas-Lift Pilot Valve Increases Gas-Lift Efficiency, SPE Latin American and Caribbean Petroleum Engineering Conference, Argentina, 25-28 March (2001).

Herald W. Winkler and Sidney S. Smith (1962): Camco Gas Lift Manual, (Camco,Incorporated, 1962).

Hussein, M.M., Al-Sarkhi, A., Badr, H.M. and Habib, M.A. (2019): CFD modeling of liquid film reversal of two-phase flow in vertical pipes. J. Petrol. Explor. and Prod. Tech. 9, 3039-3070.

Imada F. H. J., Saltara F. and Baliño J. L. (2013): Numerical determination of discharge coefficients of orifice plates and nozzles. 22nd International Congress of Mechanical Engineering (COBEM 2013) November 3-7, 2013, Ribeirão Preto, SP, Brazil

Decker K.L. and Merla T. (1986): Computer Modeling of Gas-Lift Valve Performance. 18th Annual OTC in Houston, Texas, May 5-8, 1986.

Kabir E., Emadi H., McElroy P., Elldakli F. and Young M. (2020): Optimizing Seat and Ball Combination of Actual Gas Lift Valve: An Experimental and CFD Simulation Study. SPE Artificial Lift Conference and Exhibition - Americas, Virtual, November 2020. SPE-201119-MS

Khan, M. R., Alnuaim, S., Tariq, Z.and Abdulraheem, A. (2019): Machine learning application for oil rate prediction in artificial gas lift wells. Paper presented in SPE Middle East Oil and Gas Show and Conference, Manama, Bahrain, March 18-21.

Khan M. R., Tariq Z. and Abdulraheem A. (2018): Utilizing State of the Art Computational Intelligence to Estimate Oil Flow Rate in Artificial Lift Wells SPE Kingdom of Saudi Arabia Annual Technical Symposium and Exhibition, Dammam, Saudi Arabia, April 2018. SPE-192321-MS

Latif B., McKenzie KS, Rodgers WM., Stephenson GB. and Wildman SL. (2018): Life-of-well gas lift installations for unconventional resources. SPE Artificial Lift Conference and Exhibition - Americas, The Woodlands, Texas, USA, August 2018. SPE-190959-MS

Li L.J., Zhang H., Davis G.R., Kalb F.D. and Hamid S. (2005): Improving the closing characteristics of subsurface safety valve with combined FEA and CFD Modeling/Numerical Analysis. SPE Western Regional Meeting, Irvine, California, March 2005. SPE-93941-MS

Liao, T., Schmidt, Z. and Doty, D.R. (1995): Investigation of Intermittent Gas Lift by Using Mechanistic Modeling. SPE Production Operations Symposium, Oklahoma City, Oklahoma, April 1995. SPE-29454-MS

Maria A. C., Sandro G. and Luis R. R. (2000): Numerical simulation of the flow through an intermittent gas lift valve, Conference Energy for the New Millenium, February 14-17, 2000, New Orleans.

Mazin ZA. (2000): Analysis of Gas Lift Installation Problems. 9th Abu Dhabi International Petroleum Exhibition and Conference held in Abu Dhabi, U. A. E., 15-18 October 2000.

Milano, P.E. (1999): Dynamic performance of the intermittent gas-lift valve. M.S. Thesis. The University of Tulsa, Tulsa, Oklahoma.

Mohammed M., Khan M. B. and Bashie E. B. M. (2017): Machine Learning Algorithms and Applications, Taylor and Francis book, 2017.

Sami N.A. and Turzo Z. (2020): Computational fluid dynamic (CFD) simulation of pilot operated intermittent gas lift valve, J. Pet. Res., 5 , 254-264.

Sami N.A. and Turzo Z. (2020): Computational fluid dynamic (CFD) modelling of transient flow in the intermittent gas lift, J. Pet. Res. 5 , 144-153.

Sami N.A. and Turzo Z. (2021): CFD Modeling of Dynamic Flow Behavior of Intermittent Gas Lift Components. Journal of Pet. and Coal. 63(1), 106-115

Sami N.A. and Turzo Z. (2020): Tracking sequence of oil well production with artificial gas-lift installations. Műszaki Földtudományi Közlemények, 89(2), pp. 83–91.

Neely, A.B., Montgomery, J.W. and Vogel, J.B. (1974): A field test and analytical study of intermittent gas lift. SPE Journal. 14 (05): 502–512.

Nieberding, M.A., Zelimlr, S., Blais, R.N. and Doty, D.R. (1993): Normalization of Nitrogen-Loaded Gas-Lift Valve Performance Data. SPE Production & Facilities. 8(3), 203-210.

Odedele T. O. and Ibrahim H. D. (2016): Predicting oil well gas lift performance and production optimization using hybrid particle swarm optimization and fuzzy support vector machines. Proceedings of the World Congress on Engineering 2016 Vol I, 110-116.

Ortiz, J.L. and Lagoven, S.A. (1990): Gas-lift troubleshooting engineering: an improved approach. SPE Annual Technical Conference and Exhibition, New Orleans, Louisiana, September 1990. SPE-20674-MS

Ounsakul, T., Sirirattanachatchawan, T., Pattarachupong, W., Yokrat, Y. and Ekkawong, P. (2019): Artificial Lift Selection Using Machine Learning. International Petroleum Technology Conference, Beijing, China, March 2019. IPTC-19423-MS

Parsi, M., Vieira, R.E., Agrawal, M., Srinivasan, V., Laury, B.S.M., Shirazi, S.A., Schleicher, E. and Hampel, U. (2015): Computational fluid dynamic (CFD) simulation of multiphase flow and validating using wire mesh sensor. 17th International Conference on Multiphase Production Technology, Cannes, France, June 2015. BHR-2015-D4

Pestana, T., Bordalo, S. and Almeida, M. B. F. (2013): Numerical simulation in the time domain of the intermittent gas lift and its variants for petroleum wells. Paper presented in SPE Artificial Lift Conference-Americas, Cartagena, Colombia, May 21-22.

Poletto V. G., De Lai F. C., Ferreira M. V. D., Martins A. L. and Junqueira S. L. M. (2020): Numerical simulation to study scale formation on SSV valves. SPE International Oilfield Scale Conference and Exhibition, Virtual, June 2020. SPE-200689-MS

Pourtousi, M., Ganesan, P. and Sahu, J. (2015): Effect of bubble diameter size on prediction of flow pattern in Euler–Euler simulation of homogeneous bubble column regime. Measurement, 76, 255-270.

Ranjan A., Verma S. and Singh Y. (2015): Gas Lift Optimization using Artificial Neural Network. SPE Middle East Oil & Gas Show and Conference, Manama, Bahrain, March 2015. SPE-172610-MS

Gasbarri S., Marcano L. J. E. and Faustinelli J. G. (1999): Insert Chamber Lift Experiences in Mara-La Paz Field, Venezuela, SPE Asia Pacific Oil and Gas Conference and Exhibition, Jakarta, Indonesia, April 1999. SPE-54389-MS

Sandoval, S., Solórzano, L.R. and Gasbarri, S. (2005): Transient two-phase-flow model for predicting column formation in intermittent gas. SPE Latin American and Caribbean Petroleum Engineering Conference, Rio de Janeiro, Brazil, June 2005. SPE-94950-MS

Sarvestani, A.D., Goodarzi, A.M. and Hadipour, A. (2019): Integrated asset management: a case study of technical and economic optimization of surface and well facilities. Petr. Sci. 16, 1221–1236.

Sattar, M., Naser, J. and Brooks, G. (2013): Numerical simulation of two-phase flow with bubble break-up and coalescence coupled with population balance modeling. Chemical Engineering and Processing: Process Intensification, 70, 66-76.

Schlumberger (1999): Gas lift design and technology. (Schlumberger, Incorporation, 1999)

Schmidt, Z., Doty, D.R., Lukong, P.B., Fernandez, O.F. and Brill, J.P. (1984): Hydrodynamic model for intermittent gas lifting of viscous oil. J Pet Technol 36 (03): 475–485

Shahaboddin A., Mostafa N. and Mahmood M. (2005): Intermittent gas lift in Aghajari oil field, a mathematical study J. Petrol. Sci. Eng. 200442, 245– 255.

Solesa, M., Cveticanin, S. and Gligoric, G. (1991): POVLIFT A computer program for designing and optimizing intermittent gas lift. Petroleum Computer Conference, Dallas, Texas, June 1991. SPE-22296-MS

Stenmark, E. (2013): On multiphase flow models in ANSYS CFD software. (Chalmers, 2013)

Taha, T.and Cui, Z.F. (2005): CFD modelling of slug flow in vertical tubes, Chem. Eng. Sci. 61, 676–687.

Tocci, F, Bos, F. and Henkes, R. (2017): CFD for multiphase flow in vertical risers. 18th International Conference on Multiphase Production Technology, Cannes, France, June 2017. BHR-2017-309

Tukiman M.M., Ghazali M. N. M., Sadikin A., Nasir N. F., Nordin N., Sapit A. and Razali M. A. (2017): CFD simulation of flow through an orifice plate, IOP Conf. Series: Materials Science and Engineering 243 (2017) 012036

Turzo, Z. and Takacs, G. (2009): CFD techniques determine gas- lift valve behavior. Oil Gas J. 107, 46-51.

Wardle K.E. and Weller H.G. (2013): Hybrid multiphase CFD solver for coupled dispersed/segregated flows in liquid-liquid extraction. Int. J. Chem. Eng. 13, 1-13.

White, G.W., O'Connell, B.T., Davis, R.C., Berry, R.F., Aim, L.A. and Stacha, M. (1963): An analytical concept of the static and dynamic parameters of intermittent gas lift. J Pet Technol 15 (03): 301–308

Yang, X., Dindoruk, B. and Lu, L. (2020): A comparative analysis of bubble point pressure prediction using advanced machine learning algorithms and classical correlations. J. Pet. Sci. Eng. 185, 106598.

Zhu J., Zhu H., Zhao O., Fu W., Shi Y. and Zhang H. Q. (2019): A Transient Plunger Lift Model for Liquid Unloading from Gas Wells. International Petroleum Technology Conference, Beijing, China, March 2019. IPTC-19211-MS

11.APPENDIXES

11.1. Appendix A: Summary of Literatures Review

Table A.1. The research on conventional intermittent gas lift (edited by the Author)

Authors, year	Characteristics	Key results
Brown and Jessen, 1962	-Experiments on a field test well of 8000ft long with 2 3/8 in. diameter	-The efficiency of intermittent gas lift increases with valve port size and surface choke size.
Beadle et al., 1963	- Experiments on field test well	- A set of pressure loss curves of the flow line at different operation conditions.
White et al., 1963	- Experiments on 93 ft long with seven different string diameters.	-Applying a dimensionless ratio of well parameters has the advantage in the analysis of the intermittent gas lift system.
Brill et al., 1967	- Experiments on 1500 ft well for two tubing sizes 1.25 &1. 5 in. - An empirical fall-back correlation - Mathematical model to calculate the tubing pressure and volume of gas injected.	- The liquid slug initially undergoes high acceleration, then reaches essentially a constant velocity and accelerates again as it is produced at the surface.
Neely et al., 1974	- Experiments in an instrumented well - **A**nalytical description of different intermittent gas lift parameter.	- The casing pressure is not equal to the tubing pressure when the valve is opened - A significant amount of liquid produced is contributed to after flow
Schmidt et al., 1984	- Hydrodynamic model. - Experimental of 18 m long pipe with 7.6 cm in diameter	- The liquid slug velocity is continuously accelerating and does not reach a constant velocity - The production increase with increasing injection pressure - A significant amount of liquid produced is contributed to after flow
Solesa et al., 1991	- Mathematical model	- Developed POVELIFT program to simulate the intermittent gas lift
Chacin, 1994	-Review of the key modeling works regarding intermittent gas lift	-Two weakness of developed mechanistic models in the literature, the lack of field adjustment and the complex of the models.

Table A.1. (Cont.)The research on conventional intermittent gas lift (edited by the Author)

Authors, year	Characteristics	Key results
Liao et al., 1995	- Mechanistic model	- Sensitivity analysis to study the effect of different operation parameters on the performance of intermittent gas lift using the developed model
Hernandez et al., 1998	- Mathematical analysis using Temperature and pressure survey	Evaluating the optimum cycle time, productivity index, true liquid gradient, liquid column length, static reservoir pressure, and liquid fall back.
Hernandez et al., 1999	- Experimental in field scale test well 8000 ft length with 2 7/8 in. diameter	- Measure the important effect of different parameter in the efficiency of intermittent gas lift using the conditions similar to the real well
Caicedo, 2001	- A numerical method to solve equations that relate to Vogel's model with field data for intermittent gas lift wells	- Developed an equation to estimate IPR in the intermittent gas lift well
Cheung and Gasbarri, 2002	- Numerical model based on pressure drop correlations of Hagendorn and Brown's, and a combination of Aziz's and Wallis'.	- Develop a mathematical model to estimate the fluid column accumulated in intermittent gas lift wells.
Sandoval et al., 2005	- Laboratory measurement to develop the model for accumulation stage in intermittent gas lift of 20 m long pipe with 2in. diameter.	- Developed a two-phase flow model to estimate a height of a fluid column
Cedeno and Ortiz, 2007	- Mathematical model using SOLAG computer system	- Estimate the optimum gas liquid ratio in a continuous flow gas lift. Also, optimize liquid flow rate in the intermittent gas lift
Pestana et al., 2013	- A mathematical model based on Liao and Carvalho model	- Developed a Simulator based on mathematical model to estimate the liquid production rate, fallback, and required injection gas
Alahmed and Bordalo 2017	- Laboratory Experiments in 15 m length of vertical well with three different diameters 1, 1.5 and 2 in.	- Study the stability and behavior of the intermittent gas lift cycle - Determine the liquid fall back for different operation condition

Table A.2. Summary of the research on multi-phase flow regime using CFD simulation. (edited by the Author)

Author, year	Model	Fluid	Geometry	Study
Taha and Cui, 2005	-CFD-Fluent -VOF with RANS k – ε	Air and water	2 D of Vertical pipe length 11d	Taylor bubble movement in stagnant and moving liquid
Behbahani et al., 2012	-CFD fluent - Euler-Euler with Realizable k-ε turbulent model	Air and water	2 D of Vertical pipe length 80 d	Bubble flow in vertical pipe
Dakshinamoorthy et al., 2013	-CFD-Fluent -Hybrid model, Eulerian-Eulerian with multifluid VOF	Nitrogen (gas) and naphtha (liquid)	3D of vertical pipe length with 30d	Bubble, slug, and annular flow
Wardle and Weller, 2013	-Open FOAM CFD -Hybrid model of Euler-Euler with multi-fluid VOF	Water-oil and air	2D and 3D geometry of Liquid-liquid extraction device	Multiple regimes from fully segregated to fully disperse.
Garcia et al., 2015	- CFD with commercial code Trans AT	Air and different liquids	3D vertical and inclined pipe	Taylor bubble movement in stagnant liquid
Parsi et al., 2015	- CFD- Fluent - Hybrid model, Eulerian- multifluid VOF	Air and water	3D pipe with elbow 3m Vertical pipe with 6in elbow and 1.9m horizontal	Slug and Churn flow
Dabirian et al., 2015	-CFD fluent - VOF with Realizable k-ε turbulent model	-Water and air	3D of Horizontal pipeline of 3.4 m length and 0.096 m in diameter	Stratified wavy flow
Emmerson et al., 2015	-STAR CMM+CFD - VOF with Large eddy turbulent model	Water and air	3D of 180-degree bend pipe	Slug flow
Abdulkadir et al., 2015	- CFD codes, Star-CD and Star-CCM+. - VOF with RANS k – ε turbulent model	Air with silicon oil	3D vertical pipe of 6 m length with a 0.067 m internal diameter	Slug flow
Tocci et al., 2017	-CFD Open Foam -Hybrid model of Eulerian -multifluid VOF with RANS k – ε turbulent model	Air and water	3D Vertical pipe of 50D length and 50.8 mm and 67 mm in diameter	Slug and Churn flow
Hussein et al.,2019	-CFD Fluent 18.5 - Eulerian with RNG k – ε turbulent model	Air with water	2D of 3 in. vertical pipe	Transient flow from mist to churn flow

11.2. Appendix B: User Defined Function in C Language for CFD Modeling.

```
#include "udf.h"
#INCLUDE"sg_mphase.h"
DEFINE_PROFILE(pressure_magnitude, thread, i)
{
real pressure_mag;
face_t f;
Thread*t_outlet;
int Zone_ID = 10;/*outlet zone ID*/
Domain*domain;
domain=Get_Domain(2);/*to get liquid phase*/
t_outlet =Lookup_Thread(domain,Zone_ID);
begin_f_loop(f,thread)
{
if (F_VOF(f,t_outlet)<=0)
{
F_PROFILE(f,thread,i) =15600;
}
else
{
F_PROFILE(f,thread,i) =0;
}
}
end_f_loop(f,thread)
}
```

11.3. Appendix C: Data Set for Machine Learning Models

Table C.1. Sample of intermittent data set from Algyo oil wells. (edited by the Author)

Samples ID	**Input parameters**									**Output parameters**
	Pt@s	**Tt@s**	**P@cs**	**Tc@s**	**Depth**	**Oil sp.gr.**	**Tubing dia.**	**Cycle time**	**Inj. time**	**P@tv**
	[MPa]	**[ºC]**	**[MPa]**	**[ºC]**	**[m]**	**[-]**	**[m]**	**[min]**	**[min]**	**[MPa]**
1	1.439	10.2	5.641	10.1	1872	0.831	0.062	60	12	7.691
2	1.438	10.2	5.774	10.0	1872	0.831	0.062	60	12	7.934
3	1.441	10.1	5.797	10.0	1872	0.831	0.062	60	12	8.106
4	1.407	9.1	5.329	8.8	1872	0.831	0.062	120	25	7.908
5	1.362	10.3	7.659	10.1	2394	0.872	0.052	240	22	9.201
6	1.454	11.5	5.467	11.5	2394	0.872	0.052	60	15	10.316
… …										
9593	1.404	11.4	4.000	11.3	2394	0.872	0.052	60	15	9.896

Table C.2. Statistical description of (a) Training dataset and (b) Testing dataset. (edited by the Author)

a) Training dataset	Pt@s [MPa]	Tt@s [ºC]	Pc@s [MPa]	Tt@v [ºC]	Cycle time [min]	injection time [min]	Pt@v [MPa]
count	6715	6715	6715	6715	6715	6715	6715
mean	1.470	8.734	9.068	113.53	126.272	20.767	6.230
std	0.156	3.148	0.939	15.415	58.252	4.284	1.335
min	1.337	0.760	6.723	75.848	60.000	12.000	3.926
max	2.787	11.575	10.60	127.860	240.000	25.000	9.809
Coefficient of Variation	0.106	0.360	0.103	0.135	0.461	0.206	0.214
Skewness	3.667	-1.586	-0.292	-0.666	0.776	-0.816	0.218

b)Testing dataset	Pt@s	Tt@s	Pc@s	Tt@v	cycle time	injection time	pt@v
count	2879	2879	2879	2879	2879	2879	2879
mean	1.467	8.796	9.045	113.48	126.064	20.786	6.256
std	0.151	3.033	0.931	15.434	57.656	4.284	1.309
min	1.337	0.766	6.726	75.851	60	12	3.926
max	2.625	11.573	10.60	127.86	240	25	9.809
Coefficient of Variation	0.102	0.344	0.102	0.136	0.457	0.206	0.209
Skewness	3.481	-1.679	-0.275	-0.654	0.808	-0.856	0.1708

Table C.3. Coefficient of Determination (R^2) and Root Mean Square Error (RMSE). (edited by the Author)

Model	Training set		Testing set	
	R^2	RMSE	R^2	RMSE
Decision Tree Regression (DT)	1.0000	0.0000	0.9997	1.99
Random Forest Regression (RF)	0.9999	0.0077	0.9998	1.31
k-Nearest Neighbors Regression (KNN)	0.9997	0.021	0.9991	3.75

11.4. Appendix D: CFD Visualization for Two Phase Intermittent Flow

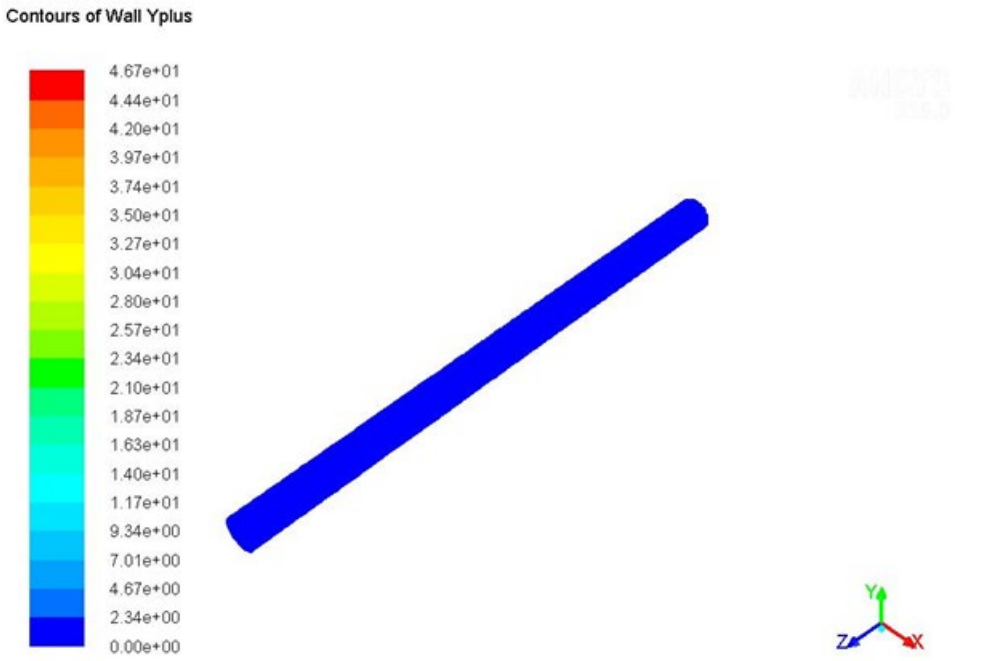

Figure D.1 Contour plot of Y+ value over the geometry wall. (edited by the Author)

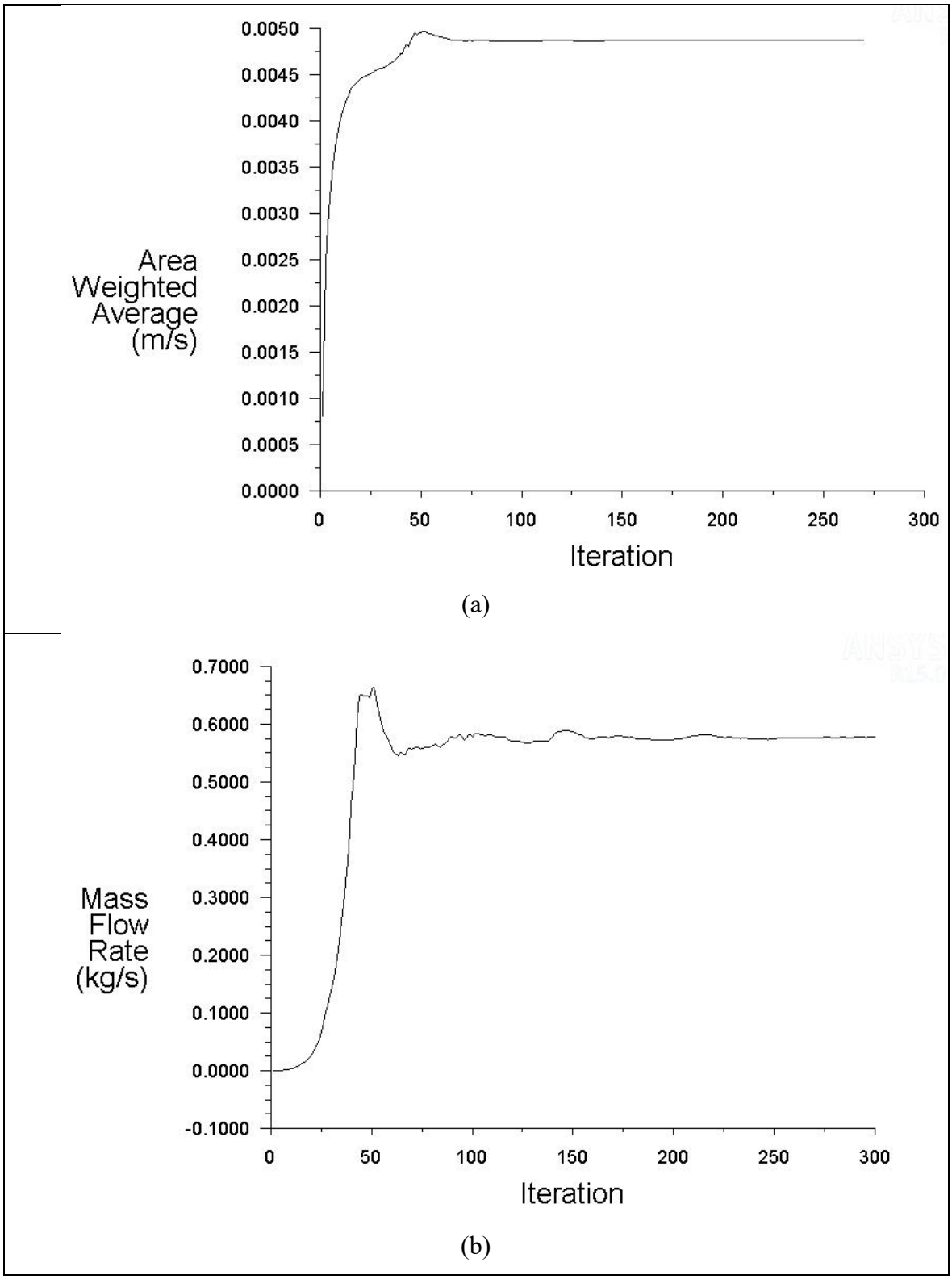

Figure D.2. (a) Convergence of area weighted average velocity at the inlet (b) Convergence of mass flow rate at the inlet. (edited by the Author)

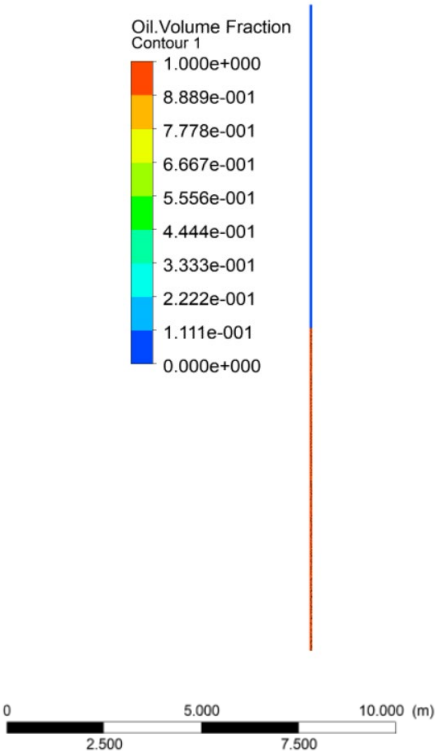

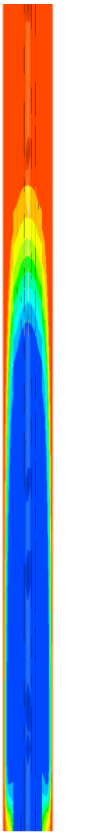

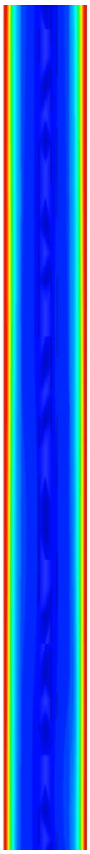

t = 0 s	Region A	Region B	t =0.8 s	t= 8 s
	t=0.2 s		Pi=40 psig, (3.7-4.2) m	

Figure D.3. Contours of oil phase volume fraction at different injection time (Case 1) (edited by the Author)

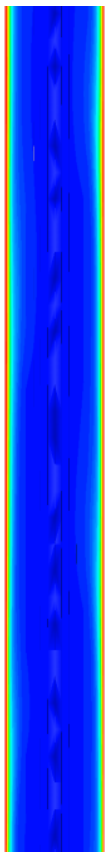

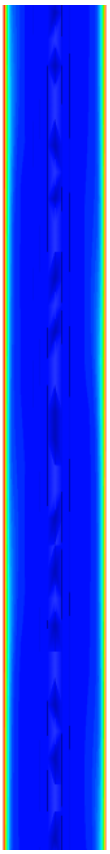

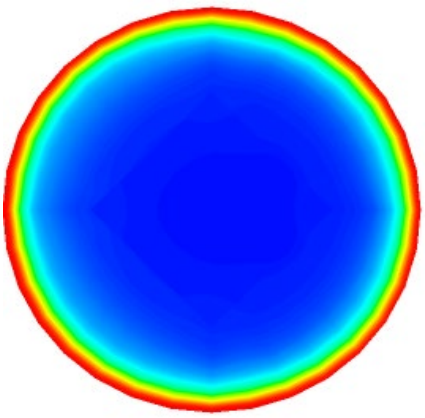

@4 m for 40 psig

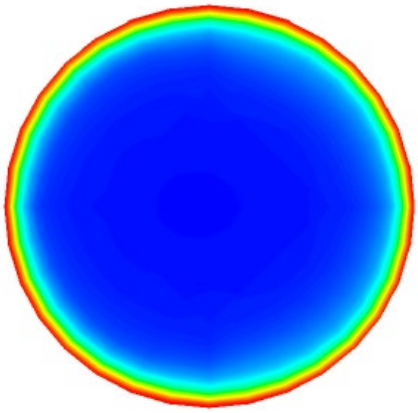

Pi = 40 psig, (3.7-4.2) m	Pi = 50 psig, (3.7-4.2) m	@4 m for 50 psig
(E) At time = 1.3 s		

Figure D.4. Contours of oil phase volume fraction at different injection pressure (Case 1) (edited by the Author)

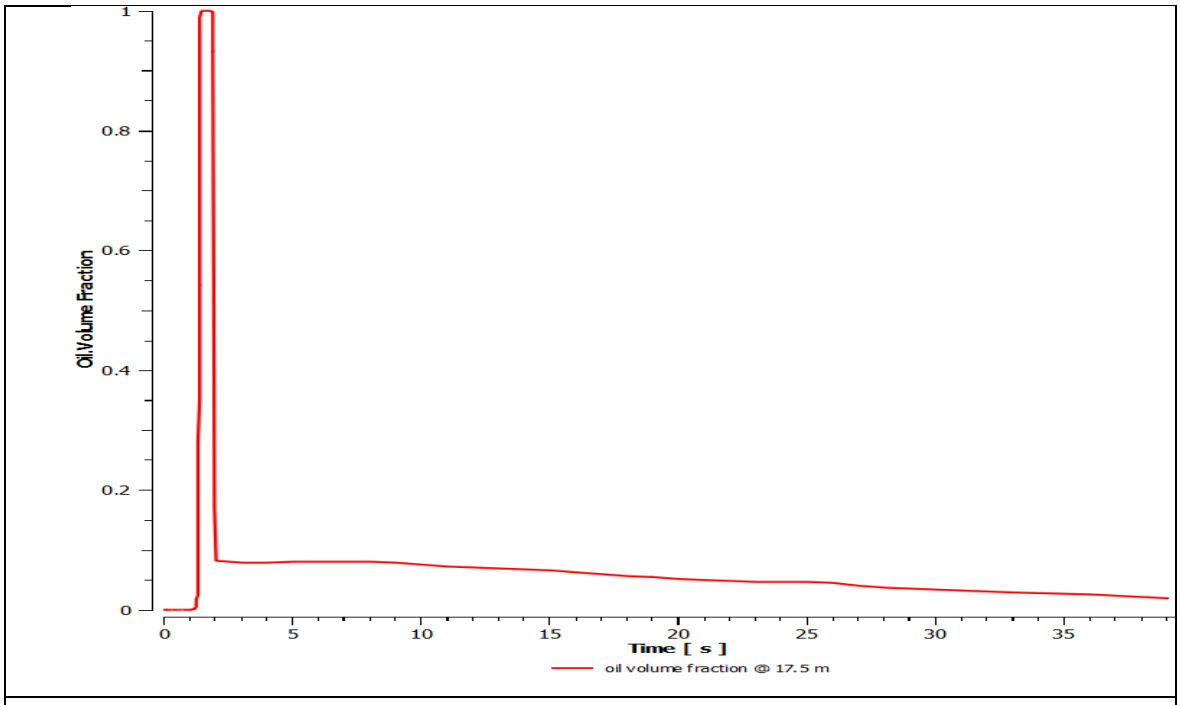

(A)

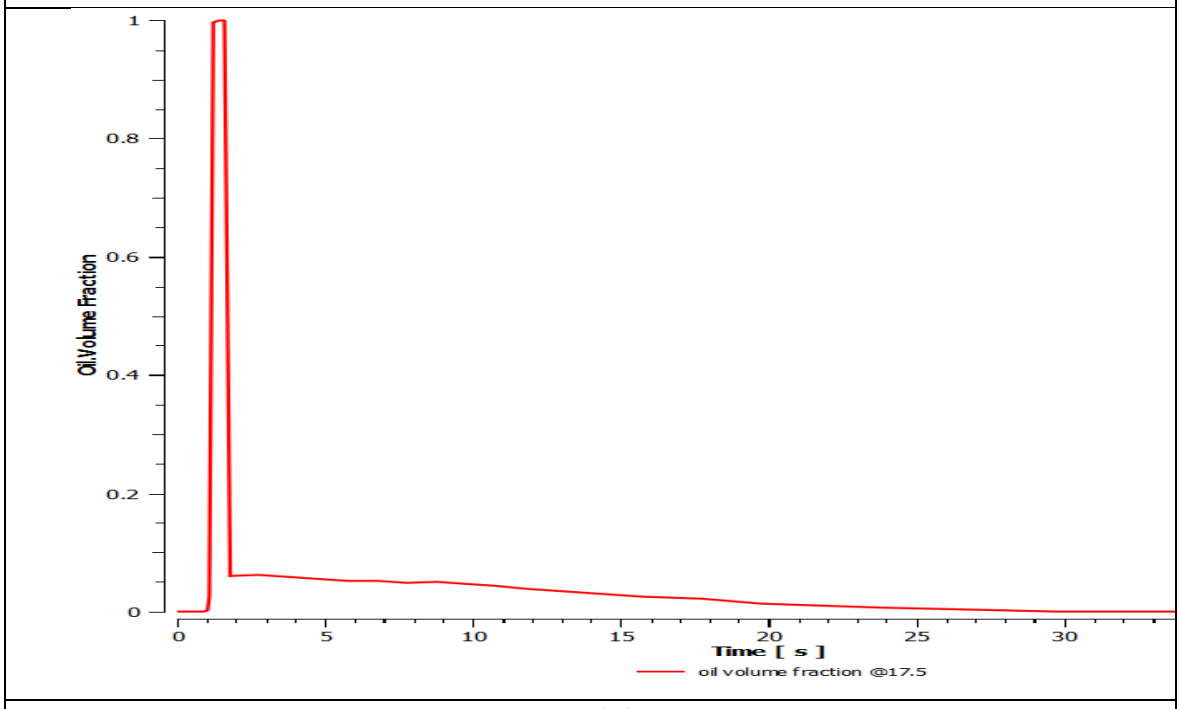

(B)

Figure D.5. Oil volume fraction vs time at the pipe outlet (A) injection pressure 40 psig, (B) injection pressure 50 psig. (edited by the Author)

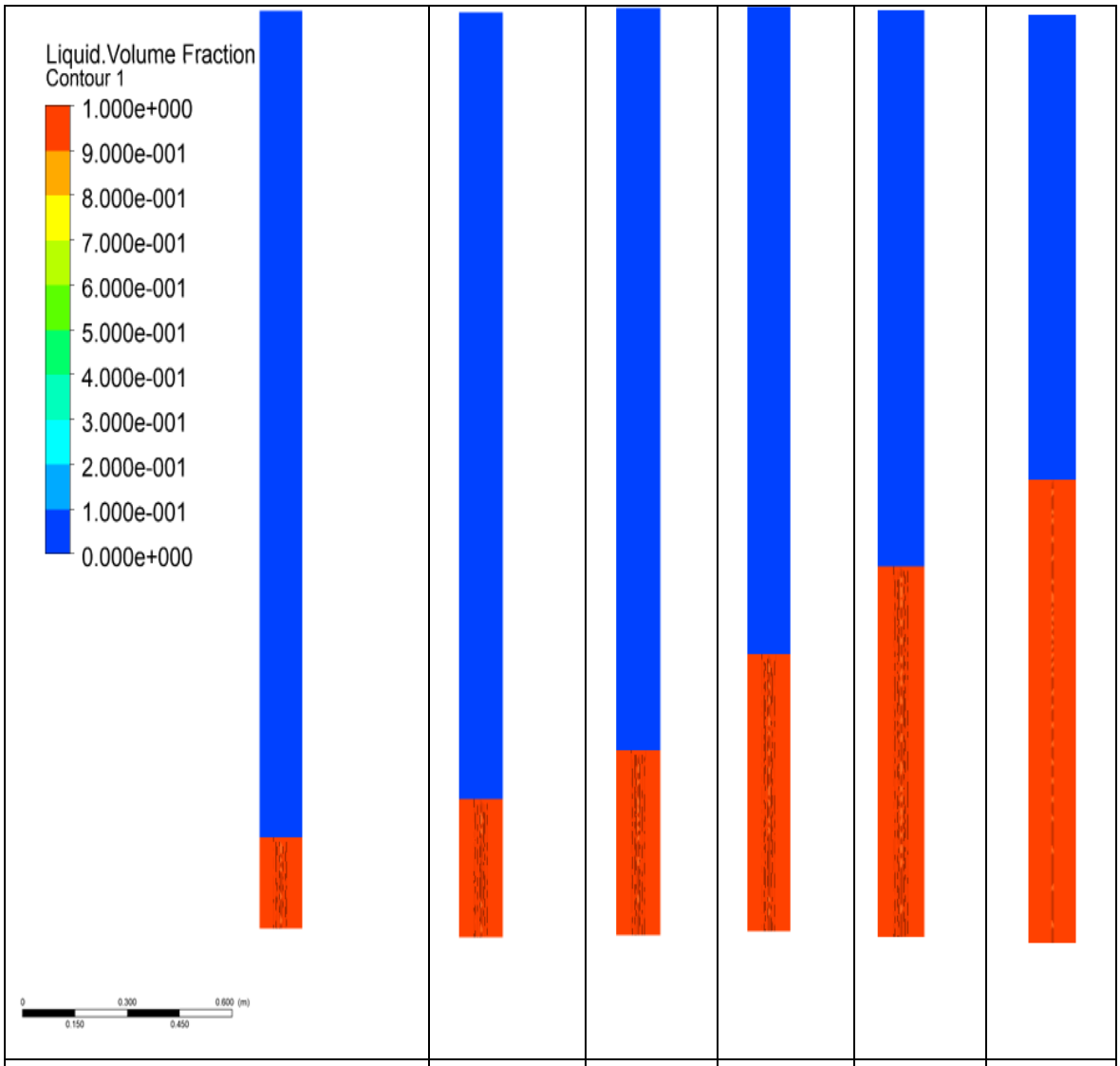

S/D=0.1	S/D=0.15	S/D=0.2	S/D=0.3	S/D=0.4	S/D=0.5

Figure D.6. The vertical cross section plane of different geometry used in CFD simulation (Case 2). (edited by the Author)

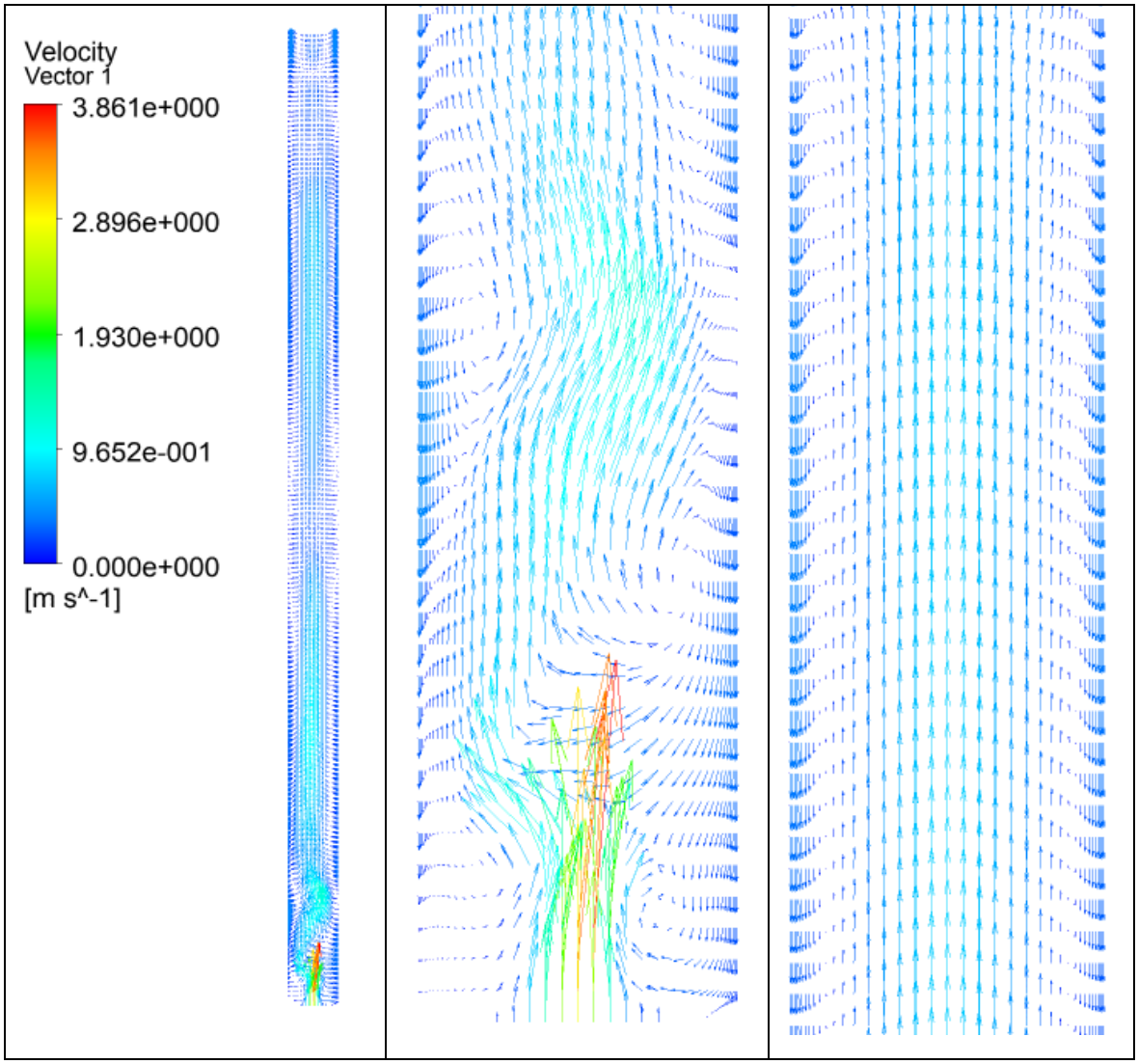

Figure D.7. Velocity vector plots for the liquid fall back. (edited by the Author)

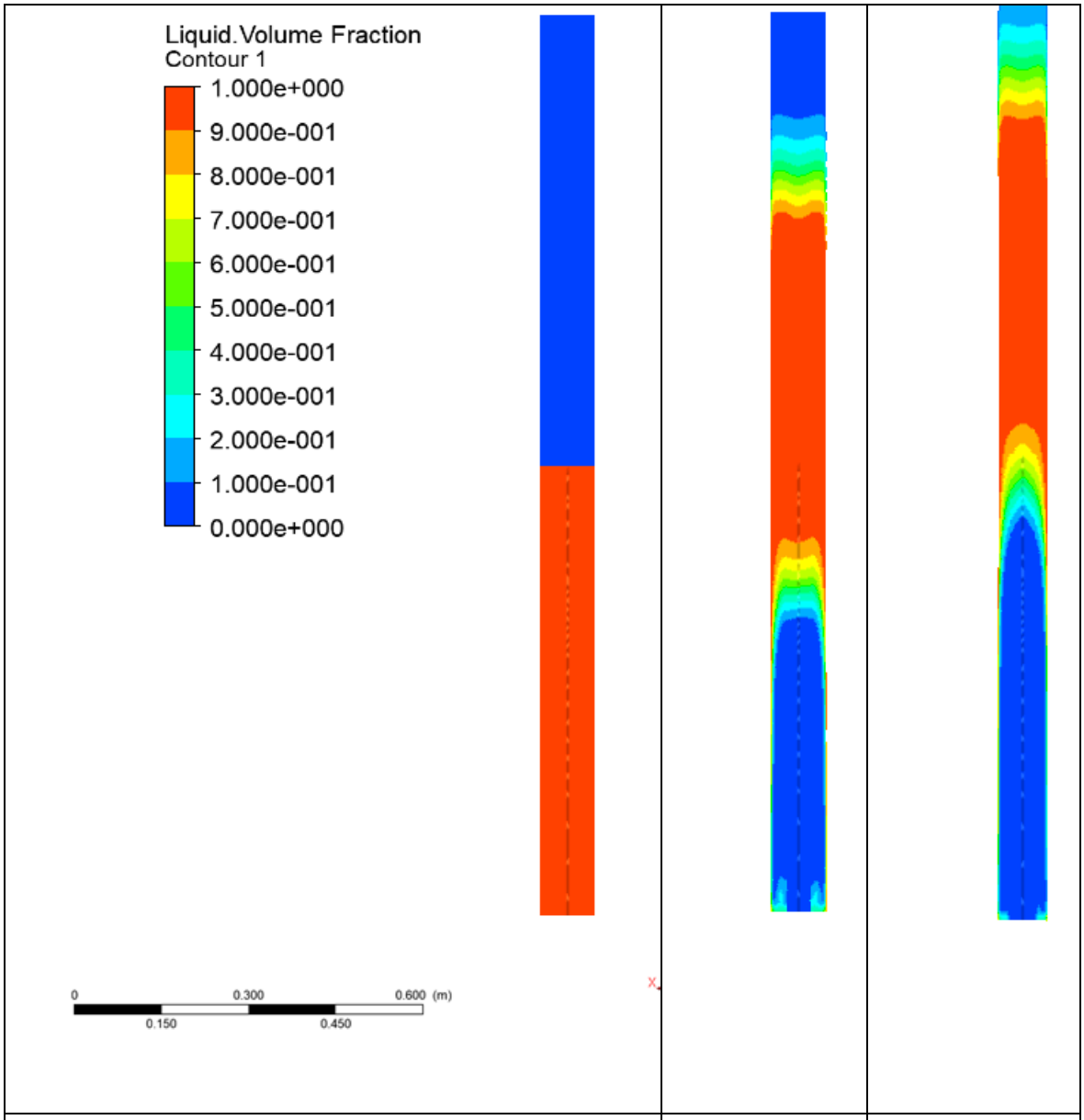

S/D=0.5 at t=0 s	Pi/Pt=2 at t=0.4 s	Pi/Pt=3 at t=0.4 s

Figure D.8. Slug proceeding for two different injection pressure at same tubing size 2.375 in. (edited by the Author)

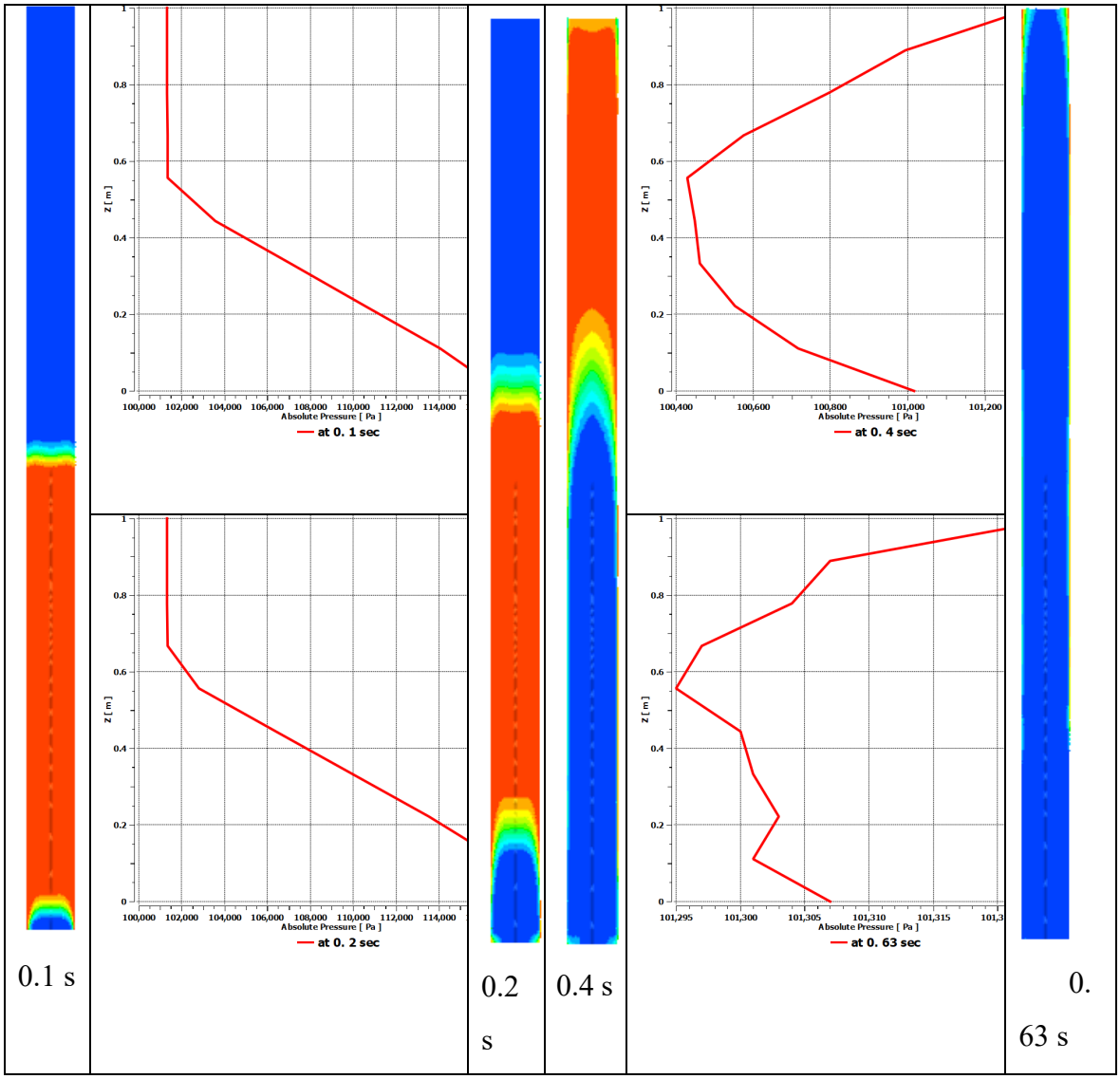

Figure D.9. Pressure along the tubing string for different injection time (tubing size 2 in. port size 0.5 in. Pi/Pt 3 and S/D 0.5). (edited by the Author)

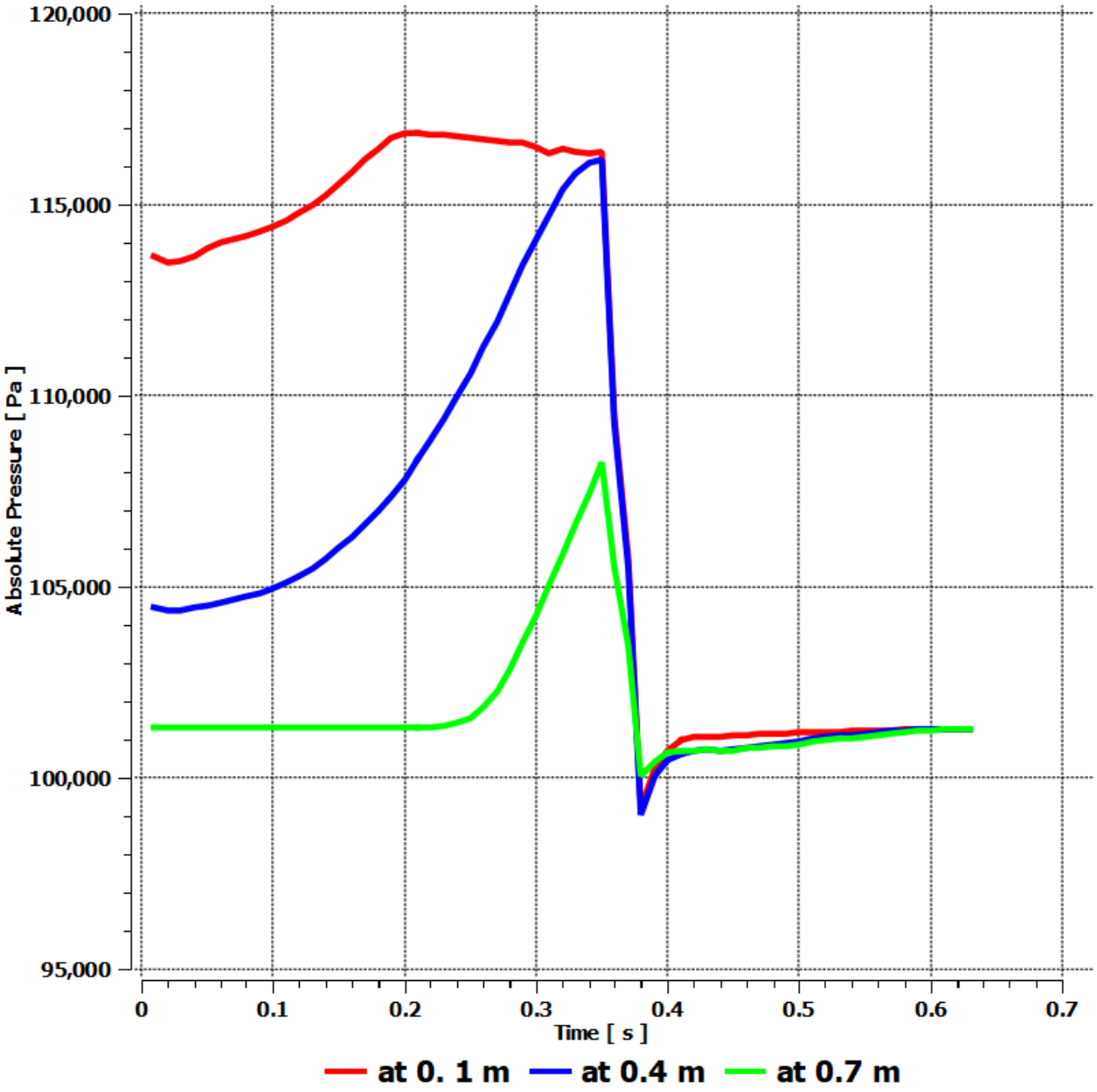

Figure D.10. Pressure versus time at different positions along the tubing (tubing size of 2 in., Pi/Pt=3, port size of 0.5 in. and S/D 0.5). (edited by the Author)

11.5. Appendix E: CFD Visualization for Pilot Valve

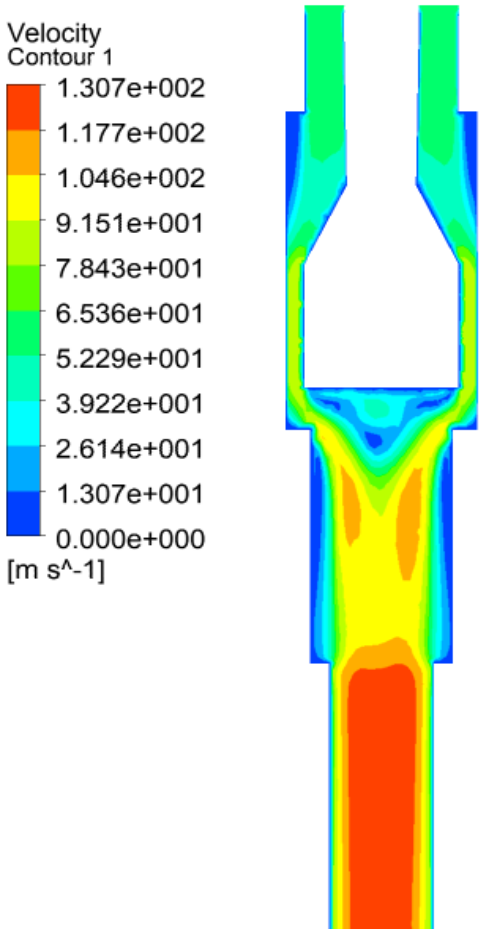

Figure E.1. Velocity contour field through pilot at Pi = 80 bar, Pp= 60 bar, and T= 300 K^{o,} (edited by the Author)

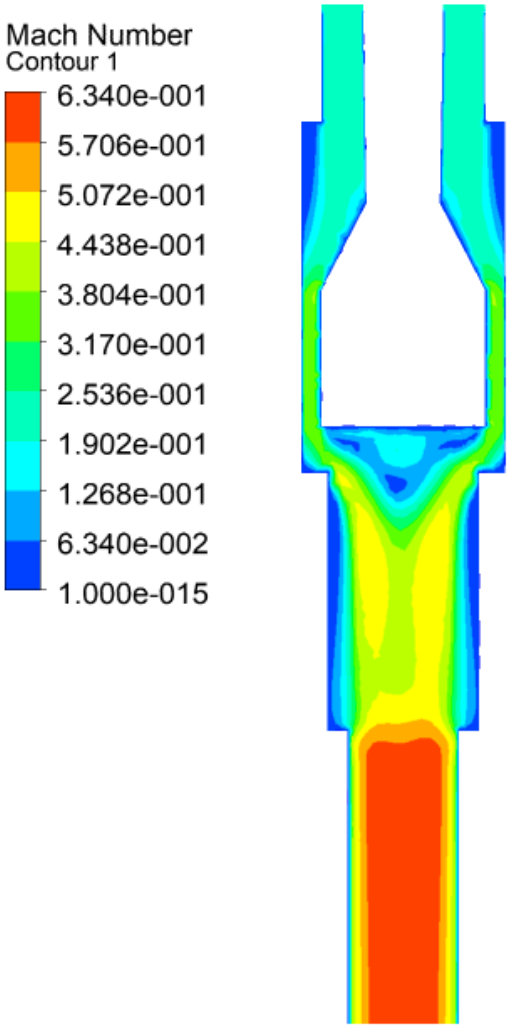

Figure E.2. Mach number contour through pilot valve at Pi = 70 bar, Pp= 60 bar, and T= 300 K^{o} (edited by the Author)

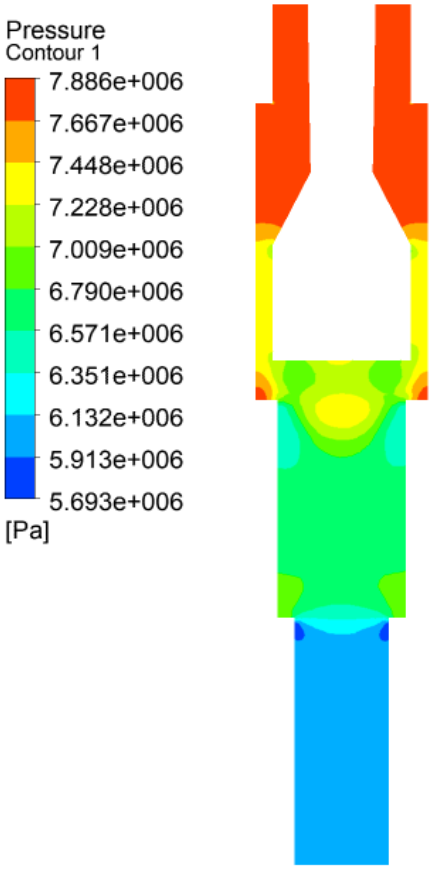

Figure E.3. Pressure contour through pilot valve at Pi = 80 bar, Pp= 60 bar, and T= 300 K° (edited by the Author)

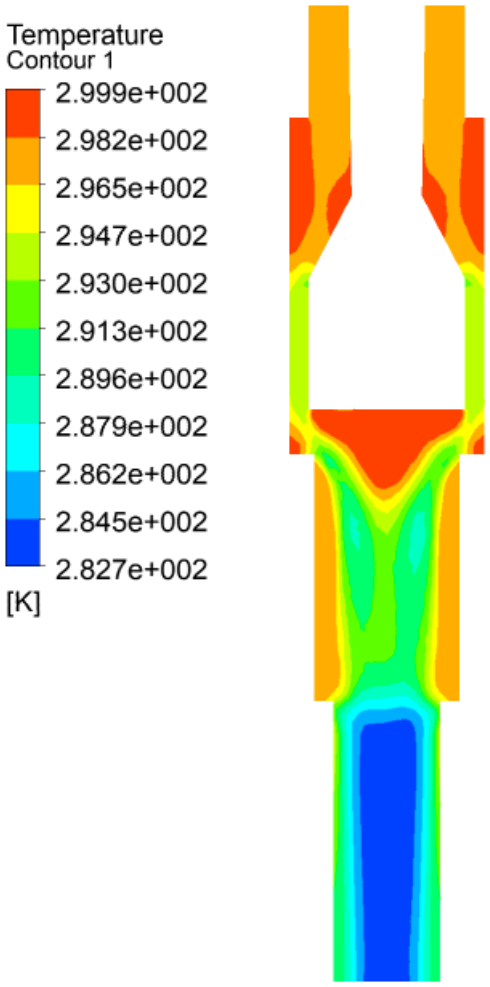

Figure E.4. Temperature contour through pilot valve at Pi = 80 bar, Pp= 60 bar, and T= 300 K^{o} (edited by the Author)

11.6. Appendix F: Pilot Valve Operation Conditions

Table F.1. Gas flow rate from CFD simulation for different operation conditions (Injected gas: Methane, Temperature= 300 ^{o}K, main port diameter = 0.551 in. (edited by the Author)

Injection pressure (P_i) [bar]	Production pressure (P_p) [bar]	Gas flow rate (Q_{sc}) [MMscf/d]
50	50	0
	45	1.297
	40	1.748
	30	2.200
	20	2.316
	10	2.320
70	70	0
	65	1.553
	60	2.125
	55	2.511
	50	2.786
	40	3.120
	30	3.232
	20	3.232
	10	3.232
80	80	0
	75	1.665
	70	2.288
	60	3.046
	50	3.451
	40	3.651
	30	3.651
	20	3.651
	10	3.651

Table F.1. (Cont.) Gas flow rate from CFD simulation for different operation conditions (Injected gas: Methane, Temperature= 300 ^{o}K, main port diameter = 0.551 in.

Injection pressure (P_i) [bar]	Production pressure (P_p) [bar]	Gas flow rate (Q_{sc}) [MMscf/d]
90	90	0
	85	1.860
	80	2.446
	70	3.269
	60	3.724
	50	4.032
	40	4.134
	30	4.144
	20	4.148
	10	4.148
100	100	0
	95	1.874
	90	2.590
	80	3.488
	70	4.0372
	60	4.376
	50	4.558
	40	4.600
	30	4.600
	20	4.600
	10	4.600

Table F.2. The operation conditions used to calculate the C_dY. (edited by the Author)

P_i [bar]	P_p [bar]	Q_{sc} [MMscf/d]	k [-]	γ [–]	T_v [^oK]	A_v [in^2]	Z_v [-]	C_dY [-]
70	65	1.553	1.32	0.553	300	0.238	0.875	0.311
70	60	2.125	1.32	0.553	300	0.238	0.875	0.301
70	55	2.511	1.32	0.553	300	0.238	0.875	0.290
70	50	2.786	1.32	0.553	300	0.238	0.875	0.279
70	40	3.120	1.32	0.553	300	0.238	0.875	0.255
70	30	3.232	1.32	0.553	300	0.238	0.875	0.228
70	20	3.232	1.32	0.553	300	0.238	0.875	0.204
70	10	3.232	1.32	0.553	300	0.238	0.875	0.187
80	75	1.665	1.32	0.553	300	0.238	0.863	0.309
80	70	2.288	1.32	0.553	300	0.238	0.863	0.301
80	60	3.046	1.32	0.553	300	0.238	0.863	0.283
80	50	3.451	1.32	0.553	300	0.238	0.863	0.262
80	40	3.651	1.32	0.553	300	0.238	0.863	0.240
80	30	3.651	1.32	0.553	300	0.238	0.863	0.215
80	20	3.651	1.32	0.553	300	0.238	0.863	0.196
80	10	3.651	1.32	0.553	300	0.238	0.863	0.180

12.LIST OF APPENDIXES